Center for Systems Engineering and Applied Mechanics
-
Physical Medicine and Rehabilitation Unit

Fingertip skin as an optimal interface to manipulate objects: the role of moisture

by Thibaut ANDRE

Thesis submitted in partial fulfillment of the requirements for the degree of
Docteur en Sciences Appliquées

<u>Jury :</u>

Prof. V. Blondel	Univ. catholique de Louvain	Belgium
Prof. J. Delbeke	Univ. catholique de Louvain	Belgium
Prof. V. Hayward	Univ. Pierre et Marie Curie (Paris)	France
Prof. P. Lefèvre (supervisor)	Univ. catholique de Louvain	Belgium
Dr. V. Pletser	ESA - ESTEC	The Netherlands
Prof. A.M. Smith	Univ. de Montréal	Canada
Prof. J-L. Thonnard (supervisor)	Univ. catholique de Louvain	Belgium

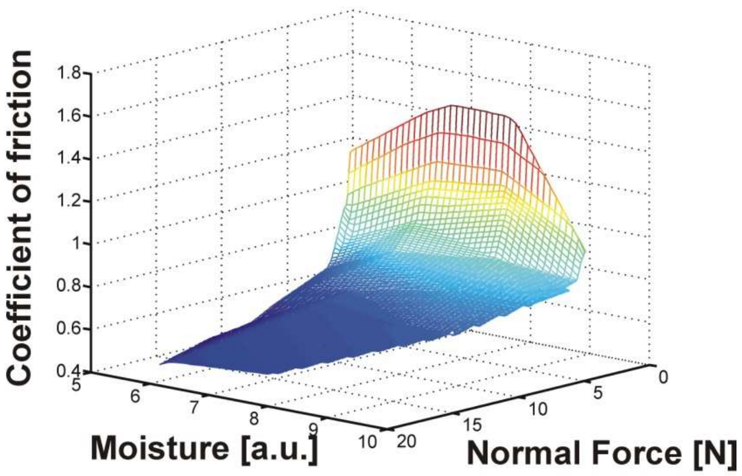

To my grand-parents…

REMERCIEMENTS

Avant de commencer cette thèse, j'aimerais adresser toute une série de remerciements aux personnes qui m'ont permis de mener à bien ce travail de recherche.

Mes premiers et plus profonds remerciements se tournent vers mes promoteurs, Jean-Louis Thonnard et Philippe Lefèvre. En effet leur disponibilité et le cadre de travail qu'ils m'ont offerts, m'ont permis de travailler dans des conditions exceptionnelles. Leurs conseils, commentaires et remarques ont toujours été judicieux et positifs, et m'ont permis d'avancer et de valoriser mon travail. La confiance qu'ils m'ont témoignée ainsi que les nombreuses expériences passionnantes qu'ils m'ont permis de vivre (vols paraboliques, conférences, collaboration étrangère,…) ont rendu ce travail de recherche unique et épanouissant.

Je tiens également à remercier les membres de mon comité d'encadrement, Jean Delbeke et Vincent Hayward. L'intérêt qu'ils ont porté à mon travail, le suivi régulier qu'ils m'ont offert et leurs remarques éclairées ont efficacement contribué à l'aboutissement de cette thèse. Je suis également très reconnaissant envers les membres extérieurs de mon jury d'avoir lu cette thèse, accepté d'être dans le jury, et pour leurs commentaires intéressants et utiles à l'amélioration de mon manuscrit.

Frédéric Crevecoeur a été un « binôme » génial durant toutes ces années de thèse et je pense qu'une réelle complicité est née au cours de nos multiples aventures. J'espère avoir encore l'occasion de travailler avec Fred et que de nouvelles collaborations naîtront dans le futur.

De nombreuses personnes ont directement contribué à l'aboutissement de mes projets et je tiens à les remercier : Michel De Wan pour sa précieuse aide lors du développement du Moisture Evaluator ; Vincent Lévesque et Vincent Hayward pour notre collaboration et l'accueil qu'ils m'ont offert à Montréal ; Christian Lebègue pour toutes ses réalisations techniques ; Damienne De Limbourg et Isabelle Hisette pour leur aide administrative ; Florent Baudrier et Matthieu Bouchain pour leur travail d'acquisition de données pendant leur mémoire.

La recherche manquerait de vie sans l'existence d'équipes et de laboratoires. Je suis très reconnaissant envers tous les membres des anciennes unités READ, NEFY et CESAME pour leur convivialité et l'excellente ambiance de travail mais également pour leur aide précieuse et leur disponibilité lorsque je cherchais des sujets. Dans la même idée, je remercie tous les membres de l'Haptics Laboratory (Mc Gill, Montréal) pour leur accueil, leur aide et les excellentes conditions de travail. Enfin, je voudrais particulièrement remercier Olivier White pour son encadrement et ses précieux conseils au début de ma thèse.

Finalement, je voudrais remercier tous les membres de ma famille, tous mes amis ainsi que toutes les personnes que j'ai rencontrées et qui ont pris le temps d'essayer de comprendre mon travail et mon sujet de thèse en m'écoutant. Grâce à eux, j'ai dû apprendre à simplifier, condenser, prendre du recul et ils m'ont même souvent apporté de nouvelles idées.

Ce travail a été supporté par le Fonds National de la Recherche Scientifique, la Fondation pour la Recherche Scientifique Médicale, le Programme Belge des Pôles d'Attraction Interuniversitaire initié par le Bureau de la Politique Scientifique Belge Fédérale, Actions de Recherche Concertées (Communauté française, Belgique), une bourse interne de recherche (Fonds Spéciaux de Recherche) de l'Université catholique de Louvain, une bourse de Prodex (contract numbers 90063, 90064, 90231, 90232), ESA (European Space Agency) et NANOBIOTACT-project (EU-FPG-NMP-033287).

TABLE OF CONTENTS

LIST OF ABBREVIATIONS

ANOVA	Analysis of variance
a.u.	Arbitrary units
CCD	Charge-coupled device
CF	Coefficient of friction
CNS	Central nervous system
CP	Center of pressure
EEG	Electroencephalogram
EMG	Electromyography
ERP	Evoked response potential
F	Force
FA-1	Fast adapting type 1
FA-2	Fast adapting type 2
FE	Finite element
FTIR	Frustrated total internal reflection
FzL	Left normal force
FzR	Right normal force
GF	Grip force
GFs	Static grip force
LED	Light-emitting diodes
LF	Load force

N	Newton
NF	Normal force
R^2	Coefficient of determination
S	Subject
SA-1	Slow adapting type 1
SA-2	Slow adapting type 2
SEP	Somatosensory evoked potential
SD	Standard deviation
SR	Stick ratio
T	Torque
TF	Tangential force
yr	Years old

DEFINITIONS OF VARIABLES

- Fx, Fy and Fz: forces measured by the F/T sensor in the x-axis, y-axis and z-axis with respect to the reference frame of the sensor. The x-axis, y-axis and z-axis correspond to the tangential horizontal axis, tangential vertical axis and normal axis, respectively.

- FzR and FzL: when the manipulandum was used, there were 2 sensors. R and L mean right and left respectively.

- NF = Fz (normal force).

- TF = sqrt(Fx^2+Fy^2) = Ft (tangential force): global value of the tangential constraints. FtR and FtL mean right tangential force and left tangential force.

- GF = (FzR+FzL)/2 (grip force).

- LF = FtR+FtL (load force).

- CF = TF/NF at slip onset (coefficient of friction).

- CP = T/NF (center of pressure)

Chapter 1

INTRODUCTION

AND BACKGROUND

“Nobody in Rugby should be called a genius. A genius is a guy like Norman Einstein."

Jono Gibbs (Chiefs)

Humans constantly interact with objects by touching, displacing, or manipulating them, and tactile information from the fingertip skin is of primary importance in this process. The skin is a viscoelastic tissue that contains thousands of mechanoreceptors, which are stimulated by skin deformation and provide information about a touched surface or an object held. To optimally control arm movement or fingertip force, the central nervous system (CNS) integrates sensory information from different receptors (vision, proprioception, touch). In particular, the CNS requires tactile information to efficiently manipulate objects. Johansson and Westling (1984b) introduced a new paradigm to study dexterous object manipulation, utilizing the thumb and index finger in a precision grip configuration (Figure 1-1) to lift and move an object. The contribution of cutaneous feedback during object manipulation has been described frequently in published literature, and plays a central role when an object’s properties are changed. This thesis seeks to explain the close link between skin mechanical properties and motor control of precision grip.

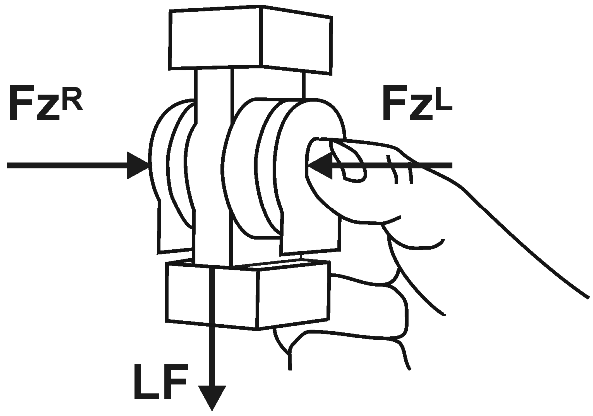

Figure 1-1 : Precision grip configuration

The fingertip skin structure and mechanical properties

The skin is a protective interface between the body and the external environment. It regulates fluid and electrolyte balance, and is an essential organ in temperature regulation (Mountcastle 2005). Hairy skin covers most of the body and differs from the glabrous (hairless) skin located on the ventral surfaces of the palms, fingers, and soles of the feet. The glabrous skin is characterized by alternating papillary ridges and grooves (see Figure 1-2), which have different functions, such as sweat evacuation ("gutter effect") or vibration creation during tactile perception.

The glabrous skin is comprised of two major tissue layers: the epidermis and the dermis. The outer epidermal layer has a fairly constant thickness; the distance from the skin surface to the dermal papillae is typically 0.6 mm and can reach 1.0 mm for the primary ridge containing the sweat ducts (Yantis and Pashler 2002). The epidermis is relatively tough and hard (Adams et al. 2007). The inner dermal layer situated between the epidermis and subcutaneous tissue is 2 to 3 mm thick and provides mechanical support to the epidermis. It contains connective tissue, blood vessels, sweat glands, and nerve plexuses. The connected fibers that compose the dermis are essentially collagen and elastin fibers mixed in a semi semi-fluid structure. The collagen fibers constitute around 70% of the dermis and give it its strength. Elastin fibers give it its elastic properties. Both the epidermis and dermis are comprised of several sub-layers with their own mechanical properties. At a deeper level there is sub-cutaneous tissue, which is a fat layer with a fluid phase volume of about 60-70% (Fawcett 1986). All these layers confer to the glabrous fingertip skin a multi-layered structure that constitutes a non-linear, non-homogeneous, and anisotropic system, which is water absorbing (Daly 1982; Edwards and Marks 1995).

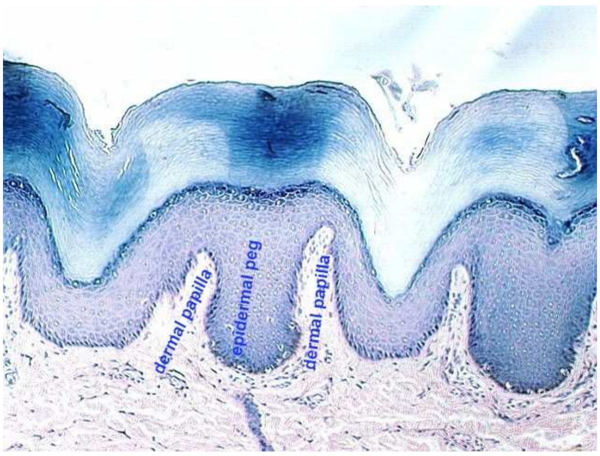

Figure 1-2 : The skin

Most research on fingertip skin mechanical properties has focused on characteristics in the normal direction with respect to the skin surface (Kinoshita and Mori 1972; Phillips and Johnson 1981; Srinivasan et al. 1992; Kim et al. 1994; Srinivasan and Dandekar 1996; Maeno et al. 1998). Such studies have used an elastic or viscoelastic model (Kelvin model) of the skin and have mainly focused on the stress/strain relationship to determine the Young's modulus. Philipps and Johnson (1981) developed a continuum mechanics model to predict the stress and strain at specific locations within the skin. Their model allowed the prediction of mechanoreceptor responses to bars, edges, and grating. In contrast to this use of static stimuli, Pawluk and Howe (1999b) investigated the dynamic response of the fingerpad. They used a quasi-linear viscoelastic model (Fung 1993) to successfully explain the experimental data. Numerous other authors have also used viscoelastic models to explain skin deformation under normal indentation, and to determine the mechanical impedance of the fingerpad (Gulati and Srinivasan 1995; Serina et al. 1997; Serina et al. 1998; Cohen et al. 1999).

Finite element (FE) analysis is widely used to model the fingertip. Srinivasan and Dandekar (1996) considered the fingertip skin as a block, without specific distinctions between the different layers. Interestingly, they found the maximum compressive strain and strain energy density at typical mechanoreceptor locations. Maeno et al. (1998) distinguished the three main layers and measured the stiffness of the finger tissue on cadavers to develop their FE model. They determined epidermis, dermis, and subcutaneous tissue Young's moduli of 1.36×10^5 Pa, 8.0×10^4 Pa, and 3.4×10^4 Pa, respectively. More recently, Tada et al. (2006c) developed an iterative process that compared the results of the FE analysis and images provided by magnetic resonance. Using these comparisons, they adjusted the FE model parameters to find a simulation that was similar to the real images. They then estimated the material constants of living soft tissue with the final parameters.

Nevertheless, few studies have addressed skin properties in the tangential direction. Focusing on the relationship between the human finger tissue and the location of tactile receptors, Maeno et al. (1998) calculated fingertip deformation with respect to the shearing force using FE analysis. Nakazawa et al. (2000) characterized human fingertips in the shearing direction, using the Kelvin model to experimentally determine the shearing stiffness and viscosity. The viscoelastic response to incremental tangential displacement was also studied by Pataky et al. (2005), who mainly focused on skin relaxation after loading, stiffness, and hysteresis. Consistent with previous works, they observed linear viscoelasticity during incremental loading but large hysteresis upon unloading, which is indicative of nonlinear viscoelastic behavior. Finally, Wang and Hayward (2007) described the biomechanics of the fingerpad skin in vivo under local tangential traction, and found that incremental loading (both stretching and shearing) induced nonlinear behaviors.

The mechanical properties of the fingertip skin at the contact interface with an object are also important parameters that have been investigated by various authors. Recently, Tada et al. (2006b) studied the mechanics of partial slippage using a theoretical model, and compared these results with experimental data obtained from a tactile imaging system. Their approximation of the constitutive law of the contact interface depended on the coefficient of friction, tangential force, and normal force. The coefficient of friction at the interface between the skin and a contact surface has been widely studied. The static coefficient of friction between two contacting surfaces is defined as the ratio between the tangential force and the normal force when slippage is initiated (Bowden and Tabor 1982; Blau 2001). Amontons' law indicates that the CF is a constant for any pair of surfaces. Accordingly, the frictional force is directly proportional to the applied load and independent of the contact surface. Naylor (1955) first described the skin surface and friction between a "friction head" (made of polythene or silver) and the skin situated over the middle third of the anterior surface of the tibia. His results did not show any effect of the loading weight, respected Amontons' law, and revealed a friction coefficient of 0.5. However, Naylor had previously found that the skin surface condition strongly affects the friction coefficient, which decreased when the skin was dry, greasy, or wet and increased when the skin was moist. Even if Naylor did not measure the moisture content, his observations introduced part of the work developed in this thesis where the influence of moisture on the coefficient of friction will be quantified.

Comaish and Bottoms (1971) showed that Amontons' law does not hold for skin in vitro. They observed that the skin coefficient of friction depends on the applied load, and proposed a new relationship between the friction force (F) and the applied load (W):

$$F=k\ W^n \quad (1)$$

where n is a real number and k is the load-dependent friction coefficient equal to the conventional coefficient at unit normal load ($\mu=k\ W^{n-1}$). Consequently, the unit of k is $[N^{1-n}]$. According to this equation, the coefficient of friction strongly increases with a low level of applied load. The coefficient of friction has been studied for various body sites like the forearm (Koudine et al. 2000; Adams et al. 2007), and significant attention has been given to the fingertip. Different measurement techniques (Sivamani et al. 2003; Gee et al. 2005; Savescu et al. 2008), several materials (Buchholz et al. 1988; Dinç et al. 1991; Derler et al. 2007; Derler et al. 2008), and various moisture levels (Nacht et al. 1981; Smith et al. 1997; Li et al. 2001; Derler et al. 2007) have also been studied. However, although several authors consider skin hydration in their results, not one has precisely and continuously quantified the effect of moisture on the skin deformation and coefficient of friction.

The skin mechanoreceptors and the sweat glands

The role of the cutaneous receptors and the correlation between receptor morphology and receptor physiology has been debated for more than a century. The physiologist Johannes Müller (1842) first introduced the notion of "specific nerve energies" that would represent coded or symbolic data concerning a tactile stimulus. Müller wrote about the sense of touch that: "the sensations of itching, of pleasure and pain, of heat and cold, and those excited by the act of touch in its more limited sense, are varieties of this mode of sensation." Later von Frey (1895) tried to account for the different qualities of somesthetic experience by postulating four separate cutaneous modalities (touch, cold, warm and pain) that were subserved by specific type of receptors: Meissner corpuscules for touch, Ruffini endings for warmth, Krause end-bulbs for cold, and free nerve ending for pain. This concept of physiological specificity of skin receptors provided the power of von Frey's theory and it became accepted that for each modality of cutaneous sensation there existed a specific type of end organ, a specific nerve fiber, and anatomically distinct specific pathways within the nervous system. Nevertheless, this concept was mainly theoretical and anatomical experiments using histological examinations of the skin could not support von Frey's correlation. It is worth mentioning that the definition of specificity was of such broad importance that many investigators preferred to retain the theory. In 1955, Weddell and Sinclair challenged this codification and advanced a 'temporo-spatial pattern' hypothesis. They wrote that "there are no specific fibers and no specific endings… what leaves the skin as a result of cutaneous stimulation is a complex spatially and temporally dispersed pattern of impulses, and this appears to be what arrives at… the brain". The pattern theory was based upon electrophysiological findings in cats and frog and it postulated that every sensation resulted from a particular kind of pattern carried by a wholly non-specific apparatus, and that there was no stimulus-specificity at all (Sinclair 1981). Then, Melzack and Wall (1962) believed that "recognition of receptor specialization for transduction of particular cutaneous stimuli does not preclude acceptance of the concept that the information generated by skin receptors is coded in the form of patterns of nerve impulses". They introduced the "gate control" theory of pain which stated that pain was the result of messages aroused in small myelinated and unmyelinated fibres. Later, Iggo, Vallbo, Johansson and colleagues (Iggo and Andres 1982; Johansson and Vallbo 1983; Iggo 1984; Vallbo and Johansson 1984) described the electrophysiological responses of 4 types of mechanoreceptors and suggested they were related to the following morphologies. The Meissner corpuscles for the fast-adapting (type 1) afferents, the Merkel cells for the slow-adapting (type 1) afferents, the Pacinian corpuscles for the fast-adapting (type 2), and the Ruffini complexes for the slow-adapting (type 2). Moreover, they aimed at attributing specific functions to morphologically distinct cutaneous sensory receptors. Despite its widespread acceptance, there has never been any real proof that the FA-1 axons terminate in Meissner corpuscles or that SA-1 fibers terminate on Merkel cells.

Meissner corpuscles

The Meissner corpuscles are located in the tips of the dermal papillae (Figure 1-3), placing them within the dermis but at a minimal distance from the skin surface. Meissner corpuscles have a capsule enclosing flattened sheets of nervous tissue interleaved with flattened lamina cells. Anatomical studies based on the direct count of Meissner corpuscles showed that the innervation density in the fingerpad is about 12-38/mm² in human (Bolton et al. 1966) and 47-60/mm² in monkey (Pare et al. 2001). Meissner corpuscles are supposed to end the nervous fast adapting type 1 (FA-1) afferents, which are responsible for the detection and discrimination of low frequency vibrations. FA-1 afferents are insensitive to static skin deformation, but are sensitive to dynamic skin deformation in the frequency range of 1 to 300 Hz. Their receptive field size is between 10 and 50 mm² with a spatial acuity of 3 mm (Johnson 2001). Numerous authors aimed at correlating morphology, physiology and the functions of the receptors and it has been suggested that the FA-1 afferents are responsible for detecting lateral skin stretch between skin and an object held in precision grip, providing them with an important function in producing feedback signals for grip control (Johansson and Westling 1984b; Srinivasan et al. 1990; Macefield et al. 1996; Johnson 2001). However, the recent studies by Birznieks et al. (2001; 2009; 2010) show that all the skin mechanoreceptors detect tangential shearing forces. This would appear to contradict their earlier papers. Finally, it is worth noting that Meissner corpuscles are not only mechanoreceptors, but they also responds to substances which are associated to nociception. It suggested that Meissner corpuscles also have nociceptive capabilities (Pare et al. 2001).

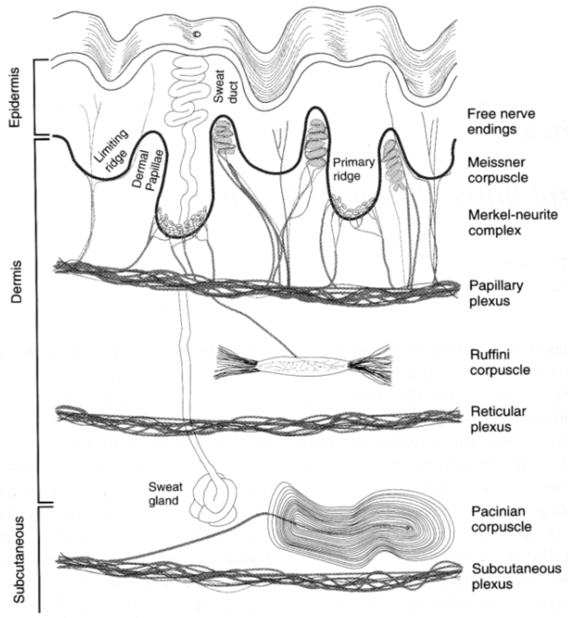

Figure 1-3 : Human glabrous skin. From (Yantis and Pashler 2002).

Merkel cells

Merkel cells are found in the tips of the primary epidermal ridge, in the basal epidermal layer (Figure 1-3). Pare et al. (2002) showed that about 70-85% of the surface area at the base of the epidermal ridges was covered by Merkel cells. They form neurite complexes that are supposed to enclose the endings of myelinated axons of the slow adapting type 1 (SA-1) afferents. The receptive field size of the SA-1 afferents is ~ 5 mm^2 (diameters of 2-3 mm). SA-1 afferents are sensitive to low-frequency dynamic skin deformation (< 5 Hz) and static force. Due to their selective sensitivity to strain energy density, SA-1 afferents are sensitive to points, edges, and curvature. Their spatial resolution of 0.5 mm provides the SA-1 population with an acute spatial representation. Therefore, they are mainly involved in form and texture perception (Johnson 2001; Johansson and Flanagan 2009).

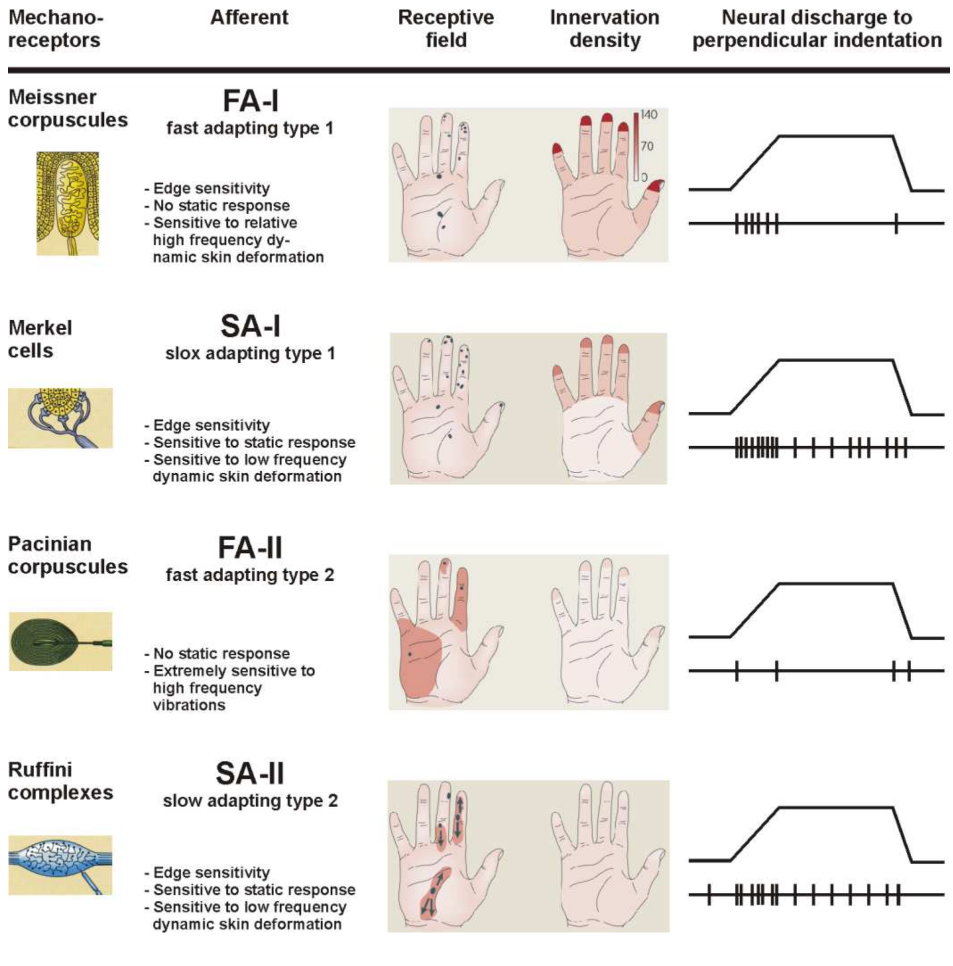

Figure 1-4 : The skin mechanoreceptors (Adapted from Johansson and Flanagan(2009))

Pacinian corpuscles

The Pacinian corpuscles are located in the deeper skin layers and subcutaneous tissue (Figure 1-3). Each corpuscle is comprised of layers of concentric lamellae that filter mechanical deformation. A Pacinian corpuscle terminates a fast adapting type 2 (FA-II) afferent, and its physical characteristics provide it with a low-frequency filter property. It is sensitive to high-frequency stimuli, from 5 to 1000 Hz (with a peak at 200Hz). These corpuscles have an innervation density of 20/cm² (~ 350 corpuscles per finger) and almost no spatial resolution (> 10 mm). Their receptive field may include an entire finger or hand. Finally, the FA-II afferents provide a high-fidelity neural image of transient and vibratory stimuli transmitted to the hand by held objects.

Ruffini complexes

The existence of Ruffini complexes remains controversial, although they are commonly thought to be located in the dermis (Figure 1-3). These encapsulated strands of connective tissue and nerve endings are reportedly anchored in the dermal collagen at their poles. Ruffini complexes are thought to be the end organ of the slow adapting type 2 (SA-II) afferents. They are sensitive to very low frequency stimuli (peak sensitivity of 0.5 Hz), have a small density innervation (10/cm²) and a large receptive field (60 mm²). The SA-II units transmit a neural image of the skin stretch and are thus sensitive to tangential force (forces acting parallel to the skin surface), hand shape, and motion direction. Information of this nature may help monitor shearing forces between the skin surface and a hand-held object. Nevertheless, Pare et al. studied cutaneous mechanoreceptors in the glabrous fingerpads of monkeys (Pare et al. 2002) and humans (Johnson

2001; Pare et al. 2003), and did not identify any Ruffini corpuscule or Ruffini-like ending in the glabrous skin. It has been suggested that the SA-II units might be a subset of Merkel endings with special morphological features. However, they detected Ruffini-like endings at the fingernail base. As Johnson (2001) wrote, "SA-II afferents present a puzzle. They are reported regularly in microneurographic studies of mechanoreceptors in human hand but have never been observed in neurophysiological studies of mechanoreceptors in the monkey hand".

Sweat glands

There are three main types of exocrine glands in the human skin: sebaceous, apocrine, and eccrine (Collins 1988; Folk and Semken 1991). Sebaceous glands are classified as holocrine glands (i.e., the whole secretory cell is secreted) and are associated with hair follicles (Figure 1-5). They secrete into hair follicles an oily matter, called sebum, to lubricate the skin. The two other glands (apocrine and eccrine) are sweat glands that are generally associated with body thermoregulation but also respond to emotional stress (emotional sweating) or spicy food consumption (gustatory sweating). Sweat gland activity is directly controlled by the CNS via the hypothalamus. The efferent central sudomotor pathway consists of the cerebral cortex to hypothalamus, hypothalamus to medulla, medulla to lateral horn of the spinal cord, lateral horn to sympathetic ganglia, and sympathetic ganglia to sweat glands as postganglionic sympathetic fibers (Sato et al. 1989; Wilke et al. 2007).

Apocrine glands are only found in the axial, mammary, perineal, and genital regions. They consist of a coiled gland in the deep dermis and a short straight duct in close vicinity to the hair follicle (Figure 1-5). Fluid secreted by the apocrine is an oily substance containing proteins, lipids, and steroids. Apocrine glands respond to emotional stimuli (e.g. anxiety, pain, or sexual arousal), and although their exact function is unclear, they are thought to represent scent glands (Wilke et al. 2007).

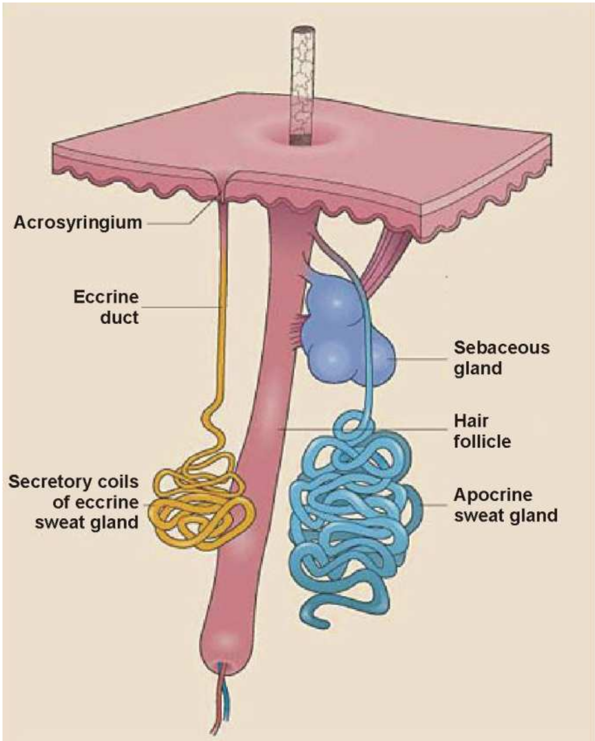

Figure 1-5 : The exocrine glands in human skin

Eccrine glands are more numerous (> 2 million) than apocrine glands and are present at high densities on the palms and soles (~700/cm²). They are coiled tubular systems comprised of acrosyringium, eccrine duct, and secretory portions (Figure 1-5). The secretory portion is located shallow in the dermis and consists of a tubule of about 60 to 80 µm in diameter and

2 to 5 mm in length. There are three different cell types in the secretory portion: clear, dark, and myoepithelial cells. Contractions squeeze the gland and provoke the discharge of the accumulated secretions. Myoepithelial cells contract in response to cholinergic stimuli and provide mechanical support for the secretory portion (Sato et al. 1989). Eccrine sweat is composed of 99% water, with different solutes: sodium, potassium, chloride, lactate, urea, ammonia, amino acids, calcium, magnesium and bicarbonate (Wilke et al. 2007). Although the main function of eccrine sweat glands is thermoregulation, it has been found that palm or sole sweating is mainly induced by emotive stimuli (Kerassidis 1994) and that palmar sweat glands respond to both thermal and emotive stimuli, each of which can be superimposed on the other (Robertshaw 1977). Some authors have described a human perspiration system that depends on the mammalian eccrine glands, which are separately controlled by the nervous system and provide an adhesive surface (increased friction) for grasping and walking (Adams and Hunter 1969; Adelman et al. 1975; Folk and Semken 1991).

The control mechanisms of sweating have been widely studied in the field of psychology and psychophysiology. Sweat secretion is divided into secretory and expulsive components (Bligh 1967). As previously said, the secretory portion of eccrine glands is surrounded by myoepithelial cells. As a consequence, a sudden increase in moisture implies myoepithelial cell contraction; whereas a slow, gradual increase in moisture suggests that the secretion rate has increased without contraction. Therefore, sweating may occur because of increased secretion alone, myoepithelial contraction without an increase in the rate of secretion, or an increased rate of secretion combined with myoepithelial contraction (Robertshaw 1977). The eccrine glands are innervated largely by cholinergic nerves and respond to different hormones. On one hand, catecholamines (e.g. adrenaline or noradrenaline) increase sweat secretion and intradermal injections can evoke local sweating (Venables and Christie 1973). On the other hand, antidiuretic hormone produces a decrease in sweat rate and aldosterone increases the ductal reabsorption (Robertshaw 1977). Centrally, the neural control of sweating in human has been studied by Critchley et al. (2000) using functional magnetic resonance imaging. They showed that the generation of discrete skin conductance responses events was associated with significant activity in the left medial prefrontal cortex, bilateral extrastriate visual cortices, and cerebellum. Their findings provide evidence for involvement of areas implicated in emotional behavior and attention.

Through fingers and hand…

Hand anatomy: bones, nerves and muscles

The human hand is a complex, multi-fingered body part located at the end of each of the two arms. It is comprised of five fingers: the thumb, and the index, middle, ring, and little fingers. The basic skeleton of the hand and wrist consists of 27 bones grouped into carpals, metacarpals, and phalanges (Figure 1-6).

The 8 carpal bones constitute the wrist and are grouped in two rows. The hand contains 5 metacarpal bones that constitute the palm. These are the longest bones of the hand. The first metacarpal bone (corresponding to the thumb) is short, strong, and the most mobile of the metacarpals. Each digit contains 3 phalanges, except for the thumb which contains 2 phalanges.

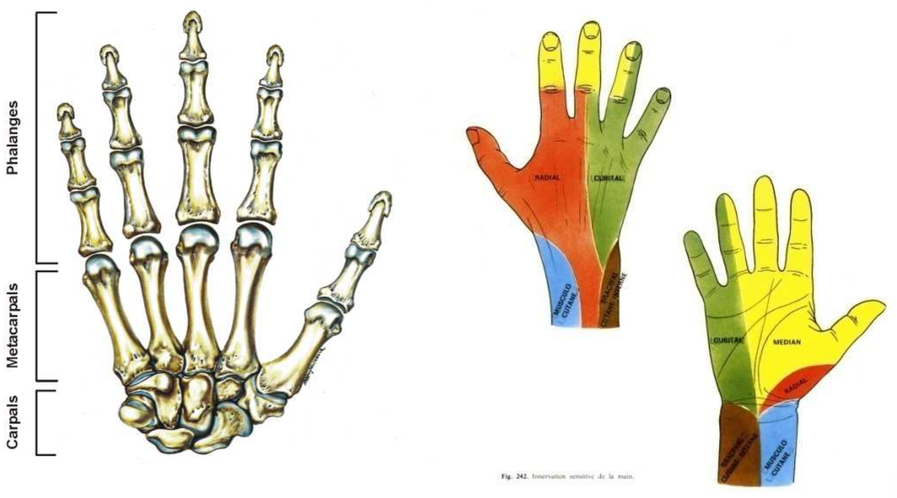

Figure 1-6 : Skeleton and innervations of the human hand (Adapted from Bonola et al. (1988))

Three nerves, the median, ulnar, and radial, innervate the hand. The median nerve mainly originates from C6-C7-C8. The motor branches of the median nerve innervate the muscles involved in the precision grip function (more details in the next paragraph). The sensory branches provide signals from the palmar side of the thumb, index, and long finger (Figure 1-6). The ulnar nerve originates from C8-T1 and the motor branches innervate the muscles involved in power grasping. The sensory branches provide signals from the small and ring fingers. Finally, the radial nerve (from C5-C6-C7-C8) innervates the fingers and wrist extensor, and the sensory branches provide signals from the dorsum of the hand (Figure 1-6).

The muscles that allow hand movement are divided into extrinsic and intrinsic muscle groups. The extrinsic muscles, which are located in the forearm, include extensors and flexors. The extrinsic extensor muscles are innervated by the radial nerve and consist of wrist extensors and a large group of thumb and digit extensors. The extrinsic flexor muscles are mainly innervated by the median nerve (although some are innervated by the ulnar nerve) and consist of wrist flexors and a large group of thumb and digit flexors. The intrinsic muscles, including the thenar, hypothenar, lumbrical and interossei muscles, are the muscles for which the proximal and distal insertions are exclusively within the hand. The interossei muscles consist of 3 volar and 4 dorsal muscles and are all innervated by the ulnar nerve. The lumbrical muscles are 4 little flexors that are innervated by the median nerve for the first and second lumbricals and the ulnar nerve for the third and fourth lumbricals. The hypothenar muscles are associated with small finger abduction. The thenar muscles are the opponens pollicis, flexor pollicis brevis, abductor pollicis brevis, and adductor pollicis (Figure 1-7). This group of muscles is associated with extension, abduction and flexion of the thumb and actually controls and stabilizes the posture of the thumb. They are of prime importance when manipulating object because they enable the thumb to have a position of opposition with respect to other fingers (Forrest and Basmajian 1965).

The hand in precision grip

Napier et al. (1956) first defined two hand postures, the power grip and precision grip, for classifying prehensile movements. The power grip is defined as the forcible activities of the fingers and thumb acting against the palm. It requires the whole hand and seeks to transmit force to an object. In the power grip configuration, the extrinsic muscles provide the major gripping force. In contrast, the precision grip is defined as the manipulation of an object that is pinched between the thumb and fingers using the fingerpad. Although Landsmeer (1962) proposed using the terminology "precision handling" in lieu of "precision grip" because of the manipulative nature of the configuration, most authors use the latter phrase. In the precision grip configuration, thumb abduction ensures that the pulp surfaces of the thumb and fingers can place themselves opposite to each other. In the rest of this manuscript, we will mainly focus on the two-digit precision grip involving the thumb and index finger.

The precision grip requires precise control of the finger and thumb positions, and involves the co-contraction of all the intrinsic and extrinsic muscles of the forearm (Forrest and Basmajian 1965; Long et al. 1970; Smith 1981; Smith and Bourbonnais 1981; Bonola et al. 1988; Johansson and Westling 1988). These muscles (Figure 1-7) stabilize the held object by providing an adequate pinch force. Maier and Hepp-Reymond (1995) studied the electromyography (EMG) activation patterns during force production in precision grip, using linear regression to quantify EMG activity as a function of force. They found that the intrinsic muscles and long flexors of the index were tightly related to force, as were the adductor and short flexor of the thumb.

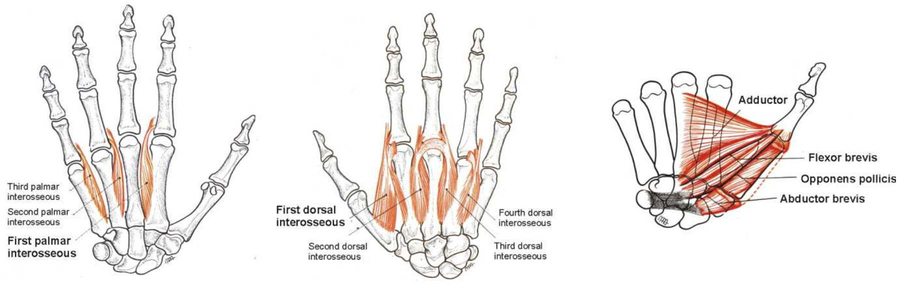

Figure 1-7 : The main hand muscles involved in precision grip

To the brain.

Three main steps are generally described when studying object manipulation: the reaching phase, lifting phase, and transporting phase. During the reaching phase, the arm is moved towards the target object and the hand posture is adapted with the object size and shape. The lifting phase starts when the digits come in contact with the object, and consists of increasing the grip force (normal to the object surface) to overcome the tangential load force (sum of the constraints tangential to the object surface) associated with object lifting. Finally, during the transporting phase, the grip force must be adapted to load force variations (due to inertia) to keep the object from slipping. Moreover, Saels et al. (1999) showed that the surface slipperiness of grasped objects influences the arm kinematics (i.e. acceleration). The CNS plays an essential role during each phase, by integrating motor commands, predictions, and sensory feedbacks.

<u>The reaching phase</u>

To manipulate an object, it must first be reached. During the reaching phase, motor commands are sent to the arm and hand to approach the target object, to orient the hand using the wrist, and to appropriately adjust the finger aperture with the object size. The object is first localized in space using vision, and visual information from the retina is transformed by the CNS to encode the target location with respect to the body frame reference (Desmurget et al. 1998). Using this target location and proprioception information about the hand location, the CNS plans hand displacement and determines a desired trajectory. The motor commands that must be sent to the muscles to realize a desired trajectory depend on "prior" information and feedback information. This "prior" information is comprised of arm-dynamics models and the external environment, and is updated using sensory feedback information. It is commonly proposed that the CNS internally simulates the dynamic behavior of the motor system. The internal model concept has been defined as the neural mechanisms that mimic the arm-dynamics behavior (Wolpert et al. 1995; Kawato 1999; Wolpert and Flanagan 2001). There are two varieties of internal models: inverse internal models that calculate motor commands from the desired trajectory information, and forward internal models that predict sensory consequences from the efference copy of the motor commands (see Figure 1-8). The forward models are vital for anticipating the sensory effects of movement and compensating for physiological delay (i.e., ~ 80 ms, (Miall et al. 1993)).

During the reaching phase, internal models can be updated with respect to unusual or novel environments. To change the internal models, sensory feedback available from vision and proprioception is internally compared with the task goal and predictions (Atkeson 1989; Shadmehr and Mussa-Ivaldi 1994). When studying reaching movement in a new force field, after a learning time the motor commands were well adapted to the new environment (Lackner and DiZio 2005). Several studies showed this adaptation using a new force field created by a robot (Shadmehr and Mussa-Ivaldi 1994; Kurtzer et al. 2005), Coriolis acceleration (Lackner and Dizio 1994; Dizio and Lackner 1995; Pigeon et al. 2003), or new gravitational field like weightlessness or hypergravity (Papaxanthis et al. 1998; Papaxanthis et al. 2005; White et al. 2008; Crevecoeur et al. 2009b). The interaction between multiple sensory feedback sources has also been studied, revealing that both vision and proprioception are very important (van Beers et al. 2002).

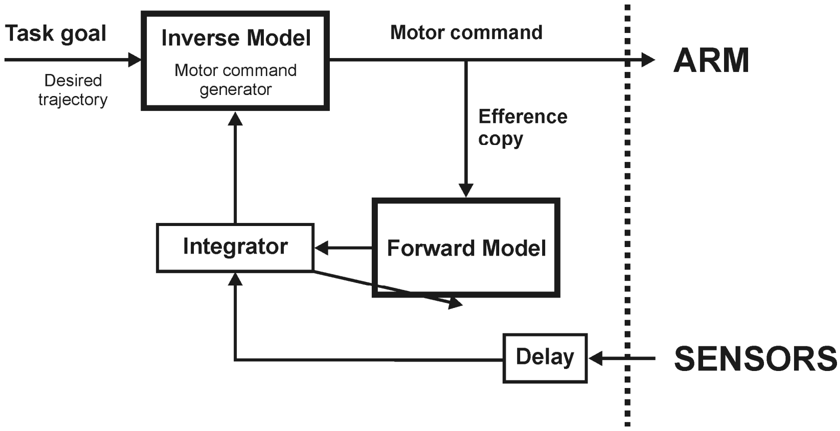

Figure 1-8 : Internal models

Another important issue is determining the optimal motor control (i.e., the motor command that minimizes the cost function). Numerous authors have explained human behaviors using an upper limb–dynamics model, revealing that the motor command movement that minimizes the model's cost function is similar to human experimental results (see Todorov (2004) for review). Nevertheless, the results strongly depended on penalized parameters and the cost function (Jordan and Wolpert 1999). The cost function can be based on a kinematic criteria where the squared jerk (third position derivative) is minimized (Hogan 1984; Flash and Hogan 1985); on a dynamic criteria that depends on variables such as the torque change, muscle tension, or motor commands (Uno et al. 1989; Kawato 1992); or on the minimization of the signal-dependent noise (the minimum-variance theory of motor planning; Harris and Wolpert (1998)).

The hand grip aperture (separation between the thumb and index finger) evolves during the reaching phase. During a reach-to-grasp movement, there is first a progressive opening followed by a gradual closing of the grip until it matches the object's size (Jeannerod 1981; 1984) (Figure 1-9). The maximum grip aperture occurs within 60-70% of the movement duration, and is correlated with the object's size (Castiello 2005). Numerous factors, such as the object size, contact surface size, texture, and weight, influence the grasping kinematics. For instance, Smeets and Brenner (1999) showed that grasping a heavy object or a slippery object requires a large grip aperture.

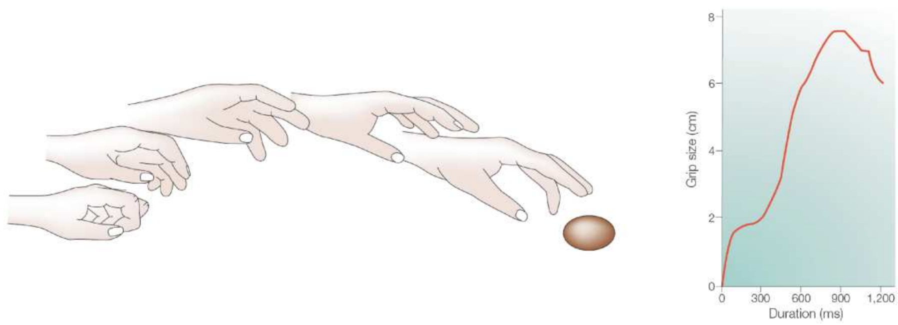

Figure 1-9 : Grip aperture evolution during reach-to-grasp movement (adapted from Castiello (2005))

<u>The lifting phase</u>

When humans lift an object using precision grip, they apply a normal grip force with the thumb and index finger that is large enough to prevent the object from slipping but small enough to avoid damaging the object or causing unnecessary fatigue. The CNS adjusts the grip force in parallel with the tangential LF variation (Johansson and Westling 1984b; Westling and Johansson 1984). The CNS first uses visual information about the object's properties (size, shape, and identity) and estimates the object's weight and friction (Gordon et al. 1991; Mon-Williams and Murray 2000) before beginning to touch the object. When the fingers are in contact with the object, cutaneous information from the fingertip mechanoreceptors sensory feedback provides more information about the contact surface friction and the object's weight and shape (curvature). The CNS adapts its grip/lift strategy depending on the frictional variation (Westling and Johansson 1984; Cole and Johansson 1993; Cadoret and Smith 1996; Saels et al. 1999) or object curvature (Jenmalm et al. 1998; Jenmalm et al. 2000). Flanagan et al. (1995) also showed that the perceived weight depends on the object's surface texture. The importance of cutaneous information has been shown while recording the sensory afference from the skin mechanoreceptors with the microneurography technique (Johansson and Westling 1984a; Johansson and Cole 1992) and following thumb and index finger anaesthetization (Monzee et al. 2003). Grip control is strongly affected by a lack of sensory feedback.

The transporting phase

When an object is lifted in precision grip, arm movements generate tangential LF variations that must be considered when adjusting the grip force. Experimental evidence indicates that an increase (or decrease) in grip force automatically and instantaneously compensates for an increase (or decrease) in LF. Therefore, the CNS must anticipate the LF variation; the programmed grip force is an integral part of the planning process (Flanagan and Wing 1993; Danion and Sarlegna 2007; Danion et al. 2009). Indeed, if the CNS were to wait for sensory feedback (delayed about 80 ms), then the grip and load forces would not be synchronous. Authors have suggested that anticipatory adjustments of the grip force provide evidence for an internal forward model (Flanagan and Wing 1997; Kawato 1999; Davidson and Wolpert 2004; Flanagan et al. 2006): the forward model uses an efference copy of the motor commands to anticipate the consequence of the movement and efficiently adjust the grip force (Figure 1-10). Forward models are based on prior knowledge of the arm and object dynamics model, and must be adapted to environmental changes. Flanagan et al. (2001) showed that the inertial anisotropy of the arm is predicted during movement planning. Microgravity provides a completely new environment that changes arm dynamics. Experiments performed during parabolic flights provide evidence that the internal models are updated with respect to the new environment (Hermsdorfer et al. 2000; Nowak et al. 2001b; Augurelle et al. 2003a; White et al. 2005; Crevecoeur et al. 2009a). An adapted forward model allows subjects to manipulate an object efficiently after a certain learning period.

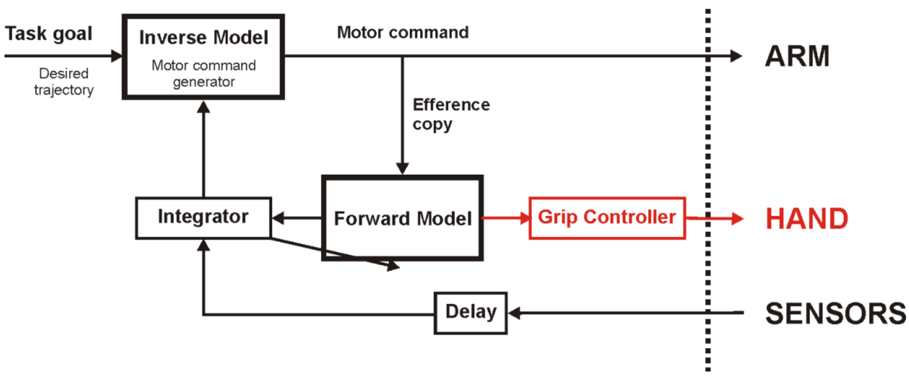

Figure 1-10 : Forward model to anticipate for grip force adjustment

The importance of cutaneous feedback during the transporting phase has also been studied (Nowak et al. 2001a; Augurelle et al. 2003b; Witney et al. 2004). Cutaneous afferents are required to maintain a background level of grip force, to detect slip, and to adapt the grip force to friction. Moreover, cutaneous feedback allows correction and maintenance of an internal model of the object's physical properties.

Open questions and content of the thesis

The skin is a multi-layered tissue that contains numerous receptors and sweat glands. It has been described as a hydrophilic viscoelastic material which properties could change with hydration, but little is actually known about its mechanical properties or its deformation under tangential constraints. Even less is known about the influence of hydration on its deformation. When an object is held in precision grip, the minimal grip force required to avoid object slippage strongly depends on the friction at the skin-object interface. Although the skin coefficient of friction is of prime importance and is influenced by skin hydration, few studies have quantified the effect of moisture or continuously measured the moisture content and friction. Prior information about an object's properties is essential during dexterous manipulation, and the CNS updates its models using sensory feedback. However, even if skin biomechanics change with hydration level, few studies have addressed the effects of a change in an object's properties during a task, and no study has analyzed the effects of skin moisture variations on grip control. Moreover, the problem of a peripheral or central control of sweat gland activity has never been developed when studying motor control of movement and no study linked skin physiology and motor control.

Important questions in this area include:

- What are the effects of the skin's hydration level on skin surface deformation during loading and slipping?

- How can we continuously measure the fingertip skin moisture during a manipulation task?

- What are the effects of moisture on the fingertip friction?

- Can we continuously measure the fingertip friction during object manipulation?

- What is the influence of skin moisture on the grip strategy?

- Is there an optimal fingertip moisture regulation?

In the introduction (Chapter 1), we will present the general context of the thesis using a "bottom-up" approach, to describe the link between skin mechanical properties and brain motor control of movement. Skin mechanical deformation at the interface between the fingertip and a glass surface and the effect of moisture content will be addressed in Chapter 2. The subjects performed slippages with their index finger on a glass surface, a video of the skin interface was recorded during loading and slipping, and the normal and tangential forces exerted by the finger and moisture content were measured. We will also analyze the effect of interaction force components and moisture on the surface skin deformation. We will show that the moisture content can strongly influence skin properties, leading us to develop a task-specific instrument to measure skin moisture during object manipulation (Chapter 3). This instrument consists of a probe and an electronic circuit, and is based on the principle of conductance. The instrument has been calibrated and validated using a commercial device (Corneometer®) and is perfectly adapted to our grip/lift force dynamometer.

The coefficient of friction at the interface between the fingers and an object held in precision grip will be studied in Chapter 4. We will show that the effect of the normal force and moisture content on the fingertip friction highlights the optimal moisture value that maximizes the coefficient of friction. These results provided us with a new technique to continuously measure the fingertip friction. In Chapter 5, we will present an experiment investigating the effect of the fingertip moisture content on the grip control during dexterous manipulation. We will show that the fingertip moisture is optimally modulated during object manipulation. Finally, in Chapter 6, we will summarize the contribution of this thesis, provide new global hypotheses, discuss the limitations of our work, and describe possible future investigations.

Publications and communications

Journal papers:

- **Fingertip Moisture Is Optimally Modulated During Object Manipulation.** André T., Lefèvre P. and Thonnard J-L., Journal of Neurophysiology (2009) 103: 402-408.

- **A Continuous Measure of Fingertip Friction during Precision Grip**. André T., Lefèvre P. and Thonnard J-L., Journal of Neuroscience Methods (2009) 179: 224-229.

- **Moisture Evaluator: a direct measure of fingertip skin hydration during object manipulation**. André T., De Wan M., Lefèvre P. and Thonnard, J-L., Skin Research and Technology (2008) 14: 385-389.

Submitted paper:

- **Effect of skin hydration on the dynamics of fingertip gripping contact.** André T., Lévesque V., Hayward V., Lefèvre P. and Thonnard J-L. Submitted in the Journal of the Royal Society Interface.

Conference papers:

- **Does slippage influence the EEG response to load force variations during object manipulation?** André T., Delbeke J., Lefèvre P. and Thonnard J-L. IFMBE Proceedings; Vol. 22. 4th European Conference of the International Federation for Medical and Biomedical Engineering (2008): 2097-2100.

- **Measurement and Influence of the Skin Moisture in Dexterous Manipulation**. André T., Lefèvre P. and Thonnard J-L. Lecture Notes In Computer Science; Vol. 5024. Proceedings of the 6th international conference on Haptics: Perception, Devices and Scenarios (2008): 373-377.

Work in progress papers:

- **Are EEG responses to load force variations influenced by the slipping of objects during manipulation?** André T., Delbeke J., Lefèvre P. and Thonnard J-L.

Conference communications:

- **The effects of moisture on fingertip skin deformation during loading and slipping.** André T., Lévesque V., Hayward V., Lefèvre P. and Thonnard J-L., 39th Annual Meeting of the Society for Neuroscience, Chicago, USA (2009). Poster presentation.

- **Does slippage influence the EEG response to load force variations during object manipulation?** André T., Delbeke J., Lefèvre P. and Thonnard J-L. 4th European Conference of the International Federation for Medical and Biomedical Engineering, Antwerp, Belgium (2008). Oral presentation.

- **Are EEG responses to load force variations influenced by the slipping of objects during manipulation?** André T., Delbeke J., Lefèvre P. and Thonnard J-L., 38th Annual Meeting of the Society for Neuroscience, Washington, USA (2008). Poster presentation.

- **Measurement and Influence of the Skin Moisture in Dexterous Manipulation**. André T., Lefèvre P. and Thonnard J-L., 6th international conference on Haptics: Perception, Devices and Scenarios, Madrid, Spain (2008). Poster Presentation.

- **Influence of the skin moisture at fingertip on the static grip force during dexterous manipulation**. André T., Lefèvre P. and Thonnard J-L., 37th Annual Meeting of the Society for Neuroscience, San Diego, USA (2007). Poster presentation.

- **The effects of grip force and skin moisture on friction during dextrous manipulations.** André T., White O., Lefèvre P. and Thonnard J-L., 17th Annual Meeting of the Neural Control of Movement Society, Sevilla, Spain (2007). Poster presentation.

Chapter 2

EFFECT OF SKIN HYDRATION ON THE DYNAMICS OF FINGERTIP GRIPPING CONTACT

"Rugby is a game for the mentally deficient... That is why it was invented by the British. Who else but an Englishman could invent an oval ball?"

Peter Pook

Submitted as: T. André, V. Lévesque, V. Hayward, P. Lefèvre and J-L. Thonnard. **Effect of Skin Hydration on the Dynamics of Fingertip Gripping Contact.** Journal of the Royal Society Interface (2010).

Abstract

The dynamics of fingertip contact manifest themselves in the complex skin movements observed during the transition from a stuck state to a fully developed slip. While investigating this transition, we found that it depended strongly on skin hydration. To quantify this dependency, we asked subjects to slide their index fingertip on a glass surface while keeping the normal component of the interaction force constant. Skin deformation

inside the contact region was imaged with an optical apparatus that allowed us to quantify the relative sizes of the slipping and sticking regions. The ratio of the amount of stuck skin to the total amount of contact decreased linearly from one to zero when the tangential force component increased from zero to a maximum. The slope of this relationship was inversely correlated to the normal force component. The dynamics were profoundly affected by the skin hydration level. For any given contact state between a fully sticking and a fully slipping contact, increases in the skin hydration level moved the fingertip further from slipping. Since grips were more unstable under dry skin conditions, our results suggest that the nervous system responds to dry skin by exaggerated grip forces.

Introduction

Human haptic behavior depends critically on the efficient integration of afferent tactile signals. Such signals are produced by thousands of mechanoreceptors that innervate the glabrous skin and are stimulated by skin deformation (Johansson and Vallbo 1983; Johansson and Westling 1984b; Srinivasan et al. 1990; Johnson 2001; Johansson and Flanagan 2009). These signals enable the central nervous system (CNS) to be aware of the properties of a touched surface, allowing the CNS to adapt its motor strategy to the intended task (see (Augurelle et al. 2003b; Witney et al. 2004) for recent surveys). When holding an object, the normal component of the grip force must be sufficiently large to induce a tangential force component that can prevent slip (Johansson and Westling 1984b). The smallest grip force providing a stable grasp depends on the properties of the gripped object, including its mass, geometry, material, and surface finish. Humans rely on tactile afference to adjust the grip force in accordance with such object properties (Westling and Johansson 1984; Flanagan et al. 1995; Cadoret and Smith 1996). Frictional properties and grip stability, however, also depend on skin hydration as much as they depend of the object itself (André et al. 2010).

Here, we experimentally investigated the details of the mechanical events occurring during the transition period between a stuck contact state and a fully developed slip, and the dependency of these events on skin hydration. When performing a dynamic gripping task, external loading reportedly initially deforms the skin; when slip occurs, it does so first at the periphery of the contact region. Contact dynamics during the transition stage may inform the nervous system of a corrective behavior to adopt to maintain grip stability. These transitional events, however, have not yet been directly visualized.

While many authors have considered models of finger deformation under strictly normal finger loading (Kinoshita and Mori 1972; Phillips and Johnson 1981; Srinivasan et al. 1992; Fung 1993; Kim et al. 1994; Srinivasan and Dandekar 1996; Maeno et al. 1998; Cohen et al. 1999; Pawluk and Howe 1999a), composite loads that include significant tangential components are particularly relevant in the investigation of grip behavior. Few studies have evaluated the lumped biomechanical behavior of the fingertip. Nakazawa et al. (2000) characterized the lumped stiffness and viscosity of the human fingertip under tangential isometric loading, and Pataky et al. (2005) studied bulk relaxation after quasi-static loading. The micromechanical behavior of the skin was studied by Wang and Hayward (2007), who used miniature cantilevered benders to test the biomechanical properties of the fingerpad skin in vivo at a submillemetric scale. They found that the viscoelastic behavior of the skin under local tangential loading was strongly nonlinear, and that the skin became very stiff beyond a 50% strain. Significantly, these properties depended on the direction of the loading relative to the orientation of the ridges, suggesting that bulk behavior may be difficult to predict with any level of accuracy from global simulation studies. As a result, the most reliable method to analyze the properties of a realistic finger contact still remains direct observation (Tada et al. 2000; Levesque and Hayward 2003).

The conventional coefficient of friction, defined as the ratio of the tangential to normal components of a net interaction force, remains a convenient abstraction, even if it depends on many exogenous and endogenous factors in a contact pair. Skin hydration is perhaps the most important of those exogenous factors, since it depends both on physiological and environmental conditions (Naylor 1955; Nacht et al. 1981; Adams et al. 2007; Derler et al. 2007; André et al. 2009). We previously developed an apparatus that can continuously measure skin hydration during precision gripping behavior (André et al. 2008), and showed that subjects with naturally dry skin not only respond with a tighter grip to compensate for a reduced coefficient of friction, but clearly overcompensate. This observation suggested that lumped friction was not the sole factor considered by the CNS to provide a stable grip. It could be that the nervous system is sensitive to the skin micro deformations that occur before a full slip develops, and that these micromechanical events depend strongly on skin hydration. Here, we characterized the distributed skin deformation under composite loading to realistically assess the effect of hydration on slip onset.

Methods

Materials

Optical system:

We used an optical fingerprint recording technique based on the principle of frustrated total internal reflection. The apparatus included an intense diffuse light source, right-angle prism, and camera (Figure 2-1.A). Light propagated toward the 45° face of the prism where the fingertip was in contact. When there was no contact, light was totally reflected toward the camera, creating a bright, uniform image. When the fingerprint ridges were in contact with the prism, total internal reflection was frustrated, resulting in a high-contrast pattern of black ridges on a white background.

The optical system, originally developed by Levesque and Hayward (2003), used a 250 W halogen lamp as light source and a right-angle prism ($50 \times 50 \times 70$ mm) made of BK7 glass. A monochrome, progressive scan CCD camera (TM-6703, Pulnix America, Inc., Sunnyvale, CA) recorded the reflected images with 8-bit pixel depth and a resolution of 640×484 at 60 Hz. A zoom (Zoom 7000, Navitar Inc., Rochester, NY) allowed the system to focus on the region of interest from a distance of 15 cm. Images were acquired in streaming mode by a frame grabber (Meteor-II/Multi-Channel, Matrox Electronic Systems Ltd., Dorval, Canada) connected to a personal computer. Images were processed using Matrox Imaging Library (MIL) version 6.1. An electronic signal generated by the frame grabber at the onset of video recording allowed synchronization with force measurements.

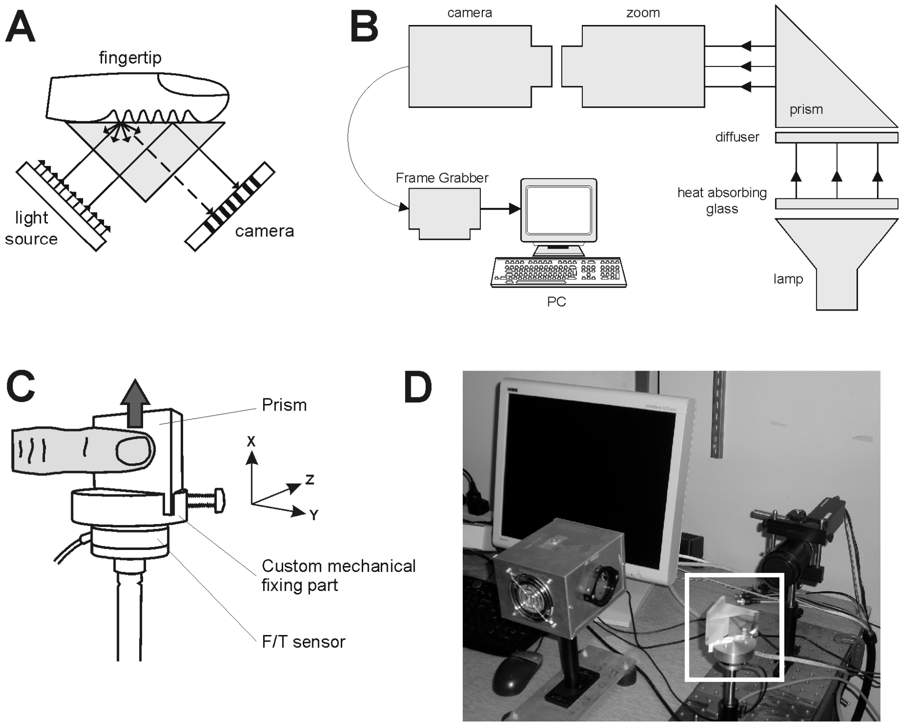

Figure 2-1: Adapted from Lévesque and Hayward (2003). A- Illustration of the principle of frustrated total internal reflection (FTIR) with a prism-based fingerprint imager. B- Illustration of the optical platform. The light source was directed toward the prism and the camera recorded the reflected light. C- Mechanical interface to record the forces applied to the prism. The task performed by the subjects is also illustrated. Subjects applied a constant normal force component and slipped in the indicated direction. D- Picture of the complete system.

Mechanical system:

The forces and torques applied to the prism were measured by a force/torque sensor (Mini40 F/T Transducer; ATI Industrial Automation, NC, USA) on which the prism was rigidly mounted (Figure 2-1.C,D). This setup allowed us to determine the three components of the interaction force, Fx, Fy, Fz, in the ranges ± 40, ± 40, and ± 120 N, respectively, with 0.01, 0.01, and 0.02 N resolution, respectively.

Skin hydration measurement:

Skin hydration was measured with a Corneometer® CM825, which operates using a capacitance principle. The probe comprises a 7-mm square ceramic tile with many closely spaced gold electrodes that act as capacitor plates. Electrodes are protected by a 20-µm-thick vitrified dielectric material. Measurements are given in arbitrary units ranging from 20 (very dry) to 120 (very moist). The Corneometer is fully described in Fluhr et al. (1999; 2000).

Experimental procedure

Ten healthy Caucasian subjects (from 20 to 30 years of age) participated in this study. Fifteen minutes before the experiment, subjects washed their hands with soap and water and the experimenter verified that their hands were rinsed and dried carefully. All subjects provided informed consent, and the experimental protocol was approved by the local ethics committee. Subjects were seated in front of the experimental setup and were instructed to apply a constant normal force on the imaged face of the prism with their right index fingertip. Visual feedback provided them with the normal force component actually exerted. The experimenter checked visually that the initial angle between the glass surface and their distal phalange was within 20 to 30 degrees. When the normal force was stabilized at a given level (specified by the experimenter), subjects performed an ulno-radial tangential slip (vertical arrow, Figure 2-1.C). The fingertip skin moisture was measured before and after each trial. Each subject performed five trials for six levels of normal force: 0.2, 0.5, 1, 2, 5, and 10 N.

Data processing and variables studied

The force transducer signals and the trigger signal from the CCD camera were acquired with a 12-bit 6071E analog-to-digital converter in a PXI chassis (National Instruments, Austin, TX, USA). The trigger signal allowed synchronization of the video frames with the force recordings. Force signals were low-pass filtered with a fourth-order, zero phase-lag Butterworth filter, which has a cut-off frequency of 10 Hz.

Image processing:

Optical flow is a technique commonly used in computer vision. Its simplest realization involves overlaying two or more frames taken at different instants in time (Zitova and Flusser 2003). This technique allows estimation of a displacement vector for each pixel of the original image, and registration of the two images into the same coordinate system. We compared each selected frame of the fingertip surface of contact (Im(t), Figure 2-2) to the previous frame (Im(t-1), Figure 2-2). The displacement vector was coded using a gray scale, where black indicated a null displacement and white indicated a displacement of 20 pixels. The optical flow computation revealed a contact region represented by a gray region on a black background, and a stuck region was represented by a black region within a gray region (Figure 2-2). Inside the contact region, the gray levels indicated the displacement gradient.

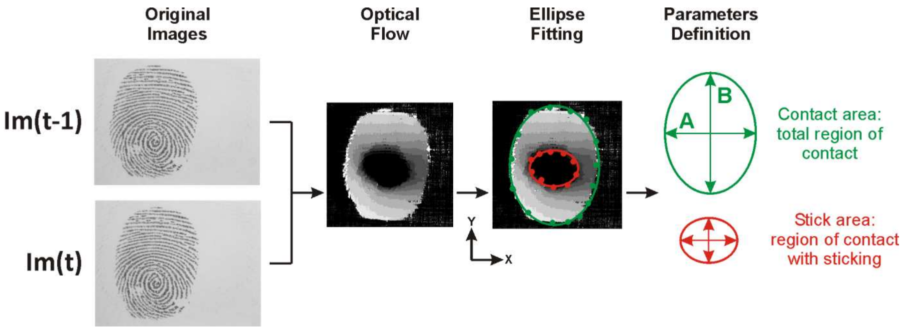

Figure 2-2: Image processing using the optical flow technique. By comparing two images, a gradient of displacement was estimated for each pixel. Black corresponds to zero displacement and gray levels correspond to the displacement magnitude (lighter color indicates greater magnitude). Ellipses were fitted to quantify the contact region (green ellipse) and the stuck region (red ellipse).

The Lucas-Kanade method (Lucas and Kanade 1981) was used to quantify displacement. Considering an image *F(x)* at time *t-1* and *G(x)* at time *t*, we sought vector *h* such that *G(x)=F(x+h)*:

$$h \approx \left[\sum_x \left(\frac{\partial F}{\partial x} \right)^T [G(x) - F(x)] \right] \left[\sum_x \left(\frac{\partial F}{\partial x} \right)^T \left(\frac{\partial F}{\partial x} \right) \right]^{-1}, \quad (1)$$

where $\frac{\partial}{\partial x} = \left[\frac{\partial}{\partial x_1} \frac{\partial}{\partial x_2} \right]^T$ in 2-D images. While *h* corresponds to the global displacement between two images, the displacement can also be estimated for any image portion. Further characterization of the different regions was done by fitting an ellipse at the outer border of each region. The experimenter selected at least 10 points on the border of the region to be quantified. The best-fitting ellipse was found using a least-squares criterion that minimized the sum of the distances between the 10 points and the curve (Figure 2-2, Ellipse Fitting).

Considering the ellipse equation:

$$ax^2 + bxy + cy^2 + dx + ey + f = 0\,, \qquad (2)$$

and letting $P = (a,b,c,d,e)$ be the vector of parameters to be estimated normalized to f, then

$$P = \sum(X)/(X^T X)\,, \qquad (3)$$

where X is a matrix of the form $\left(x^2\ xy\ y^2\ x\ y\right)^T$ of all the measurement vectors $\left(x\ y\right)^T$. We used this procedure to estimate the areas of the total and stuck contact regions.

Results

The temporal evolutions of the normal (NF) and tangential (TF) components of the interaction force for a typical trial are shown in Figure 2-3 (top). When NF applied to the prism by the index finger was stabilized around the target value, subjects ramped up TF during the preloading period (Figure 2-3, grey area) until slip fully occurred. At this point, the frictional force balanced TF and the magnitude of TF plateaued (Figure 2-3, black arrow). The synchronization feature of the apparatus allowed us to associate the TF and NF with each recorded frame (Figure 2-3, dashed lines). A set of seven frames 150-ms apart was used to calculate the optical flow that produced “optical flow images” (Figure 2-3, bottom), which are related to these force components. The area of the contact region varied little during the tangential loading period, while the area of the stuck region decreased significantly when TF increased. When slip was fully developed, as evidenced by optical flow processing (Figure 2-3, bottom right), TF no longer varied (Figure 2-3, top, black arrow).

Static characteristics of the contact area

The areas of the total contact region and stuck region were estimated for each optical flow image. The subjects had large anatomical differences, since the contact areas for each subject and for a 10-N normal force varied from 177 to 288 mm2 (Table 2-1).

Subjects	AC	AG	FH	GC	GT	MZ	RW	TA	VL	VM
Contact Area at 10N (mm²)	224	249	228	263	177	183	253	288	275	251

Table 2-1: Contact area of each subject when the normal force was 10 N.

To compare the results between subjects, the contact region areas were normalized to the largest contact area attained when NF was 10 N. Figure 2-4.A shows the relationship between NF and the normalized contact area when TF was zero. The normalized contact area increased logarithmically with NF. At 2 N, the contact surface was nearly 80% of its final value, and the contact area at 10 N was three times larger than that at 0.2 N. Thus, the contact area was sensitive to changes in NF at low values only, and was saturated at high values.

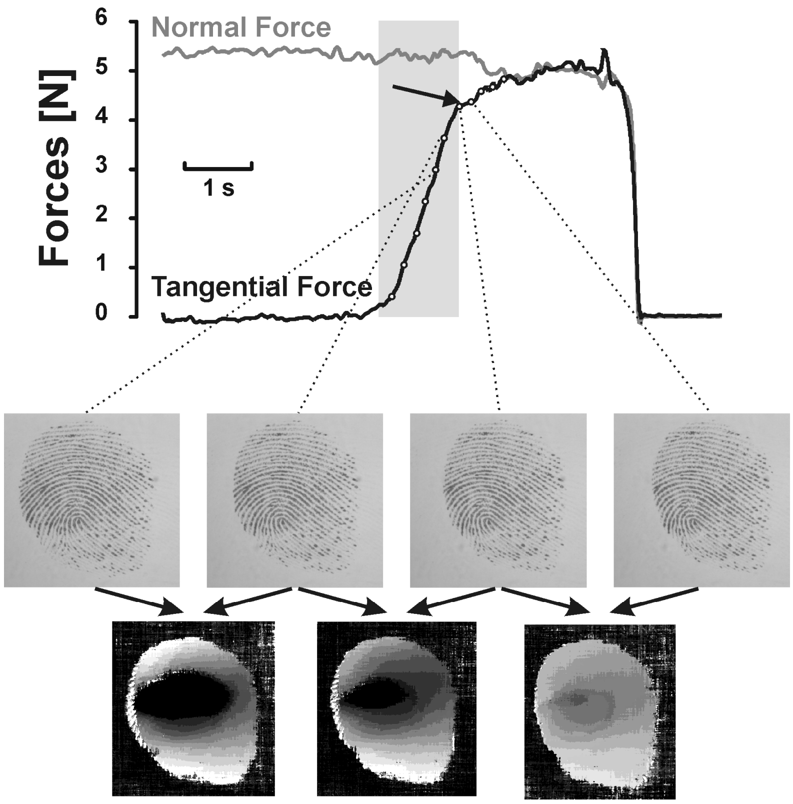

Figure 2-3: Time course of the normal and tangential force components in a typical trial, associated frames, and "optical flow images". During the tangential preloading period (grey box), the tangential force component increased until slip occurred (black arrow, top). Frames were selected during the preloading phase and compared to obtain optical flow images. The contact area is not correlated to the tangential force. The stuck area decreased when the tangential force component increased.

A typical time course of the normalized contact area for subject TA at a constant NF of 5 N is shown in Figure 2-4.B (black dots). The normalized contact area decreased moderately over time until it reached a constant value, which corresponded to the normalized contact during full slip. The decrease in the contact area correlated with fingertip skin loading in the direction of movement (Figure 2-2). During slip, there was very little variation in the contact area.

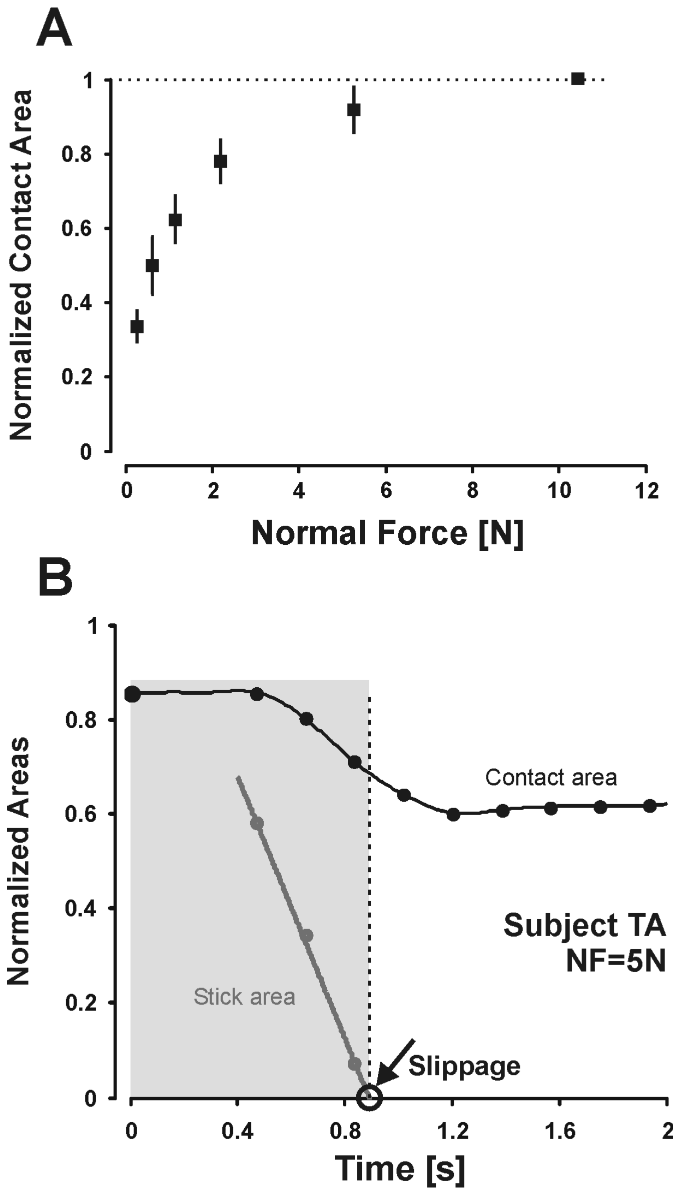

Figure 2-4: A- Normalized contact area increased logarithmically with the normal force component. The normalized contact area was defined as the ratio between the contact area and the contact area for a normal force of 10 N. Each data point corresponds to the mean normalized contact area across all subjects. Standard deviations (vertical lines) are plotted around the corresponding means. B- Typical trial showing the time course of the normalized contact area (black dots and curve) and the normalized stick area (grey dots and curve) for one subject applying a normal force component of 5 N. When the stuck area vanishes, slip is fully developed (circle and dashed line). The grey box corresponds to the tangential preloading phase.

Lumped dynamics of the contact

Figure 2-4.B shows the time course of the normalized stick area (grey dots and line). During the preloading phase (grey zone, Figure 2-3, top) when TF increased, the area of the stuck region decreased linearly until it reached zero (Figure 2-4.B), at which point full slip occurred. Since it is a fundamental property of friction that adhesive forces are smaller than friction forces once the transients have settled, the measured interaction force must correlate with the stick ratio, SR, of the areas of the stuck region and the contact region:

$$SR=\frac{\text{stuck area}}{\text{contact area}}, \tag{4}$$

which varies from 1 (unloaded contact) to 0 (fully slipping contact). We averaged the SR and hydration levels from five consecutive trials for each subject and for each value of NF. Interestingly, the hydration level did not vary significantly over the five trials (standard deviation = 5 a.u.). This was also the case for each individual subject.

Normal Force [N]	0.2	0.5	1	2	5	10
Slope	-1.81 ± 0.47	-1.29 ± 0.43	-0.85 ± 0.27	-0.44 ± 0.12	-0.31 ± 0.10	-0.19 ± 0.06

Table 2-2: Mean value (± SD) of the slope of the linear relationship between tangential force and stick ratio, for each level of normal force across all subjects.

Since SR captures the contact state by a single number, one can relate the contact state to TF (Figure 2-5). Figure 2-5.A and B display the results from two subjects with obvious skin differences for NF values of 0.5 N or 5.0 N. Subject AG (green trace) had dry skin (mean hydration = 49 a.u.), while subject GC (blue trace) had moist skin (mean hydration = 110 a.u.).

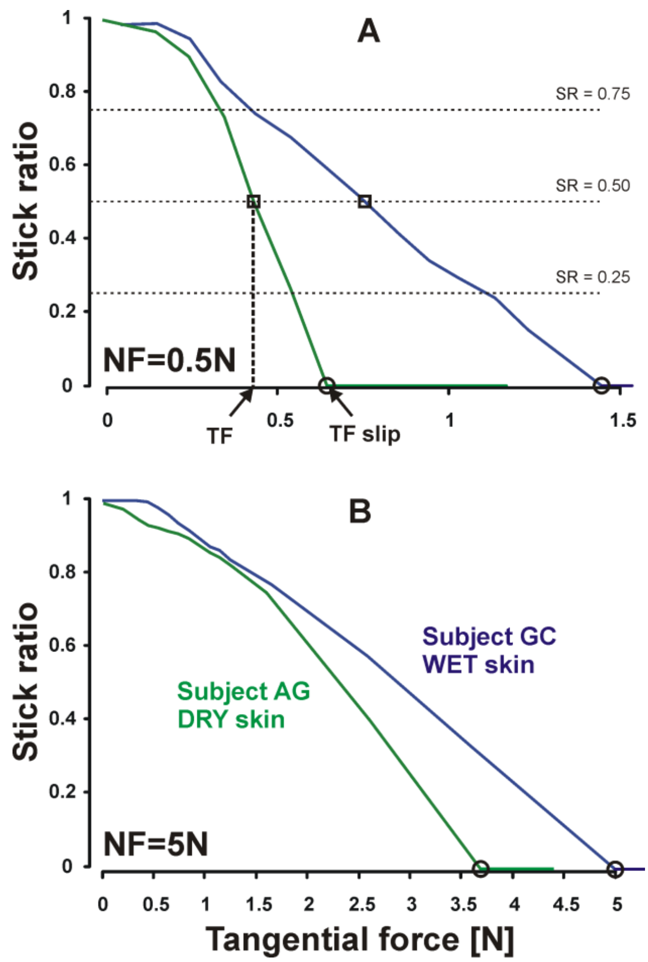

Figure 2-5: Relationship between the stick ratio and the tangential force for two subjects with very different hydration levels (green or blue curves) and for two normal forces (0.5 N, A, and 5 N, B). Each curve corresponds to the mean of 5 trials for a given subject and a given normal force. A- The horizontal dashed lines underline three stick ratio values (SR = 0.25, 0.5 or 0.75). The tangential force component is found where the lines cross the curves (e.g., for SR = 0.5, black squares). The tangential force component when full slip occurs is found when the stick ratio is zero (black circles). B- Colors are associated with subjects: green trace for subject AG who had the driest skin and blue trace for subject GC who had the wettest skin.

The lowest TF magnitudes were not correlated to SR. However, with higher TF magnitudes, SR decreased almost linearly with TF, and the decay rate strongly correlated to the hydration level, especially at low NF values. This effect was quantified by computing the linear regression that fit the data for SR < 0.8. Table 2-2 shows the mean slope across all subjects for different NF values. The results confirm the strong influence of the normal contact loading.

Effect of hydration

The effect of skin hydration on the finger contact dynamics can also be evaluated by comparing the relative increase in TF before slippage. Figure 2-5, shows with black squares the TF magnitudes for an SR of 0.5. Hydration levels could then be associated to the TF during full slip, i.e., SR = 0 (Figure 2-5.A and B, black circles). The ratio between TF and the ultimate tangential force component (TFslip) indicates the sensitivity of a contact to a disturbance. Figure 2-6 shows the effect of hydration on the quantity TF/TFslip at different points of a developing slip (SR = 0.25, 0.5, or 0.75).

The data is from all subjects and all NF values. On average, TF/TFslip increased as SR decreased: the sensitivity of the contact decreased when it was closer to full slip. TF/TFslip also decreased with hydration for all three SR values: dry skin always corresponded to grips that were more sensitive to disturbance. The linear regressions fitting the data were all significant (P < 0.01; $r^2 = 0.42$ for SR $= 0.25$ or 0.5, $r^2 = 0.27$ for $\text{SR} = 0.75$). Considering SR = 0.5 (when half of the contact region is sticking), at a low level of hydration the quantity TF/TFslip is ~ 0.9. This value decreases to 0.6 for a high level of moisture. Thus, when hydration is low, a 10% disturbance in tangential loading can provoke slip, whereas a 40% increase is needed to achieve the same result in well-hydrated skin. At any point of a developing slip, the higher the skin hydration is, the further the skin is from full slip. This observation holds true regardless of the NF value.

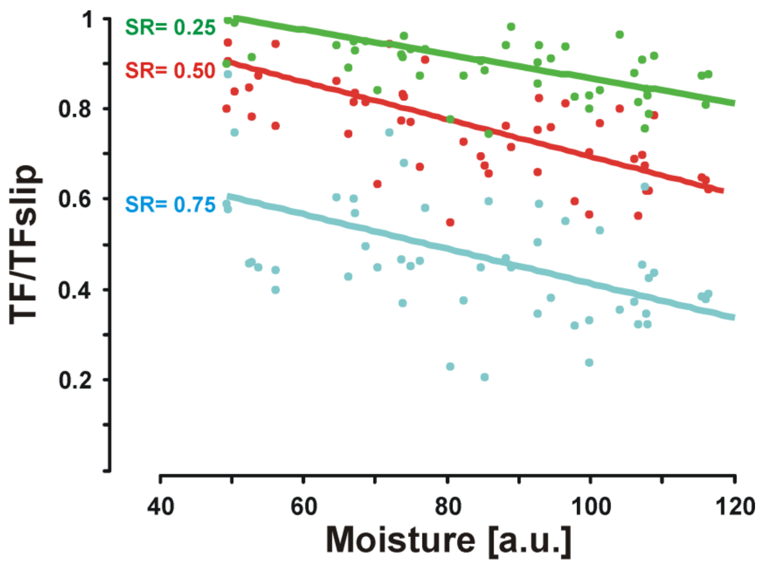

Figure 2-6: Effect of moisture on the ratio TF/TFslip for three stick ratios (SR = 0.25 in green, SR = 0.5 in red, and SR = 0.75 in blue). All subjects and all normal forces are represented. Each data point corresponds to the mean ratio TF/TFslip and moisture level for one normal force component value across the five trials and for a given stick ratio.

Discussion

This study showed that skin hydration profoundly impacts the finger contact dynamics. Previous studies considered only the effects of normal loading. Here, skin surface deformation under tangential loading was imaged, and we observed how the contact transition from adhesion to slip varied as a function of skin hydration. To quantify this effect, we first evaluated the amount of skin undergoing slip relative to the total contact region. As predicted by the laws of friction, the tangential force component TF reached a maximum when the entire contact surface slipped. More significantly, skin hydration strongly impacted the relative increment of tangential loading available before a complete slip developed, regardless of the normal force component NF and regardless of the contact state. In all cases, the greater the skin hydration magnitude was, the further the contact was from slipping.

The notion of incipient slip

Johansson and Westling (1984b) described the importance of the cutaneous sensory feedback in precision grips. They showed that the nervous system adapts the grip force as a function of object friction properties. They hypothesized that continuous tactile feedback arises from partial slips, termed "incipient slips", occurring at the periphery of the contact region. However, few studies have quantified this effect. Tada et al. (2006a) introduced the SR to quantify the contact state, and presented experimental data that were similar to ours: the SR decreased linearly when tangential loading increased. However, these authors tested proximo-distal finger movements with normal force components ≤ 1.5 N, and did not control for skin hydration. In the present study, we used ulno-radial movements that are more relevant to gripping behaviors, a much larger force range, and measured skin hydration. These factors are all significant to dexterous manipulation.

Incipient slips are widely used in robotics to develop robots that can dynamically adapt the grasp force to objects properties (Tremblay and Cutkosky 1993; Maeno et al. 2000; Tada et al. 2002; Edin et al. 2008).

Tremblay and Cutkosky (1993) made a robotic finger that had an artificial skin covered with "nibs" that formed local contact regions and could slip independently. When partial slip occurred, some "nibs" located peripherally emitted a vibration that was used to adapt the gripping force. Maeno et al. (2000) described an artificial skin with strain gauges bonded to phosphor bronze plates embedded in silicon rubber. Incipient slip was detected from the relative displacement of each plate. They showed that broad contact conditions (non-contact, slip, or stick) varied with the normal and tangential force components. Recently, Edin et al. (2008) developed an artificial tactile system with miniature strain gauges embedded in a biomechatronic hand that provides rich information during manipulation tasks, including slip information between the fingertip and an object.

<u>The effect of hydration</u>

For equivalent contact states (encoded by SR), we found that the contact safety margin increased when skin hydration increased (at least when touching a glass surface), regardless of the normal loading. This result contributes to our understanding of motor behavior when grasping or manipulating objects. Smith et al (1997) observed that people who were administered scopolamine spontaneously employ higher grip forces. Scopolamine reduces skin hydration through reduced sweat gland activity, which in turn modifies the finger/object frictional interaction. Recently, we demonstrated a causal relationship between skin hydration and grip force (André et al. 2010). Subjects with a dry skin spontaneously employed a greater grip force. Other factors were also involved, since subjects with dry skin systematically overcompensated for a frictional reduction by exerting very large grip forces. This behavior could not be explained solely by a reduction in the coefficient of friction. In the light of the present results, we speculate that the CNS ”knows” that when the skin is dry, a small disturbance could have a large effect unless the gripping force is exaggeratedly large. In terms of the time course of the motor commands needed to produce a stable grip, dry skin reduces the “time-to-slip,” making the grip potentially even more unstable.

It is possible to speculate on the mechanisms contributing to the global effect we observed. There are at least three distinct yet related phenomena. First, moist skin is more flexible than dry skin (Adams et al. 2007). As a result, the bulk dynamics of deformation are faster with dry skin, making it harder for the nervous system to sense them for corrective action. Second, hydration could have mechanical consequences at the scale of the ridges. Glabrous skin ridges determine the “effective contact area” inside a contact region (Warman and Ennos 2009). A moist, softer skin could reasonably provide a larger effective contact area than dry skin for the same contact region, increasing net friction. Third, the superficial, keratin-based, fibrous skin layers present strong affinity for endogenous or exogenous water, modifying skin mechanical behavior at the microscopic scale. Interfacial microscopic stress distributions are probably strongly dependent on the presence or absence of water, especially during interactions with smooth surfaces (Persson et al. 2008).

Perspectives

The experiment presented here was performed using active touch. Subjects exerted a force with their index finger and used visual feedback to regulate the normal component. They performed the task adequately, leading to a standard deviation of the normal component that was < 20% of the mean, even during the preloading phase. The spontaneous preloading period was nearly constant (~700 ms) suggesting another type of compensating motor behavior. To control these factors, in future studies the subjects' fingers should be stimulated by a servo-controlled apparatus where all the mechanical variables could be regulated independently, including the slip velocity. Nevertheless, the mechanics of interaction should be studied together with spontaneous, task-oriented motor behavior.

Conclusion

Skin hydration modifies the skin deformation dynamics during grip-like contacts. Certain motor behaviors observed during object manipulation could be explained by the effects of skin hydration. We suggest that the overcompensation strategy seen when skin is dry could be explained by important variations in the contact dynamics as a function of skin hydration.

Chapter 3

MOISTURE EVALUATOR: A DIRECT MEASURE OF FINGERTIP SKIN HYDRATION DURING OBJECT MANIPULATION

"The only trophy we won this day, was the blood and sweat we left on the pitch.... and it was enough"

Published as: T. André, M. De Wan, P. Lefèvre and J-L. Thonnard. **Moisture Evaluator: a direct measure of fingertip skin hydration during object manipulation.** Skin Research and Technology (2008) 14:385-389.

Abstract

The mechanical properties of the fingertip skin are very important when studying dexterous manipulation. These properties are strongly influenced by the level of skin hydration. Currently, there is no device capable of measuring skin moisture during object manipulation. Skin moisture levels during object manipulation were measured using the

Moisture Evaluator, a probe consisting of gold-covered electrodes connected to a resistor-capacitor circuit. *In vivo* calibration was performed by comparison with measurements obtained using a Corneometer® at two normal force levels (0.2 N and 2 N). Measurements from the Moisture Evaluator were well correlated with those from the Corneometer®. A new device for evaluating skin moisture at the fingertip has been designed and validated.

Introduction

Moisture influences the properties of the skin, particularly the coefficient of friction (CF). During dexterous manipulation, changes in skin hydration modulate the mechanical properties of the finger/object interface and alter the minimum pinch force required to avoid slipping of the object. Previous studies have investigated the influence of moisture on skin friction properties. Buchholz et al (1988) reported a significant interaction between the texture of the grasped object and moisture. Smith et al (1997) found that scopolamine increased prehensile force as a consequence of reduced palmar sweating. In the same way, Johansson and Westling (1984b) showed that the variation in CF induced by different levels of skin hydration resulted in behavioral differences during manipulation. These studies have demonstrated the important effect of moisture on the properties of the finger/object interface. An online measurement of moisture at the fingertip would therefore be of major interest to those investigating the role of skin properties in object manipulation.

Skin moisture is a very important parameter in other contexts as well. The fields of cosmetics and dermatology are two areas in which skin hydration is of primary interest. This has motivated the development of various devices to evaluate the moisture content of the skin. Several studies have made a quantitative comparison across different devices measuring skin moisture (Fluhr et al. 1999; Heinrich et al. 2003; Alanen et al. 2004). The effect of moisturizers and creams has also been evaluated (Fluhr et al. 2000) in order to compare different methods of skin hydration.

The moisture level of the skin is typically measured using one of two principles: capacitance or conductance. Application of these two principles is easy to understand if one considers a simple electrical model of the skin as a resistor in parallel with a capacitor. Because the value of both components is influenced by the water content of the skin, either the resistive component or the capacitive component may be measured. The geometry of the probe electrodes, the frequency of the current, and the design of the oscillating electronic circuit must be adapted to suit the desired measurement principle (Lévêque and de Rigal 1983). Barel et al. (1997) evaluated two commercial devices, each based on one of these principles: the Corneometer® (capacitance) and the Skicon-200 (conductance). They found a good correlation between the methods, with a lack of sensitivity at low levels of hydration for the conductance method and a lack of sensitivity of the capacitance method at very high levels of hydration. Other devices such as the SkinChip, the MoistureMeter, the Nova DPM 9003, and the Dermalab have been tested, calibrated and are well referenced (Fluhr et al. 1999; Leveque and Querleux 2003; Alanen et al. 2004). However, due to the size of the probe, none of these commercial devices enable measurement of skin hydration during object manipulation.

In this study, we present a simple and inexpensive instrument to measure the moisture level of the skin. This device, called the Moisture Evaluator, is based on the conductance principle and is specifically designed for the determination of skin hydration at the fingertip during object manipulation.

Methods

<u>Apparatus</u>

The Moisture Evaluator:

The Moisture Evaluator is designed to measure the conductance of the skin surface. The measuring probe (Figure 3-1.A) has a moderate surface area (12 cm^2) and weight (5 g). It consists of 56 gold-covered electrodes (spacing =0 .89 mm; width = 0.25 mm). The electrodes are alternately connected in a "comb" configuration. There is a direct galvanic contact between the electrodes and the skin. In order to measure the normal force exerted on the probe during the measurement and to assess its influence on the measurement, the probe is fixed on a force-torque transducer (Mini40 F/T transducer, ATI Industrial Automation, NC, USA). The sensing range for the normal force is +/- 120 N with 0.06 N resolution.

The measurement of conductance is based on a resistor-capacitor circuit. The electronic diagram is presented in Figure 3-1.B. In this diagram, R_X represents the combined equivalent resistance of the probe and the finger. Inside the Moisture Evaluator is a capacitor C (11 nF) that is charged and discharged at a frequency dependent on R_X. A switch within the NE555 oscillator controls the charge of the capacitor: depending on the capacitor voltage (Uc), the switch is either open (charging) or closed (discharging).

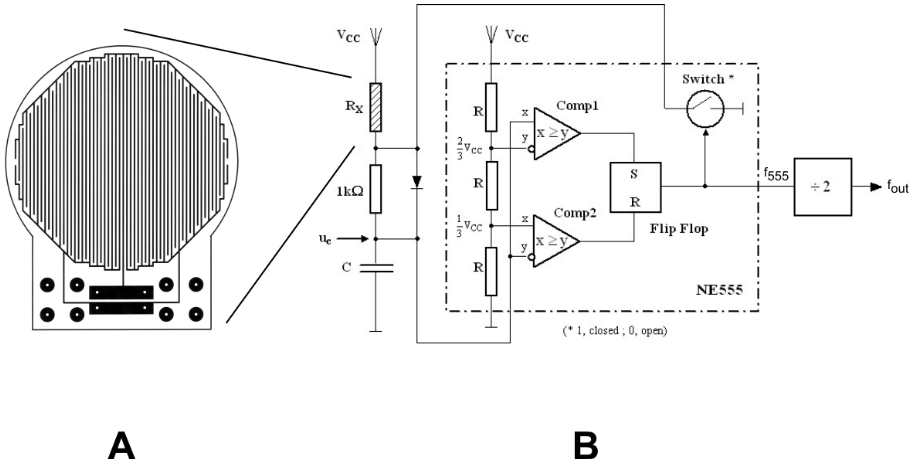

Figure 3-1: A- Network of electrodes that constitutes the probe of the Moisture Evaluator. B- Diagram of the electronic circuit measuring the conductance of the probe (represented by Rx): Vcc is the supply voltage, NE555 is the oscillator that controls the switch by comparing Uc with a reference voltage, C is the capacitor that is charged and discharged and Rx is the impedance of the probe (influenced by skin moisture). The frequency of the output signal depends on the charging time of C, which is influenced by Rx.

The capacitor voltage evolves differently during these two phases. When the capacitor is charging, Uc increases from 1/3 Vcc to 2/3 Vcc with a time constant of τ_{ch}. The output logic signal of the NE555 (f_{555}) is low and the capacitor obeys the following equation:

$$U_C = V_{CC}(1 - e^{-\frac{t}{\tau_{ch}}}) \qquad (1)$$

When the capacitor is discharging, Uc decreases from 2/3 Vcc to 1/3 Vcc with a time constant of τ_{de}. The output logic signal of the NE555 (f_{555}) is high and the capacitor voltage is described by:

$$U_C = V_{CC} e^{-\frac{t}{\tau_{de}}} \qquad (2)$$

The time constants (τ_{ch} and τ_{de}) can be easily determined. During the charging phase, the 1kΩ resistor is shunted (via the diode), the capacitor charges through R_X and the time constant $\tau_{ch} = R_X C$. During the discharging phase, the capacitor discharges through the 1kΩ resistor and the time constant $\tau_{de} = R_{1k\Omega} C$.

Considering the duration of the charging phase T_{ch} and the duration of the discharging phase T_{de}, it has been calculated that $T_{ch} = \tau_{ch} \ln 2$ and $T_{de} = \tau_{de} \ln 2$. The output signal of the NE555 is an asymmetric periodic signal with the frequency

$$f_{555} = \frac{1}{T_{ch} + T_{de}} = \frac{1}{(\tau_{ch} + \tau_{de})\ln 2} \cong \frac{1.44}{(R_X + R_{1k\Omega})C} \quad (3)$$

The last stage of the circuit is a frequency divider that is switched at each rising edge. This converts the logic signal to a symmetric square wave to prevent potential acquisition problems. The frequency of the Moisture Evaluator output signal is

$$f_{out} \cong \frac{1.44}{(R_X + R_{1k\Omega})C} \times \frac{1}{2} \quad (4)$$

Therefore, this frequency is a direct measure of the value of the resistance R_X.

The Corneometer® CM 825:

In this study, the Corneometer CM825 was used as a reference device. The Corneometer® has gained worldwide acceptance as an efficient and reliable instrument to measure the water content of the stratum corneum (O'goshi and Serup 2005).

The Corneometer is based on the capacitance principle and operates at a mean frequency of 1 MHz: 1.15 MHz - very dry ; 0.9 MHz – very hydrated (Fluhr et al. 1999). The probe consists of a 7 x 7 mm ceramic tile with many closely-spaced gold electrodes which function as capacitor plates (Fluhr et al. 2000). The electrodes are covered with a vitrified dielectric material of 20 µm thickness (Barel and Clarys 1997). This glass layer prevents any galvanic contact between the electrodes and the skin. The Corneometer is sensitive to the variable dielectric constant of the skin (in contact with the glass layer) which increases with the water content of the stratum corneum. A minimum pressure of 0.8 N is required to trigger the measurement. The measurements are given in arbitrary units (a.u.) ranging from 0 (very dry) to 120 (very wet).

<u>Experiment:</u>

Ten healthy Caucasian subjects (five women and five men) participated in this study. Fifteen minutes before the experiment, subjects were asked to wash their hands with soap and water. The experimenter verified that the hands were rinsed and dried carefully. The probes of both instruments (Moisture Evaluator and Corneometer®) were cleaned with alcohol and ether.

As illustrated in Figure 3-2, the experimenter measured the moisture of the fingers alternately with the Corneometer® (Figure 3-2.A) and the Moisture Evaluator (Figure 3-2.B). Twenty pairs of measurements were obtained at two levels of normal force exerted on the probe of the Moisture Evaluator (0.2 and 2N).

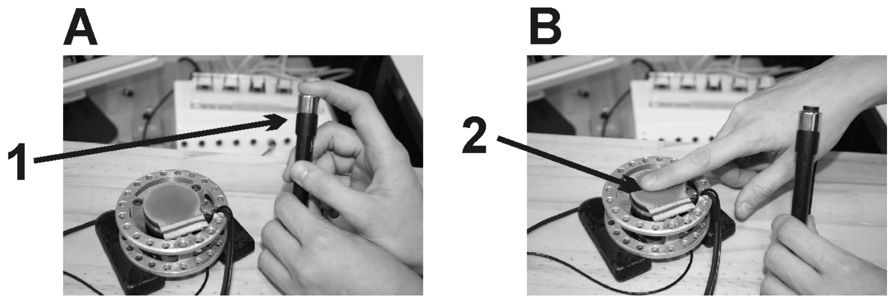

Figure 3-2: A- Measurements of fingertip moisture with the Corneometer (1). B- Measurement of fingertip moisture with the Moisture Evaluator (2) attached to the ATI force transducer.

Data processing

The conductance was determined using a frequency measurement. A higher frequency signal represented increased water content at the skin surface. The frequency of the signal was recorded and reported on a logarithmic scale. For this reason, the output of the Moisture Evaluator is expressed in a.u. corresponding to the logarithm of the measured frequency (expressed in Hz).

All statistical analyses were performed using the Statistica® software package. The coefficients of determination (R^2) of linear regressions were calculated to assess the correlation between the different measures. The analysis of covariance and the homogeneity-of-slope model have been used to evaluate the influence of normal force on the Moisture Evaluator measurements.

Results

Figure 3-3 presents the relationship between the Moisture Evaluator and the Corneometer® measurements. The coefficients of determination are large and the correlation is highly significant (0.2N: R^2 = 0.78, $P < 0.01$; 2N: R^2 = 0.83, $P < 0.01$).

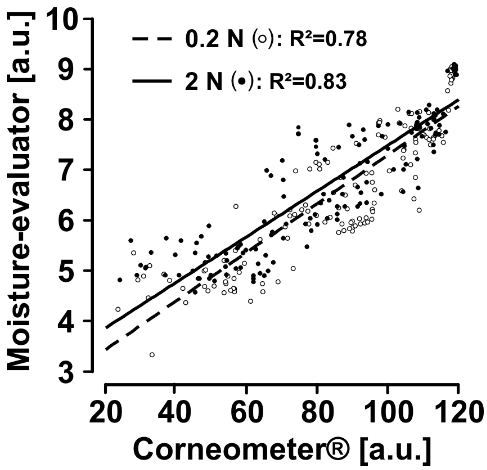

Figure 3-3: Relationship between Corneometer® and Moisture Evaluator measurements. Two levels of normal force exerted on the Moisture Evaluator are presented, 0.2 and 2 N.

The analysis of covariance and the homogeneity-of-slope model have been evaluated considering the Moisture Evaluator measurement to be the dependent variable, the Corneometer® measurement to be the continuous predictor, and the normal force exerted (0.2 - 2 N) to be the categorical predictor. The analysis of covariance indicated that the normal force had a significant effect ($P < 0.01$) on the parameters of the two regressions. However, the slopes of both regression lines were identical. Indeed, the homogeneity-of-slope model indicated that the normal force does not have a significant effect ($P > 0.05$) on the slope of the relationship between the Corneometer® and the Moisture Evaluator. A significant increase in the normal force (from 0.2 to 2 N) induced a moderate offset of the Moisture Evaluator measurements (average increase of 0.28 a.u.).

Discussion

In this study, we were interested in developing, testing and validating an original device to measure the moisture level of the fingertip skin during object manipulation. The Moisture Evaluator was designed to utilize the conductance principle and has been compared with the Corneometer®. For the two normal forces tested, the correlation between the measurements from both instruments was strong (0.2 N: $R^2 = 0.78$; 2 N: $R^2 = 0.83$). The coefficients of determination in our study were even higher than those obtained in previous studies comparing different moisture sensing devices (Fluhr et al. 1999; Alanen et al. 2004; O'goshi and Serup 2005). The Moisture Evaluator can be considered to be a well designed system to measure the moisture at the skin surface.

Moisture measurements were compared over the entire range of the Corneometer® (from 20 to 120). This range corresponds to Moisture Evaluator readings between 4 and 10. Figure 3-3 highlights the reduced sensitivity of the Moisture Evaluator for moisture values below 40 (dry skin) on the Corneometer® scale. This is compatible with the observation that the sensitivity of the conductance method is poor for low levels of hydration (Barel and Clarys 1997) and reaches a plateau for that range of moisture, because there is little change in conductance when the skin has a low level of hydration (Sekiguchi et al. 2001). Figure 3-3 also illustrates the improved sensitivity of the Moisture Evaluator at high levels of hydration. When the values measured with the Corneometer® exceed 115, the output of the Corneometer® saturates (at the maximum reading of 120) whereas the Moisture Evaluator still responds to moisture differences.

In this study, we compared two levels of normal force (0.2 and 2N) to assess whether a larger normal force improved the electrical contact between the skin and the electrodes, increasing the conductance and skewing the Moisture Evaluator output. The analysis of covariance demonstrated that the force exerted on the probe exerts an influence on the value of the measurement for the Moisture Evaluator. However, the homogeneity-of-slope model indicated that the slopes of the two curves were not statistically different. Therefore, one can consider that a variation of the normal force will only introduce a moderate offset in the measurements of the Moisture Evaluator. Indeed, we found that the mean offset between the two populations was 0.28 which corresponds to only 4.6% of the full range of measurement, suggesting that the influence of the normal force is minor.

The importance of the coefficient of friction (CF) in dexterous manipulation has been emphasized by numerous authors (Johansson and Westling 1984b; Srinivasan et al. 1990; Cadoret and Smith 1996; Augurelle et al. 2003b). Moreover, the influence of moisture on the CF has also been demonstrated. This influence has been studied by comparing only extreme conditions (dry and wet) without measuring a precise value of moisture on a numerical scale (Comaish and Bottoms 1971; Buchholz et al. 1988; Adams et al. 2007). The Moisture Evaluator may enable a major breakthrough by providing an on-line measurement of the moisture at the skin surface of the finger and its influence on CF. The Moisture Evaluator accomplishes this by coupling the probe electrodes to the same force/torque sensor used in dexterous manipulation, allowing the on-line acquisition of moisture measurements during object manipulation experiments.

The minor influence of the normal force on the Moisture Evaluator measurements (described above) is of prime importance when studying fine manipulation. Indeed, when an object is held and moved, the normal pinch force varies and is modulated with changing tangential load constraints. Moreover, the occlusion occurring at the interface between the fingers and the object being held influences the skin hydration and therefore the mechanical properties, making an online measurement of moisture at the fingertip during manipulation highly desirable.

The Moisture Evaluator enables the measurement of the water-content of the skin surface during the manipulation of objects. It consists of a simple, inexpensive, and adaptable tool. The probe shape and low weight facilitates easy attachment to a force sensor, permitting synchronous recording of moisture levels and mechanical force measurements.

Chapter 4

A Continuous Measure of Fingertip Friction during Precision Grip

"A forward's usefulness to his side varies as to the square of his distance from the ball. "

Clarrie Gibbons

Published as: T. André, P. Lefèvre and J-L. Thonnard. **A Continuous Measure of Fingertip Friction during Precision Grip.** Journal of Neuroscience Methods (2009) 179: 224-229.

Abstract

When humans manipulate an object, the minimal grip force required to avoid slipping depends on the frictional properties between the fingers and the object. As a consequence, fingertip skin friction plays a critical role during object manipulation. Here, the effects of the normal force and moisture content on the skin's static coefficient of friction (CF) for human fingertips were studied. Ten subjects were asked to pinch an object with a given normal force. Slippage of the object on the fingertips was generated for different ranges of normal force using a linear translation stage. The exerted forces and moisture of the fingertips were then measured, and the static coefficient of friction was calculated as the ratio between the tangential force and normal force at slippage. These results demonstrate that the effects of the normal force and moisture content on the CF exhibit a complex interaction. For a given moisture condition, the CF varies as a power function of the normal force; in contrast, for a given normal force, the CF is described by a “bell-shaped” function of moisture. A global expression of the CF as a function of the normal force and moisture content is derived, and a method is proposed for a continuous measure of the CF. This new method shall be of particular interest in investigating dexterous manipulation.

Introduction

Precision grip allows humans to manipulate small and/or delicate objects. In this grip configuration, the object is held between the thumb and index finger. The grasp stability is ensured by a close coordination of the forces exerted on the object by the tips of the fingers: the grip force (GF) applied normal to the object’s surface must be sufficient to counteract both the gravitational and inertial components of the tangential load force (LF) (Johansson and Westling 1984b). During tasks of precision manipulation, the grip force must be well adapted with load force variations in order to avoid slipping of the object (Flanagan and Tresilian 1994) but also to avoid damaging the object or muscle fatigue. Moreover, it has been shown that adjustments of the normal grip force anticipate tangential load force changes, provided that the physical properties of the object are predictable (Flanagan and Wing 1993; 1995). Several studies (Westling and Johansson 1984; Flanagan et al. 1995; Cadoret and Smith 1996) have pointed out that the static coefficient of friction (CF), as well as the weight and the grip configuration (McDonnell et al. 2005), are primary factors when studying object manipulation. Indeed, the minimal grip force required for the object not to slip is key to understanding human performance and is directly related to the CF (Westling and Johansson 1984).

The static coefficient of friction is defined as the ratio between the tangential force and normal force when slipping first occurs (Bowden and Tabor 1982; Blau 2001). Earlier studies found that the force of friction was directly proportional to the applied load and was independent of the contact surface. This is known as Amontons' law, indicating that the CF is a constant for two given surfaces. However, Comaish and Bottoms (1971) showed that this law does not hold for the skin and, more specifically, for low values of the normal force (<3.5 N). This study demonstrated a relationship for the CF between the skin and a probe that closely follows a negative power function and depends upon the applied normal force. Several subsequent studies have further characterized this relationship (Wolfram 1983; Koudine et al. 2000; Sivamani et al. 2003) for different body parts, such as the forearm or dorsal side of the finger.

Moisture is another factor that influences the CF between the skin and object. The effect of water on the skin has already been described in several studies (Comaish and Bottoms 1971; Buchholz et al. 1988; Adams et al. 2007). In particular, Adams et al. (2007) observed that the skin's friction actually increases in the presence of water and decreases during the subsequent drying period. Derler et al. (2007) quantified the moisture content of the skin with a commercial device named the Corneometer (Fluhr et al. 2000) and studied the dependence of the friction coefficient on the applied normal load for moist and dry skin. They found a strong increase in CF with moisture and suggested that further investigations with human subjects were needed to study the influence of skin hydration on friction in detail. Indeed, none of these previous studies precisely and continuously quantified the moisture of the skin with an adequate sensory probe. Moreover, when manipulating objects, an occlusion occurs at the finger/object interface. As a consequence, the moisture content and thus the CF vary during the task (Fluhr et al. 2000). It is therefore crucial to measure the moisture of the skin continuously during manipulation tasks in order to better understand the role of the CF in grip force control.

Different techniques have been used in the past to estimate the static coefficient of friction (Turrell et al. 2001). The most widespread approach in dexterous manipulation involved asking subjects to slowly separate the thumb and index finger until an object dropped. Using the ratio of the TF/NF when slipping was initiated, the CF could be estimated. As a consequence, this technique implied to evaluate CF before and/or after performing an object manipulation task. However, CF varies over time during object manipulation. In the present paper, we studied two variables that influence CF and we provide a method to measure CF continuously during a precision grip task. The influence of both the normal force and moisture content on the static coefficient of friction between the skin and object surface suggests that both of these factors must be taken into account when studying the CF. Indeed, the normal force and moisture content vary during a dexterous manipulation; consequently, the CF must vary as well. The CF between the fingertip and object should not be evaluated *a priori* but instead continuously estimated by considering the varying normal force and moisture. This paper studies the combined effects of both factors on the CF, and we obtain a global relationship between these three variables. A general analytical expression of the CF that depends on both the normal force and moisture content is reported, and this expression is used to propose an original method for a continuous estimation of the CF during precision grip.

Materials and Methods

Ten healthy Caucasian subjects (five women and five men) participated in this study. Their ages ranged from 20 to 53 years. All subjects provided informed consent, and the experimental protocol was approved by the local ethics committee.

Apparatus

The mechanical system used in the experiment is illustrated in Figure 4-1. A linear translation stage (NLS4 Series Precision Linear Stage, 6'' Travel, Newmark System Inc, CA, USA) controlled the displacement of a base, which in turn compressed two springs. The compression generated a vertical force on an object held in a precision grip by the participants. This object included two force/torque transducers (Mini40 F/T transducer; ATI Industrial Automation, NC, USA) and two moisture sensor probes. Each force/torque transducer measured the normal (NF, z-axis) and tangential force (TF, y-axis) at the interface with the thumb or index finger. The sensing ranges for the TF and NF were ±40 N and ±120 N with 0.01 N and 0.02 N nominal resolutions, respectively.

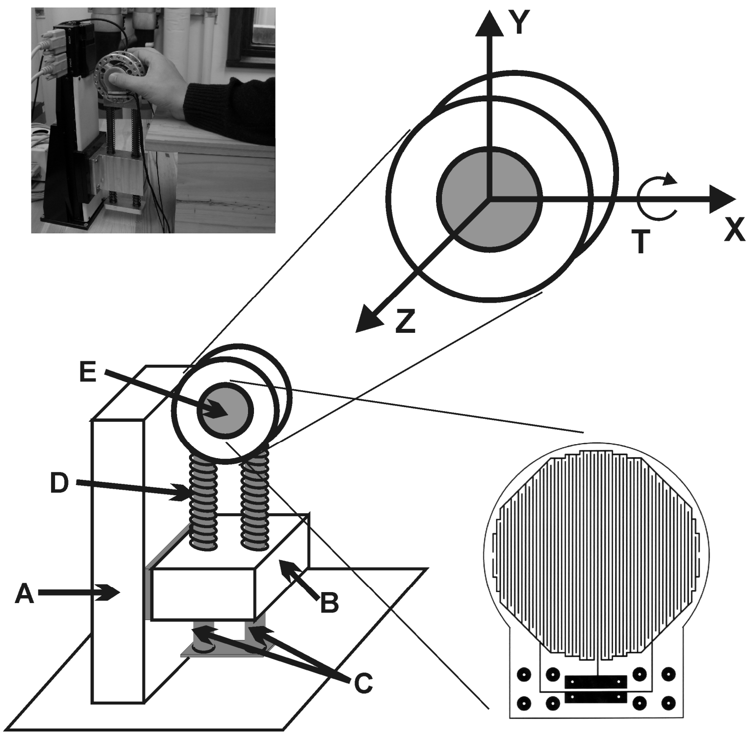

Figure 4-1: A linear translation stage (A) was fixed on a table and controlled the displacement of a base (B), which was connected to its mobile stage. Two axes (C), not linked to the base, were surrounded by springs (D) and connected to the instrumented object (E). The latter was composed of two force/torque sensors (reference frame on the right-top part of the figure) on which probes of a moisture sensor (inset on the right-bottom part of the figure) were glued. When the object was kept immobile by the subject, any vertical upward displacement of the mobile stage led to a movement of the base that then compressed the springs and generated a vertical force on the instrumented object.

The torques and forces measured by the sensors were used to determine the center of pressure at the fingertip:

$$CP = T/NF$$

where CP, T, and NF correspond to the center of pressure, torque, and normal force, respectively. CP corresponds to the coordinates of the point at which the resultant NF should be applied to generate the measured torque (T). The mechanical configuration of the setup (see Figure 4-1) allows only vertical movements of the mobile stage. As a consequence, only the y-component of CP is reported in the data. The vertical mobile stage speed was 1mm/s.

Skin hydration at the fingertip was measured with moisture sensors (Moisture Evaluator; André et al. (2008)). This task-dedicated device used the conductance principle to evaluate moisture content and provide a reliable, quantitative measure of skin hydration during the task. It consisted of an adapted probe composed of 56 gold-covered electrodes (see inset on right-bottom part in Figure 4-1) fixed on a Bakelite support and an electronic circuit to evaluate skin conductance. The numerical scale of the probe ranges from 4 to 10 in arbitrary units (a.u.), representing very dry to very wet skin, respectively. It is worth mentioning that the normal force exerted on the probe does not affect significantly the Moisture Evaluator reading (effect < 5% within 0.2N with 2N range, André et al.(2008)). For our quantitative analysis, an ordinary scale covering the whole range of moisture was arbitrarily defined and separated into four categories as follows: dry, 4 – 5.5 a.u.; normal, 5.5 – 7 a.u.; wet, 7 – 8.5 a.u.; very wet, 8.5 – 10 a.u. It is important to note that no additional water was applied at fingertip to obtain the very wet state. This classification was subject-independent. According to subjects' actual skin hydration at the time of the experiment, it permitted several subjects to cover more than one range of moisture. These intra-subject moisture variations allowed us to check that each individual subject followed the general tendency with respect to his/her own skin hydration.

Experimental procedure

Subjects were seated comfortably with a horizontal support under their forearm and wrist. They were asked to pinch the object (item E in Figure 4-1) between the thumb and index finger. Visual feedback of the NF was provided to the subject, allowing him or her to exert different levels of force on the object according to our instructions. The experiment consisted of producing slippage between the fingers and object for different levels of NF. The linear translation stage (Koudine et al. 2000; Adams et al. 2007) generated an increase in the TF exerted on each finger while subjects were instructed to keep their NF constant at the instructed level. When the TF became sufficiently large, the object slipped; the static CF was estimated at slippage by:

$$CF=TF/NF. \qquad (1)$$

Detection of slippage was performed combining two criteria: a maximum in TF associated with a steeper slope in the CP profile (Figure 4-2; vertical line C).

Each subject performed five consecutive trials for seven levels of NF: 0.2, 0.5, 1, 2, 5, 10, and 25 N.

Data processing

The signals from the force transducers were low-pass filtered with a fourth-order zero phase-lag Butterworth filter having a cut-off frequency of 10 Hz, which is consistent with the bandwidth of the signals in this task. For each trial, the static CF was estimated separately for each finger when the object slipped. Skin hydration was also measured simultaneously using the

Moisture Evaluator. The quantitative results were reported for both fingers (see Table 4-1) but the figures illustrate the data from the thumb.

Statistical analysis

The relationship between the NF and CF was quantified using a non-linear regression. The functional form was modeled according to the proposal of Wolfram (Wolfram 1983), which hypothesized a negative power function between the CF and NF. Consequently, our non-linear regression was based on the following equation:

$$CF = a\ NF^{-b}, \qquad (2)$$

where *a* and *b* are real parameters of the fit ('FIT' function of Matlab). All statistical analyses were performed using two-way analyses of variance (ANOVAs) to study the effects of seven levels of NF (factor 1) and four levels of moisture (factor 2) on the CF (data).

Results

Figure 4-2 presents the temporal variation of the normal and tangential forces, as well as the vertical component of the center of pressure (CP) and the moisture during one typical trial for the thumb. For this particular trial, the subjects were instructed to maintain a constant NF of 1 N. During phase 1 of the experiment, the subject touched the object (position A in Figure 4-2) and stabilized the normal force to approximately 1 N. For phase 2, the linear motor started to move (position B in Figure 4-2) and the TF increased monotonically. During this period, the CP moved slowly due to the skin's compliance. At the end of phase 2 (position C in Figure 4-2), slipping occurred when the NF could no longer counteract the TF. The ratio of TF/NF at this time corresponds to the static coefficient of friction. During phase 3, the TF remained roughly constant and the slope of CP increased significantly.

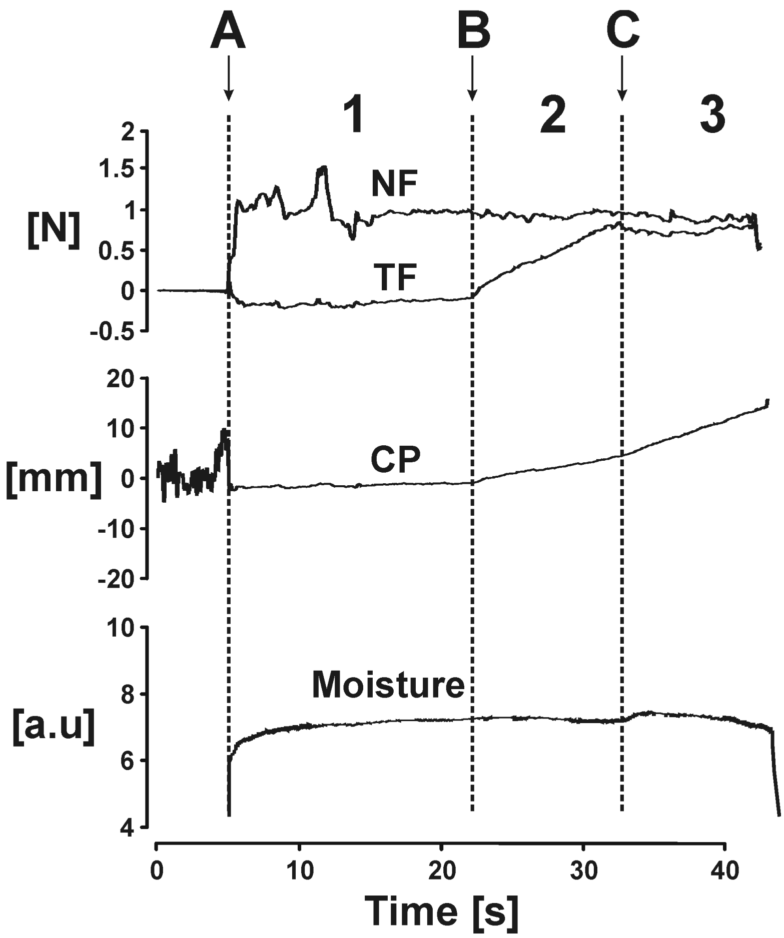

Figure 4-2: Typical trial for one subject: evolution of the NF, TF, and CP of the thumb over time. (1) The subject stabilized NF. (2) The linear translation stage started to move and generated the vertical, monotonically increasing TF. The NF stayed constant during that period, whereas the CP varied slightly due to the compliance of the skin. (3) The TF reached a maximum, and the CP variation increased; the F/T sensors started slipping across the fingertip.

Effect of normal force on the static coefficient of friction

The relationship between the normal force and static coefficient of friction for the four ranges of moisture previously defined is illustrated for the thumb in Figure 4-3. This figure shows the pooled data for all subjects. For all ranges of skin hydration, the CF was low and constant for high levels of NF (> 3.5 N). However, for three ranges of hydration (dry, normal, and wet; Figure 4-3.A-C, respectively), there was a large increase in the CF for low levels of NF (≤ 3.5 N). When the skin was very wet (Figure 4-3.D), this increase was much smaller. When the same analyses were performed on each subject individually, the same trends were observed as those in the pooled data for each range of moisture covered by each individual subject.

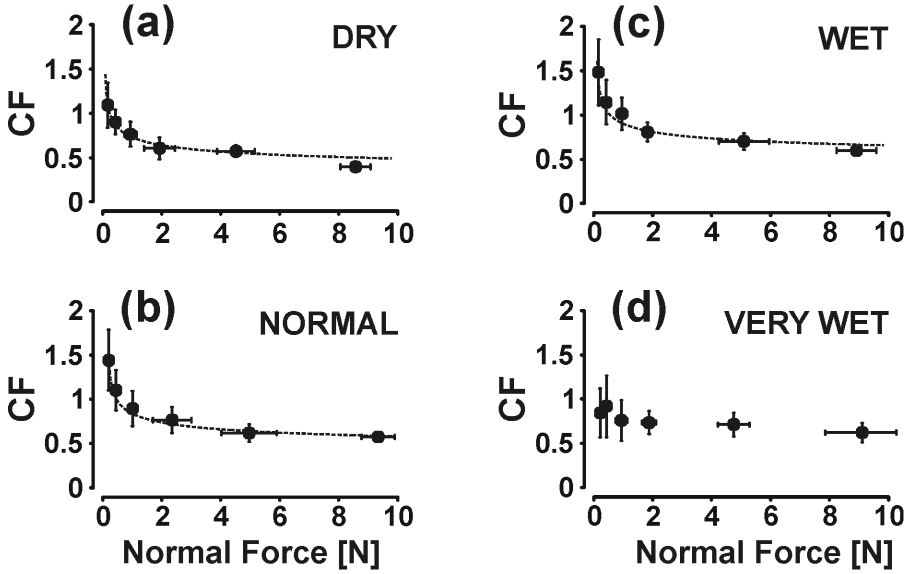

Figure 4-3: Relationship between the CF and NF for the four moisture ranges. Each data point corresponds to the mean CF and NF for a specific range of NF pooled for all subjects (data for the thumb). The associated standard deviations (vertical for the CF and horizontal for the NF) are plotted around the corresponding means. The dashed curves show the negative power function regression line fit to all raw data (Equation 2). The largest value of NF tested (NF = 25 N) is not shown due to scaling constraints.

Negative power functions were used to quantify the relationship between the CF and NF (using a non-linear fit). Table 4-1 gives the values of the parameters *a* and *b* (see Equation 2) for the thumb and index finger across the four ranges of moisture. Parameter *a* was mostly influenced by the mean level of the CF (larger for normal and wet conditions). Indeed, it corresponds to the CF value when the NF = 1 N. Parameter *b* was closely related to the shape of the curve, as determined by the influence of NF on the CF. Parameter *b* was significantly smaller for the very wet range of moisture, indicating that the influence of NF on the CF was less important in this condition.

$CF = a.NF^{-b}$	***a_thumb***	***b_thumb***	***R^2***	***a_index***	***b index***	***R^2***
DRY	0.73	0.24	0.7	0.75	0.24	0.89
NORMAL	0.93	0.25	0.72	0.79	0.22	0.55
WET	0.97	0.23	0.77	0.85	0.22	0.79
VERY WET	0.8	0.11	0.24	0.75	0.14	0.75

Table 4-1: Effect of moisture on parameters *a* and *b* in Equation 2 for the thumb and index finger.

The statistical analyses using a two-way ANOVA showed that the interaction between NF, moisture level and CF was significant ($P<0.01$). Nevertheless, the non influence of NF on CF for the very wet moisture level was confirmed: there was no significant differences across the seven levels of NF (P > 0.01, ANOVA), except when comparing the 0.5 N and 10 N groups (P < 0.01, pairwise comparison using Dunn's method).

Effect of moisture on the static coefficient of friction

Figure 4-4 presents the relationship between the moisture level and static coefficient of friction for seven different ranges of NF between 0.2 N and 20 N. There was a significant influence of moisture on the CF for levels of NF ≤ 3.5 N (Figure 4-4.A-D). Indeed, the CFs for the normal and wet conditions (filled symbols) were significantly larger (P < 0.01) than those for the dry and very wet conditions (open symbols).

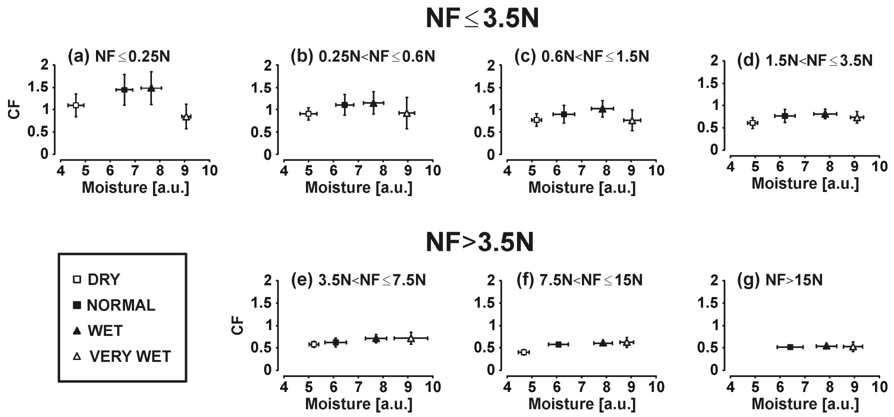

Figure 4-4: Relationship between the CF and moisture of the thumb for seven different ranges of NF from below 0.25 N to above 15 N. Each data point corresponds to the mean CF and moisture content for the specific moisture ranges and for all subjects pooled together. The associated standard deviations (vertical for the CF and horizontal for moisture) are also plotted. The inset shows the four symbols used for the four different moisture ranges: open square (dry), filled square (normal), filled triangle (wet), and open triangle (very wet).

The relationship between moisture and the CF could be approximated by a bell-shaped curve, with a peak CF for an intermediate value of moisture (approximately 7.5 a.u. on average). Moreover, when the NF increased from 0.2 N to 3.5 N, the average CF level tended to decrease for the same values of moisture (consistent with the results of Figure 4-3). For a NF > 3.5 N, the bell-shaped relationship was attenuated (Figure 4-4.E-G). The comparison between the normal and wet conditions and the dry and very wet conditions showed no statistically significant difference ($P > 0.01$) for NF > 3.5 N.

Estimation of the static coefficient of friction based on the moisture measurement and normal force

The values of parameters *a* and *b* in Equation 2 (see Table 4-1) can be used to provide for each finger an estimate of the CF for each moisture range. Here, we propose a systematic method for estimating the static coefficient of friction for each condition. This method requires only the moisture measurement and normal force. The moisture is first used to determine the best parameter values for *a* and *b* that will be used to estimate the CF on the basis of the NF. Determining these parameters is based on a linear interpolation across values formed from the four moisture ranges defined above. This is illustrated in Figure 4-5.A, which clearly shows the association of a pair (*a,b*) for each measured value of moisture. The final step simply consists of inserting the (*a,b*) pair into Equation 2 prior to estimating the CF. The final result is illustrated for the thumb in Figure 4-5.B and shows the 3D representation of the CF as a function of moisture and normal force.

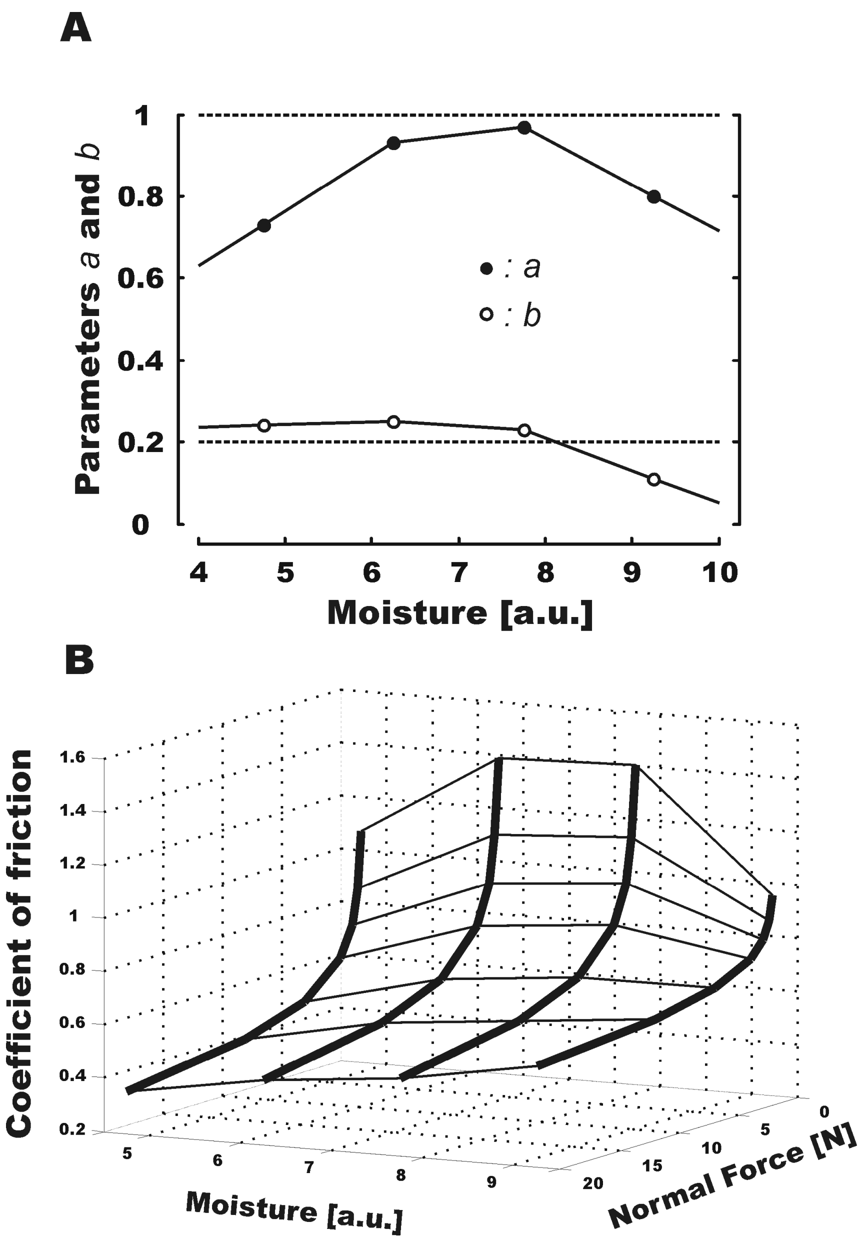

Figure 4-5: A- Estimation of *a* and *b* parameters (Equation 2) as a function of moisture (data for the thumb). The estimate is based on a linear interpolation across values found for *a* and *b* for the different moisture ranges (Table 4-1). B- Estimation of the CF of the thumb as a function of moisture and NF (3D plot).

Discussion

The aim of this paper was to study the combined effects of moisture and normal force on the static coefficient of friction of the skin for a fingertip during object manipulation. We developed a new method that allowed us to evaluate the CF during a precision grip by simultaneously measuring the normal force and skin hydration for a subject's fingertip. Our results indicate that (1) except at very high levels of skin moisture, the CF decreases with the NF according to a negative power function and (2) a bell-shaped curve characterizes the relationship between the CF and moisture, with an intermediate level of moisture maximizing the CF. This study clearly demonstrates the significant influence of both parameters on the CF, particularly at low NF levels (< 3.5 N).

The mechanical properties of the fingertip skin are of prime importance to understand human grasping and psychophysics of touch. More specifically, the coefficient of friction between fingers and objects is a critical parameter when manipulating objects. Until now, evaluation of the CF could only be done before or after a task, performing slippages and measuring the ratio of TF/NF when slipping was initiated. Our set of data combined with our method permit the continuous estimation of the CF during the entirety of any manipulation task.

Typical ranges of grip force used in dexterous manipulation are between 1 and 4 N (Johansson and Westling 1984b; Edin et al. 1992), and our results demonstrate the extent of CF variation for low levels of NF (<3.5N): the CF is strongly influenced by both the NF and moisture. Moreover, we observed important moisture variations during a manipulation task (personal observations). These observations lead to the conclusion that the CF could vary significantly and that it is crucial to assess the CF during object manipulation. Our results allow us to take these variations into account and estimate the CF continuously. New perspectives of research that will consider these variations and study the way humans adapt manipulation strategies are now possible using the methods proposed in the current paper.

The influence of the NF on the static coefficient of friction has been described by several authors. Some of these studies did not find a significant effect of NF on the CF (Buchholz et al. 1988; Savescu et al. 2008), which can be explained by the high levels of NF (> 3.5 N) used in the respective experiments. In contrast, Comaish and Bottoms (1971) demonstrated a deviation from Amonton's law and high CF levels when the NF was extremely low. This study also formalized a more complex non-linear relationship between the NF, TF, and CF. The non-linearity of the CF with respect to the NF, especially for low levels of NF (< 3.5 N), has been demonstrated by other authors as well. Wolfram (1983) argued that the static coefficient of friction of the skin decreased as a negative power function of the NF (Equation 2 with b=1/3). Similar results have been reported in publications that studied the static coefficient of friction of the skin on the dorsal side of the forearm using a glass probe or on the top of the middle finger using a steel probe (Koudine et al. 2000; Sivamani et al. 2003; Adams et al. 2007).

In the present work, we focused on the fingertip CF using a precision grip, because this approach determines the minimal grip force needed to avoid slipping of the object. Our results for the relationship between the CF and NF, expressed in Equation 2, are consistent with the previous works cited above. Moreover, it has been shown that moisture influences the CF (Adams et al. 2007) as well as the relationship between the NF and CF (Derler et al. 2007). This is consistent with our results which showed an increase in CF with moisture. Moreover, our results covered a larger range of moisture level (i.e. the very wet condition in which CF dropped) and provided estimates of CF for a continuous moisture scale. In the present study, we demonstrated the importance of the combined measure of moisture and NF for estimating the CF.

Variations of the *a* parameter in Table 4-1 suggest that the moisture content also influences the CF. Indeed, Figure 4-4 shows that CF values were strongly modulated by skin hydration. The effects of moisture on the CF varied between 46% and 4% for a NF range between 0.2 and 20 N, respectively. Up to now, various studies have considered the importance of the skin hydration level on performance during object manipulation. Smith et al. (1997) investigated the influence of scopolamine on the prehensile force during object manipulation and showed an increase of this force due to a reduction of palmar sweating. In the same way, Zackrisson et al. (2008) reported that a significant decrease of the CF and consequent significant increase of the grip force were observed when patients with very high sweating rate (hyperhidrosis) manipulated objects. These studies provide evidence for the importance of measuring skin moisture for fingertips during object manipulation, because this parameter significantly influences subject performance. Interestingly, these two studies that explore extreme ranges of moisture are fully compatible with our results (bell-shape, Figure 4-4). From a mechanical point of view, the effects of moisture on the CF have been studied by comparing dry and moist conditions (Comaish and Bottoms 1971; Buchholz et al. 1988) or by observing CF variation during drying or hydration periods (Sivamani et al. 2003; Adams et al. 2007). These studies showed an increase of the CF with moisturization. Nevertheless, none of these studies could report skin hydration measurements during the experiments. Our Moisture Evaluator (André et al. 2008) permitted a continuous measurement of moisture content and, most importantly, allowed for better discrimination of extreme and intermediate moisture values during the experiment. Figure 4-4 shows the effects of moisture level on the CF for different moisture ranges and points to an optimal level of moisture for maximizing the CF.

Interpretations of the combined effects of NF and moisture on the CF were first offered by Bowden and Tabor (1967), who argued that the visco-elastic nature of the skin causes the true area of contact to be no longer proportional to the NF level. Accordingly, Buchholz et al. (1988) hypothesized that hydration of the skin would enhance its viscous properties which would augment the adhesion effect. Recently, Adams et al. (2007) explained this by modeling the hydrated *stratum corneum* as a soft elastomer; their Young's modulus values are comparable, and the relatively large compliance of the asperities results in smooth contact on the molecular level. Both the reduction in the elastic modulus and the swelling that occurs in water would be expected to lead to extensive smoothing of wet skin's frictional contacts. Moreover, the increasing liquid-bridging between the ridges of the skin and the contacted surface increased friction (Dinç et al. 1991). Finally, the pronounced decrease in the CF at very high levels of moisture could be explained by the presence of a thin layer of water between the skin and the object (Adams et al. 2007; Tomlinson et al. 2007).

The goal of this paper was to examine the combined effects of normal force and moisture content on the static coefficient of friction between the skin of a fingertip and a manipulated object and to propose a new method for its estimation. A global relationship (illustrated in Figure 4-5.B) showed the “cross-talk” of these two parameters on the CF. Our results yielded a new method for estimating the CF with NF and moisture measurements. Indeed, as presented in our results section, the moisture level measurements provided numerical values for our *a* and *b* parameters that define the negative power function for determining the CF. Thus, a continuous estimate of the CF can be obtained during the performance of dexterous manipulation. This measurement is of prime importance, particularly during situations with variable friction. For example, variable friction occurs when there is strong moisture variation or when the level of NF exerted on the object is very low (i.e. dexterous manipulation of very small objects or manipulation in a weightless environment). In this study, we quantified the influence of moisture on the CF, assessed the strong interaction of NF and moisture on the CF, and provided a method for estimating the CF that takes into account these two variables.

The method proposed here makes a major contribution to the field of object manipulation. It provides an estimation of the CF based on the moisture and NF measurement. This estimation does not require any slippage and can take into account the moisture and NF variation during manipulation. Indeed, moisture can vary with stress and the psycho-galvanic reflex but also according to the occlusion occurring at fingers-object interface. As we already know, the NF is permanently adapted to the inertia of the manipulated object. In future investigations it will be now possible to monitor the CF continuously during object manipulation taking into account the effects of moisture and NF on CF.

Chapter 5

Fingertip Moisture is Optimally Modulated During Object Manipulation

"The relationship between the Welsh and the English is based on trust and understanding. They don't trust us and we don't understand them."

Dudley Wood (1986)

Published as: T. André, P. Lefèvre and J-L. Thonnard. **Fingertip Moisture Is Optimally Modulated During Object Manipulation.** Journal of Neurophysiology (2010) 103:402-408.

Abstract

Coordination between the normal force exerted by fingers on a held object and the tangential constraints at the fingertips helps to successfully manipulate objects. It is well established that the minimal grip force required to prevent an object from slipping strongly depends on the frictional properties at the finger-object interface. Moreover, interindividual variation in the modulation of grip force suggests that the moisture level of the skin could influence grip force strategy. In the present study we asked subjects to perform a horizontal point-to-point task holding an object with a precision grip. The object was equipped with a moisture sensor. We found large inter- and intraindividual moisture level variations. There was a strong correlation between grip force exerted and moisture level at the fingertips. Indeed, the grip force was minimal when the fingertip moisture was optimal with respect to friction. Furthermore, fingertip moisture tended toward this optimal level at which grip force is minimal. In conclusion, we showed a modulation of the grip force with moisture level and hypothesized novel mechanisms of moisture regulation that tend to stabilize moisture level toward the value that minimizes grip force.

Introduction

When handling an object or transporting it through space we apply an adequately large force normal to the grip surface (grip force) in relation to destabilizing forces tangential to the grip surface (load force). Accidental slips rarely occur because the grip force exceeds the minimal force (dependent on load force and skin-object friction) required to prevent slip (Johansson and Westling 1984b). Skin-object friction is the force resisting the relative tangential motion between skin and object. This friction depends on the properties of the surface of the held object and the glabrous skin of the fingertips. Previously, a study by Johansson and Westling (1984b) revealed that the more slippery the object the higher is the grip force at any given load force. However some pronounced interindividual variations of the friction between the skin and the surface materials were observed. Interestingly, these authors suggested that differences in sweating rates may partially account for this interindividual variability.

Although the importance of eccrine sweat secretion for controlling body temperature has been extensively investigated, the effect of sweating on the friction of glabrous skin in the palm and fingers of the hand has received comparatively little attention. Smith et al. (1997) reported that reducing spontaneous sweat gland activity of the hand by transdermal absorption of scopolamine, significantly decreased the friction of the fingers against a smooth plastic surface. In contrast, Zackrisson et al. (2008) reported that patients with primary palmar hyperhidrosis (abnormally high sweat) showed perturbed object manipulation caused by a decrease in friction. It has also been demonstrated in normal subjects that after washing and drying the hands, skin friction was greatly reduced compared with when moisture had time to accumulate (Johansson and Westling 1984a).

More recently, our group (André et al. 2009) reported that the relationship between the coefficient of friction and the moisture at the fingertip could be characterized by a bell-shaped curve, with an intermediate level of moisture maximizing the coefficient of friction. Thus, the frictional properties of dry, damp and wet skin were dissimilar. Damp skin was found to produce a higher frictional quality than either wet or dry skin. These observations led us to study the effect of fingertip moisture on grip force modulation during object manipulation. In a recent study we developed an instrument capable of measuring the moisture level of the skin (André et al. 2008). This device, called the Moisture Evaluator, enables the measurement of the water content of the skin surface during dexterous manipulation. In the present study we used the Moisture Evaluator to measure moisture variations at the fingertips during a manipulation task. We further examined the inter- and intrasubject moisture variations during the repetition of this task and the effect on grip force. We found that moisture level at the fingertip varies within and across subjects and that grip force is continuously modulated in accordance with moisture level. In this study we hypothesized novel mechanisms of moisture regulation which tend to stabilize the moisture around the value that minimizes grip force during object manipulation.

Methods

In all, eight healthy volunteers (28 ± 9.6 yr) participated in this study. All subjects were right-handed according to the Edinburgh handedness inventory (Oldfield 1971). Subjects' vision was normal, or corrected to normal, and none had a neurological history. All experimental procedures were approved by the Ethics Committee of the Université catholique de Louvain and all subjects gave written informed consent. The temperature of the room was held relatively constant (23.8 ± 1.2 °C) and air humidity was between 40 and 55 %.

Apparatus

A manipulandum was held between the thumb and the index finger using a precision grip (Figure 5-1). The manipulandum was equipped with two force-torque sensors, one under each finger (Mini40 F/T transducer; ATI Industrial Automation, Apex, NC). These sensors measured the three force components along the corresponding axes passing through the center of the corresponding grasp surface (Fx, Fy, Fz). Fx and Fy are in plane of the contact surface (Fx, horizontal and Fy, vertical; in the reference frame of the sensor), and Fz is normal to the contact surface. Sensing ranges for Fx, Fy and Fz were ±40, ±40 and ±120 N, with 0.01, 0.01, and 0.02 N nominal resolution, respectively. The mass of the manipulandum was 0.26 kg and the width between the grip surfaces was 45 mm.

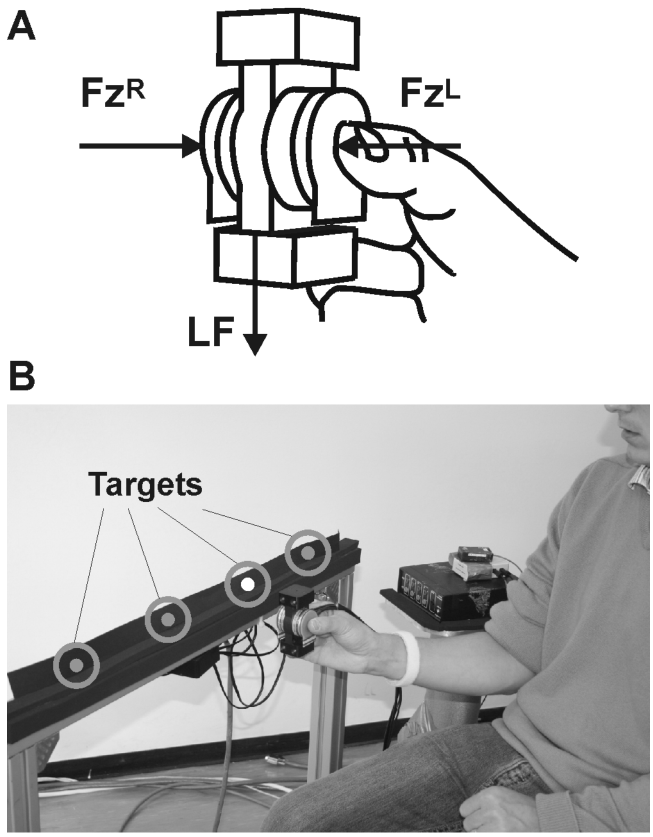

Figure 5-1: A- The manipulandum is held between the thumb and index finger. The two normal grip forces (FzR and FzL) exerted by the fingers and the tangential load force (LF) are recorded. B- Subjects were seated and told to move the manipulandum as fast as possible toward the illuminated target in order to align and stabilize the manipulandum in front of the target. Targets were randomly illuminated at the frequency of 1Hz. One alignment corresponded to one trial and subjects performed 20 blocks of 25 trials each.

On both digits, skin hydration at the fingertip was measured with the Moisture Evaluator (André et al. 2008), consisting of an adapted probe fixed on a Bakelite support and an electronic circuit to evaluate skin conductance. The measurement of conductance is based on a resistor-capacitor circuit and is determined using a frequency measurement. A higher frequency signal represents increased water content at the skin surface. The frequency of the signal is recorded and reported on a logarithmic scale. The numeric scale of the Moisture Evaluator ranges from 4 to 10 in arbitrary units (a.u.), representing very dry to very wet skin, respectively. André et al. (2008) demonstrated that the Moisture Evaluator actually measures the changes in moisture levels at the skin-object interface.

Experimental procedure

The task is illustrated in Figure 5-1.B. Four target light-emitting diodes (LEDs) were placed along a structure that was horizontally aligned with respect to the floor. The target LEDs were positioned every 15 cm. The program generated a random sequence of targets at a frequency of 1Hz. The participant was seated in front of the target axis, held the manipulandum in a precision grip, and was asked to align and stabilize the manipulandum with the lit target until the next target was illuminated. Head, eye, and arm movements were not restricted. Each participant repeated 20 blocks consisting of 25 consecutive point-to point movements each. Thus one block refers to 25 successive trials. Between each block the participant released the manipulandum for a 30 second resting period, during which fingertip moisture returned to baseline.

Data processing and variables studied

The signals from the force sensors were digitized at 800Hz with a 16-bit NI9205 analog-to-digital converter plugged into a NI cDAQ-9172 chassis. After analog-to-digital conversion, the force signals were low-passed filtered with a fourth-order, zero phase-lag Butterworth filter with a cutoff frequency set to 15Hz. The fingertip skin moisture level was measured by the Moisture Evaluator at target onset for each trial.

The normal grip force (GF) was defined as the average of the normal forces applied by the thumb and the index finger on each sensor and is represented by the following equation: $GF=(|Fz^R|+|Fz^L|)/2$, where Fz^R is the normal force component on the right sensor and Fz^L is the normal force component on the left sensor (Figure 5-1.A). The tangential force between each finger and the manipulandum was computed as: $Ft=sqrt(Fx^2+Fy^2)$. The load force (LF) was defined as the sum of the right and the left tangential forces: $LF=Ft^R+Ft^L$. It is worth mentioning that the difference between Ft^R and Ft^L was very small and always remained below 5% of their mean for each component (x and y). Finally, for each trial, an average static GF (GFs) was computed in a 100-ms time window following the target onset (Figure 5-2, grey bar). In other words, the average GFs represents the mean GF during which the manipulandum was held steady in front of the illuminated target. In each block, 25 values of GFs were associated with a corresponding value of moisture (mean of the right and left moisture values). This provided 500 pairs of GFs-moisture data points for each subject.

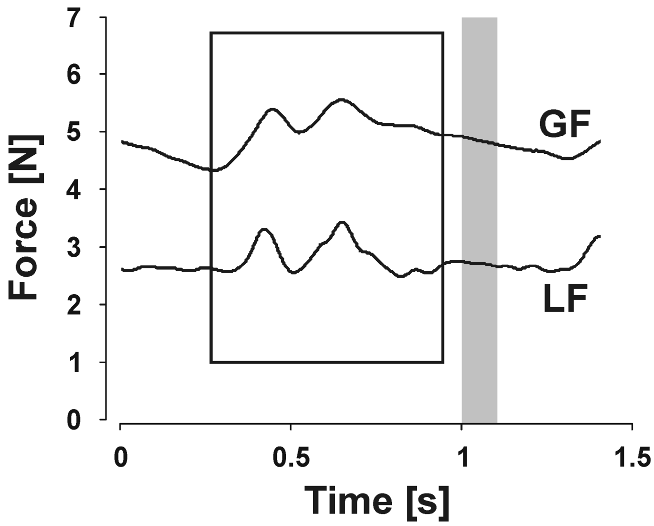

Figure 5-2: Representative temporal alterations of the grip force (GF) and the load force (LF) during a trial. During the dynamic phase (manipulandum moving toward target, rectangular box), a double peak of LF, resulting from acceleration and deceleration of the manipulandum moving toward the target, is observed. The associated GF modulation is shown. During the stable phase (manipulandum held immobile in front of target, grey bar), the LF is constant and corresponds to the weight of the object (0.26 kg). Static GF (GFs) is defined as the mean GF during this stable phase.

Statistical analyses were performed using least-squares linear regressions. The regression permitted us to evaluate the significance of a trend when testing relationship between two variables (given by the p-value). Moreover, the sign of the slope gave the nature of the effect.

Results

The temporal pattern of GF and LF for a typical trial is displayed in Figure 5-2. A dynamic phase (rectangular box) during which the manipulandum was moved toward the illuminated target preceded a static phase (grey bar) during which the manipulandum was held stationary in front of the illuminated target. During the dynamic phase, the manipulandum was accelerated and decelerated to reach the illuminated target. Typically this movement triggered a double peak in the LF trace with corresponding peaks in the GF trace. During the static phase, LF was constant and equal to the weight of the manipulandum (2.6N). In this study we concentrated on the skin moisture variation during the static phase and its influence on GFs.

Fingertip moisture, measured in arbitrary units varied significantly across participants. We ranked the subjects according to their mean moisture level across 500 trials and found that participants with either very dry or very wet skin exerted higher GFs than participants with an intermediate moisture level (Table 5-1).

Subjects	***Moisture [a.u.] (mean ± SD)***	***GFs [N] (mean ± SD)***
S1	5.6 ± 0.62	10.9 ± 2.05
S2	6.4 ± 0.89	8.6 ± 2.15
S3	7.3 ± 0.94	6.6 ± 1.34
S4	7.7 ± 0.86	5.2 ± 0.75
S5	7.8 ± 0.98	5.1 ± 0.93
S6	7.8 ± 1.06	5.7 ± 1.14
S7	8.1 ± 1.01	8.7 ± 1.01
S8	8.8 ± 0.93	8.5 ± 1.89

Table 5-1: Mean value (± SD) of moisture and static grip force (GFs) for each individual subject across 500 trials.

A significant effect ($p<0.01$) of the block number on the GFs was observed for each individual subject (see Table 5-2) except for S4. The slope of the linear regression was positive for four subjects and negative for three subjects, indicating that, depending on the subject, GFs could increase or decrease across the blocks. Accordingly, when the data were pooled across all subjects, there was no significant effect of block number on GFs (repeated-measures ANOVA, $p=0.35$; $\chi^2=20.82$; $n=19$). These results indicate that there was no clear effect of repetition on GFs across all subjects.

Subjects	***p-level***	***slope***
S1	< 0.01	0.12
S2	< 0.01	-0.36
S3	< 0.01	0.028
S4	0.49	NA
S5	< 0.01	0.029
S6	< 0.01	0.030
S7	< 0.01	-0.13
S8	< 0.01	-0.080

Table 5-2: Effect of the block number (repetition of the task) on GFs for each individual subject.

After having studied the effect of the block number on GFs, the influence of the mean moisture inside a block on GFs was studied. The relationship between the mean GFs in each block and the corresponding mean moisture is shown in Figure 5-3, pooled for the eight subjects. For low level of moisture, the GFs decreased when the moisture increased until an intermediate value of moisture for which the GFs was minimal. For a high level of moisture, the effect of moisture was inverted and GFs increased again with moisture.

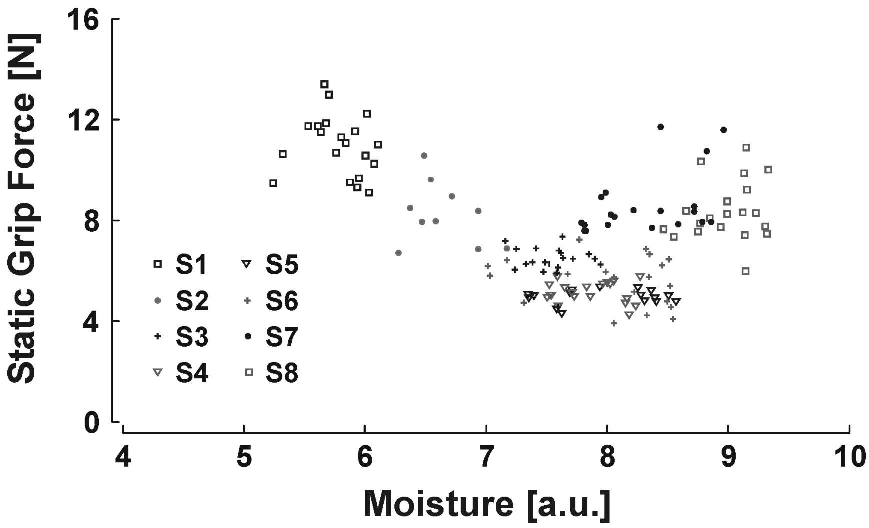

Figure 5-3: The relationship between the mean GFs of each block and the mean moisture level within the same block for each of the 8 subjects. Data for each subject are represented with a different symbol.

Fingertip moisture level during each trial was averaged across the 20 blocks for each subject (Figure 5-4). When the mean value of the moisture was low during the first trial (S1, S2, S3, and S5), the moisture increased significantly ($p<0.001$) across the 25 trials. When the moisture level was intermediate during the first trial (S4, S6, and S7) it did not change across trials ($p>0.05$). Finally, when the moisture level was high during the first trial (S8), it significantly decreased ($p<0.001$) across trials.

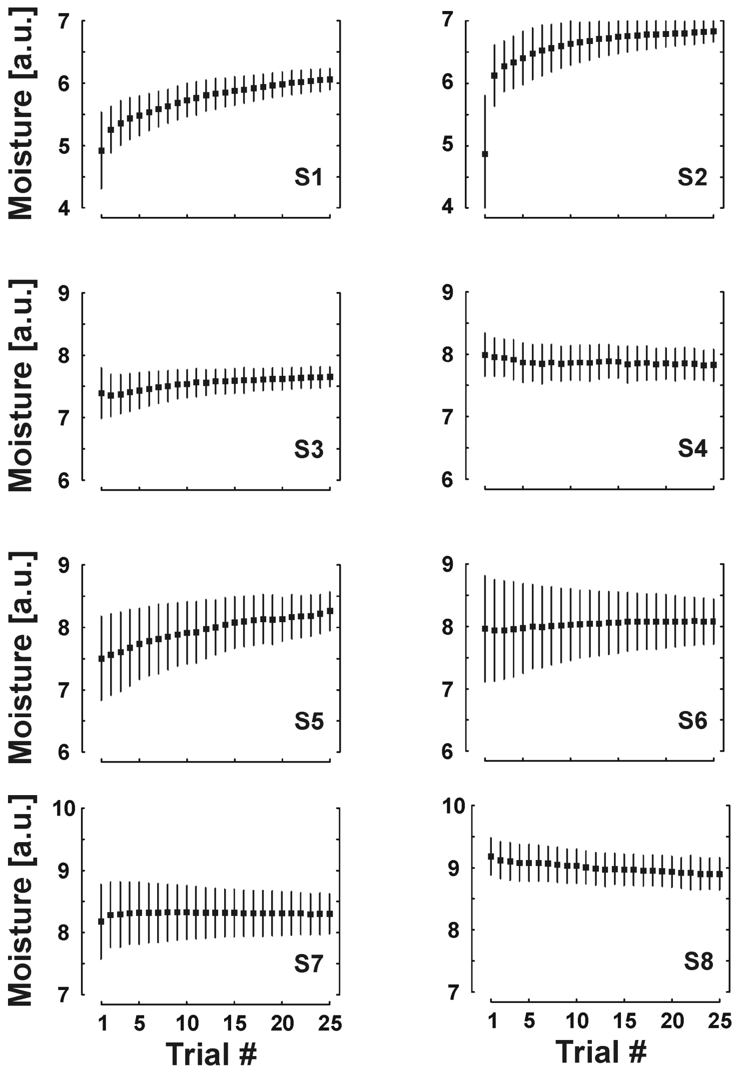

Figure 5-4: Skin moisture level at the fingertip across the 25 trials, for each of the 8 subjects. Each data point corresponds to the mean moisture level for each trial, across all blocks. The associated standard deviations (vertical line) are plotted around the corresponding means. Three tendencies are demonstrated: increase of moisture level with trials (S1, S2, S3, and S5); constant moisture level across trials (S4, S6, and S7); decrease of moisture level with trials (S8).

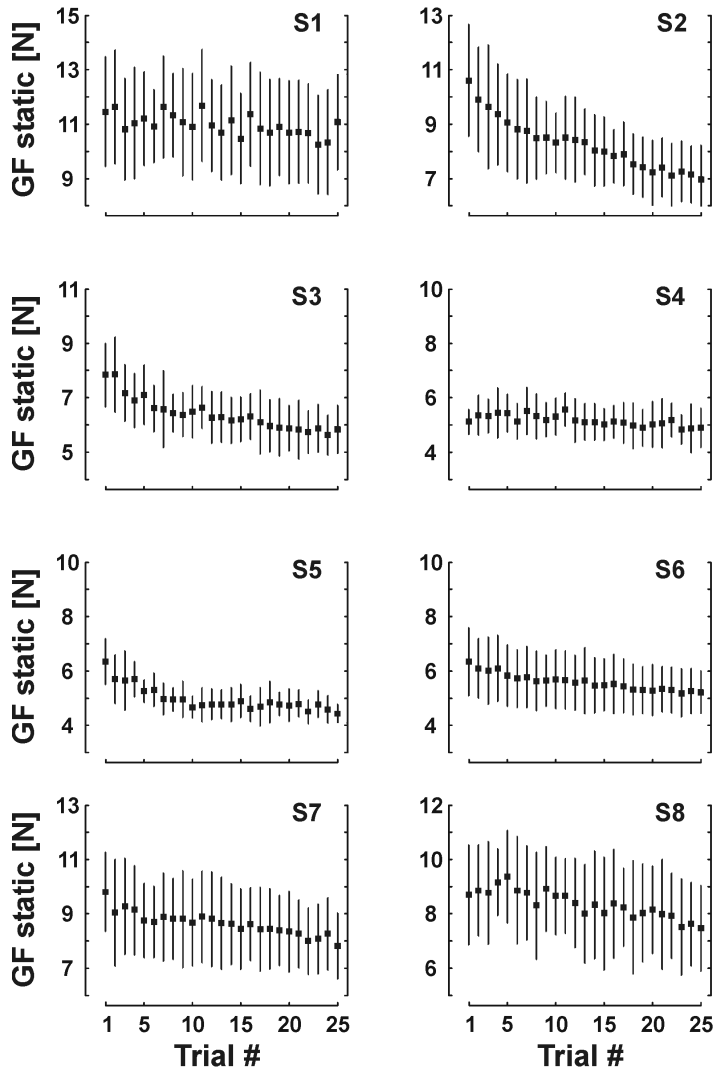

Figure 5-5: GFs exerted across the 25 trials, for each of the 8 subjects. Each data point corresponds to the mean GFs for each trial across all blocks. The associated standard deviations (vertical line) are plotted around the corresponding means. Two trends are demonstrated: a decrease in GFs with trials (all subjects except for S4) and constant GFs across trials (S4).

We were interested in the pattern of GFs across trials for each subject. Figure 5-5 illustrates, for each subject, GFs across the 25 trials averaged for the 20 blocks. GFs decreased significantly ($p<0.001$) across the trials for all subjects except for S4 presenting low and constant GFs. Interestingly, at first glance these results were not as we expected. We were interested in a correlation between moisture level and GFs. In a comparison of Figure 5-4 and Figure 5-5 a decrease in GFs across trials for S6 and S7 is associated with a constant level of moisture across trials. However, the variability of moisture level across all blocks was much higher during the first trials for these subjects, indicating that within each block the moisture could increase, remain stable, or decrease across the 25 trials.

Subjects	***Moisture increase group 1***	***Moisture constant group 2***	***Moisture decrease group 3***
S1	100%	0%	0%
S2	100%	0%	0%
S3	70%	20%	10%
S4	0%	100%	0%
S5	95%	5%	0%
S6	30%	20%	50%
S7	55%	5%	40%
S8	0%	0%	100%

Table 5-3: Percentage of blocks (across the 20 blocks) that belonged to each category, depending on the moisture variation, for each individual subject.

Thus, we performed additional analyses in order to compare the pattern of moisture with the pattern of GFs across the trials within each block. To that purpose we sorted the 20 blocks of each subject according to the moisture pattern across trials within each block (Table 5-3). A block was classified in group 2 if the moisture level remained constant (the difference between the first three and last three trials was less than ±0.15 a.u.), in group 1 if moisture level increased (the difference between the first three and last three trials was greater than +0.15 a.u.) and in group 3 if moisture level decreased (the difference between the first three and last three trials was less than -0.15 a.u.). For group 1, an increase in moisture was associated with a systematic decrease in GFs (all $p<0.001$). For group 3, there was a decrease in moisture that was also associated with a decrease in GFs (all $p<0.001$). In contrast, for group 2, neither moisture nor GFs varied (all $p>0.05$, except for S3).

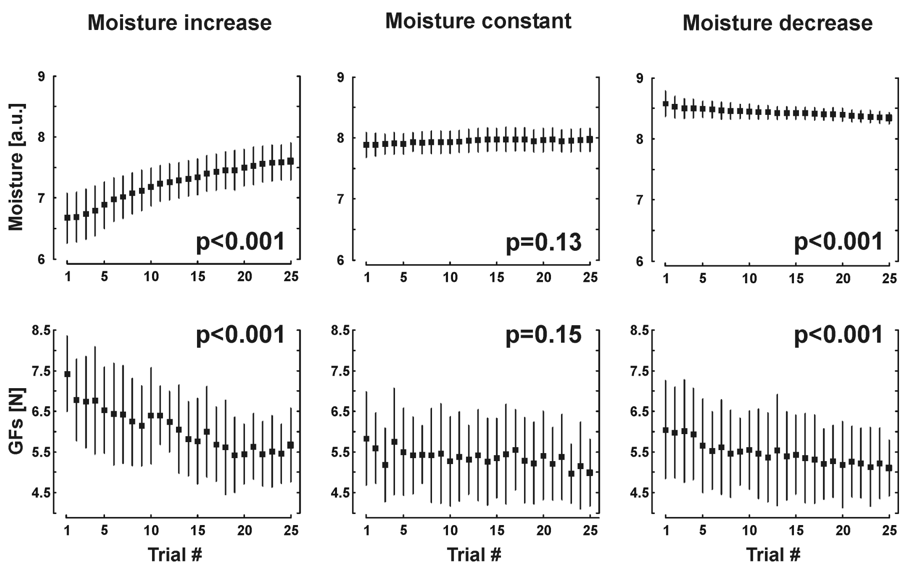

Figure 5-6: Representative alterations in moisture level and GFs with trial number (for S6). Three groups, defined by moisture variation during blocks, are represented (moisture increase, moisture constant and moisture decrease). Each data point within a graph corresponds to the mean moisture level for each trial, across all blocks. The associated standard deviations (vertical line) are plotted around the corresponding means. The p-values of the linear regression fitting the data are given for each relationship.

Figure 5-6 presents the results of S6 to illustrate the three tendencies described earlier. When moisture increased across trials (Figure 5-6, left column, low level of initial moisture), there was an associated decrease of GFs ($p<0.001$). When moisture decreased across trials (Figure 5-6, right column, high level of initial moisture), there was also an associated decrease in GFs ($p<0.001$). Interestingly, when moisture remained stable across the trials (Figure 5-6, middle column), there was no modulation of GFs ($p=0.15$). These results demonstrate that even within individual blocks, the changes in GFs were modulated by the pattern of fingertip moisture across trials.

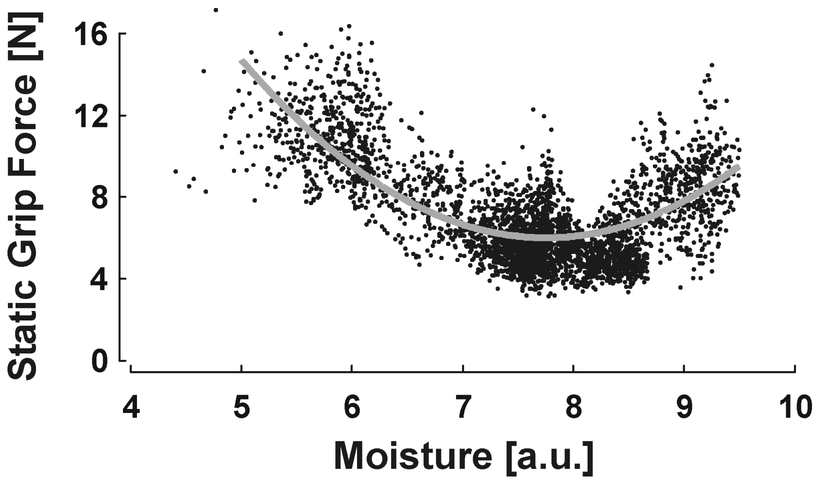

Figure 5-7: Relationship between GFs and moisture level for the raw data. Each point corresponds to a paired GFs-moisture level. The 500 paired GFs-moisture level are represented for each subject. The grey trace illustrates the quadratic regression fitting the raw data ($y=1.15x^2-17.8x+75.1$) with the minimum in GFs–moisture value pairing equal to 7.75 arbitrary units.

The modulation of GFs with skin moisture appears clearly when all 500 pairs (25 trials in 20 blocks) for each subject are plotted (Figure 5-7). It is interesting to observe that most of the trials are concentrated around the intermediate level of moisture (around 8 a.u.). Moreover, these results suggest that there is an optimal level of moisture at which GFs is minimized. The relationship between GFs and moisture level can be fitted well by a quadratic regression $y=1.15x^2-17.8x+75.1$ ($p<0.001$; $R^2=0.45$) for which a moisture value of 7.75 a.u. minimizes GFs.

Discussion

The present study focused on the effect of skin moisture at the fingertip on grip control during dexterous manipulation. By measuring the moisture level and the force exerted on an object held in a precision grip during a point-to-point task, we demonstrated that human subjects adjust grip force with moisture level. Our results showed that (1) skin moisture level at the fingertip varied significantly from one subject to another and also across trials for each subject; (2) grip force was adjusted continuously to adapt to moisture level during the task.

The influence of extreme skin moisture conditions on grip force has previously been studied. Very dry skin, resulting from the effect of aging (Cole 1991) or from scopolamine administration (Smith et al. 1997) has been shown to increase the level of grip force. Additionally, very wet skin in a patient with hyperhidrosis (Zackrisson et al. 2008) resulted in an increase in grip force. In these studies, it has been hypothesized that an increase of GF is due to a reduction in the friction coefficient. Our results agree with these prior studies (Table 5-1) and provide evidence from natural ranges of moisture observed in normal subjects. Subjects with very low or very high values of moisture exerted higher grip force. The effect of moisture on fingertip skin friction was previously analyzed. Buchholz et al. (1988) reported that the presence of moisture resulted in an increase of the friction coefficient for handling of porous materials (adhesive tape, suede, and paper). Derler et al. (2007) showed that the variations in friction coefficients measured between human skin and a reference textile were mainly attributed to differences in skin hydration and variations in the lipid content at the skin surface. More recently, we further characterized the effect of moisture at the fingertip by measuring the alterations of this value during object manipulation (André et al. 2008) and by studying its effect on the skin's static friction coefficient (André et al. 2009). In the latter study, we reported a strong influence of moisture level on friction which is especially noticeable for a low level of normal force, at which an optimal level of moisture maximizes friction. From a more mechanistic perspective, Adams et al. (2007) studied the coefficient of friction of the skin with a sphere sliding on the forearm. They compared skin behavior for different skin moisture levels and explained mechanically the role of moisture on the coefficient of friction. They distinguished three hydration states (dry, damp, and wet) and found a peak in coefficient of friction for damp skin. In the same way that Warman et al. (2009) analyzed the effects of fingerprints on fingertip friction, a model of the fingertip skin mechanical properties should be developed and should integrate the role of moisture.

Previous studies have not taken into account variability in fingertip moisture level during object manipulation. In the present study, we continuously measured skin moisture level together with force exerted on an object and found that the grip force was actively and dynamically modulated with moisture level variations. Figure 5-6 illustrates both moisture and grip force level variations in one subject. As can be seen, when fingertip moisture level starts at one extreme, it tended to increase or decrease to an intermediate value and this alteration in moisture was accompanied by a reduction of grip force. In addition, when fingertip moisture started at an intermediate level, moisture did not tend to increase or decrease and grip force remained constant (Figure 5-6, middle column). This tendency for moisture level to reach an intermediate value with a concomitant decrease in grip force was confirmed for all the subjects (Table 5-3). Moreover, it was shown that the grip force decrease was not due to repetition of the task (no block effect in Table 5-2).

Adams and Hunter (1969) studied the effects of sweat secretion via stimulation of the peripheral plantar nerve on footpad skin friction of anesthetized cats. They showed that the lowest levels of sweat secretion produced the greatest increases in friction. These results may be explained by changes in the stratum corneum, which becomes more pliable with increasing moisture level and more deformed by tangential forces. In the same study it was also reported that higher steady-state rates of sweating progressively decreased skin friction. Finally, in agreement with earlier studies (Darrow 1936; Weiner and Hellman 1960; Buettner 1965), Adams and Hunther (1969) confirmed that, rather than playing a strictly thermoregulatory role, sweat gland activity in the tactile skin modifies cutaneous mechanical properties. Later, Adelman et al. (1975) showed that sweating on the paws and palms serves several functions, all of which are advantageous to the exercising animal - it increases friction, toughness of the skin, and tactile sensitivity. Moreover, they postulated that this sweating prepared the animal to flee from stressful situations. Physiological adaptation of the palmar sweating function can theoretically be translated to humans in the context of fine pinch grip in the manipulation of small objects.

In our experiment, fingertip moisture level presented variability when performing a task and tended to stabilize by the end of each block (Figure 5-4). Additionally, when the moisture level was stable, the final value ranged from 6.5 to 8.5 a.u., whereas when it was more variable, it tended toward this range of values. Interestingly, this range can be considered optimal with respect to friction. Indeed, we have shown (André et al. 2009) that fingertip friction was maximal for moisture values ranging from 6.5 to 8.5 a.u.; with an estimated friction maximum at 7.8 a.u. Remarkably, the present data (Figure 5-7) show that the moisture value at which GFs was minimal was 7.75 a.u., and that most of the data points (62.5%) of Figure 5-7 were concentrated around this value (6.5-8.5 a.u.). The r-squared presented on Figure 5-7 is equal to 0.45 which means that 55% of the variation in grip force is due to factors other than moisture, such as the variability in the execution of the task both within and across subjects. One can observe that sweating rate always evolved toward the optimal level of moisture with respect to skin frictional properties at fingertip. Different mechanisms of active or passive regulation can be suggested at a peripheral or central level. Indeed, the regulation could be purely passive with the increase in moisture arising from occlusion at the finger-object interface when the baseline skin hydration is low and the decrease in moisture resulting from reabsorption when skin hydration is high. Another possible mechanism would be a peripheral control of the sweating gland rate that would be controlled to optimize friction. Finally, the possible control of the fingertip sweat gland activity by the central nervous system cannot be ruled out but remains speculative. Further investigations on the mechanisms of modulation of fingertip sweat are necessary to clarify this question.

It has been well described in the literature that the frictional conditions at fingertip-object interface are coded during the loading phase when performing a grip lift task (Johansson and Westling 1984b; Johansson and Westling 1984a; Johansson and Westling 1987; Johansson 1991). Stress of the skin deforms the mechanoreceptors and the microslips occurring on the border of the contact surface (called incipient slips) allow humans to code friction and adjust grip force accordingly. In our task, the dynamic phase, during which the manipulandum moved, caused skin deformation and most likely microslips. This could allow subject to "reestimate" fingertip-object friction. However, the range of GFs exerted by subjects during the task in the present study was above 3.5N which is a level of normal force we previously found associated with the moderate influence of moisture on fingertip friction (André et al. 2009). Using a method we previously developed (see André et al. 2009), we could estimate the coefficient of friction for two extreme values of GFs found in our present data. At one extreme, when the moisture was low (5 a.u.), the GFs found with the quadratic regression (Figure 5-7) was high (14.85 N). The estimated coefficient of friction was 0.4 for these conditions. On the other hand, when moisture level was optimal (7.75 a.u.), the GFs was low (6.22 N) and the estimated coefficient of friction was 0.64. We can therefore postulate that the adaptation of GFs exerted by subjects in the present study in response to moisture variation was highly sensitive: a decrease in friction of about 37.5% (from 0.64 to 0.4) was associated with an increase of about 138% in GFs (from 6.22 to 14.85 N). It is possible that this high sensitivity is a "safe" strategy used by the subjects to overcome the dramatic effect of extreme values of moisture on grip stability. Indeed, it appears that the subjects' grip adjustment was overcompensated in response to the effects of friction variation. It is also possible that at both extremes (very high and very low moisture levels) the certainty in friction estimation is more ambiguous and a greater GFs is required again as a "safe" strategy. One of the most exciting implications of this study is that the central nervous system might discern moisture level changes during object manipulation and make the necessary adjustments in grip force. The mechanism by which this information is communicated has still to be defined and is of interest for future study. Finally, it is worth noting that we tested only one surface and cannot make conclusions about the interaction between the changes in friction due to surface or moisture.

In conclusion, we found that moisture level was modulated in order to optimize skin mechanical properties. The physiological mechanism regulating moisture at fingertip still remains to be further investigated. In parallel, GFs decreased when moisture levels tended toward an optimal value. The present data show clear evidence for a continuous modulation of GFs with skin moisture variation. Our results suggest that sweat rate is modulated to optimize skin moisture and that the moisture level variation is taken into account to adequately adjust GFs.

Chapter 6

CONCLUSION AND PERSPECTIVES

"I thought I would have a quiet pint ... and about 17 noisy ones."

Gareth Chilcott (1993)

Fingertip mechanoreceptors are stimulated by skin deformation and send signals to the brain, which integrates these inputs to efficiently control the forces exerted by the finger on the held object. In addition to informing the CNS about an object's properties, tactile signals allow internal models to be updated considering any physical or dynamical object change. Within this context, we mainly focused on the influence of the skin moisture content on the skin physical properties and on the motor control of the grip during object manipulation. In this thesis, we described the skin surface deformation and the effects of moisture on this deformation during loading and slipping; we developed a new task-specific instrument to continuously measure skin moisture in the precision grip configuration; we determined a method to estimate the skin friction when manipulating an object; and we showed that the grip control integrates changes in skin moisture content during dexterous manipulation.

Main findings and new hypothesis

Although skin deformation has been studied by numerous authors, very few studies have addressed the effect of tangential strain on the skin surface deformation at the interface of the skin with another surface. Even fewer studies have assessed the effects of moisture content on this deformation. In Chapter 2, we described the effects of moisture content on index fingertip deformation during the tangential loading phase preceding complete slippage against a flat surface. The stick ratio was introduced, and we showed that for a given stick ratio, the relative increment in tangential force needed before complete slippage depended on the moisture content, with earlier slippage occurring for dry skin. We therefore hypothesized that it was less safe to manipulate an object with dry skin than with well-hydrated skin, since hydrated skin deforms more gradually than dry skin. Nevertheless, no instrument had previously been developed to continuously measure the skin moisture content at the interface between the fingertips and an object held in precision grip.

Therefore, in Chapter 3 we focused on developing, calibrating, and validating a task-specific instrument to measure fingertip skin hydration. This conductance-based instrument (Moisture-Evaluator) is comprised of a network of electrodes fixed to an adapted probe and an electronic circuit. By comparing measurements from the Moisture-Evaluator and Corneometer® (a commercial device used in the field of dermatology), we calibrated and validated our device. We found a very strong correlation between the two instruments, with the Moisture-Evaluator being minimally influenced by the normal force exerted by the finger on the probe.

Using the Moisture-Evaluator, we proposed a new method to continuously estimate the fingertip skin friction (Chapter 4). We first showed that the normal force exerted by the fingers on an object held in precision grip strongly influenced the skin friction, and found the optimal moisture level that maximized the skin friction at a low level of normal force. Finally, we described a novel method to estimate fingertip friction using the normal force and moisture content measurements. In the last chapter (Chapter 5), subjects performed a horizontal point-to-point task, and we recorded the grip force exerted on the object held and the fingertip moisture content. We determined the optimal moisture level that minimized the grip force, which was equal to the moisture value maximizing the friction. Moreover, we proved that the subjects' fingertip moisture always tended toward this optimal level, and that the grip force was continuously adapted to the moisture variation. Finally, we showed that subjects with dry or very wet skin overcompensated for the frictional variation by presenting a greater safety margin.

These results led us to some new questions and hypotheses. First, published studies frequently indicate that the CNS uses the partial slippage at the contact surface between the fingertips and an object to determine the object's friction. Nevertheless, we showed that when moving an object held in precision grip, the grip control overcompensated for the frictional variation due to a moisture level change. Consequently, the safety margin was higher for subjects with dry skin. In parallel, we also demonstrated that for a given stick ratio, fingertip slippage occurs earlier for dry skin. We hypothesize that the overcompensation observed in the manipulative task is a safe strategy to compensate for dry skin mechanical behavior and to prevent object slippage. Moreover, it could be interesting to question the previous assumption stating that the CNS uses the partial slippage to code friction. Indeed, when partial slipping occurs, the shearing stress on the stuck contact area increases, and the CNS could also use this information to evaluate friction and to anticipate complete slip risk. It is worth mentioning that the skin deformation is maximal on the border between slipping contact area and stuck contact area. As a consequence, mechanoreceptors could be more activated in this region and that could be taken into account by the CNS.

Second, we observed that the fingertip moisture content evolves toward the optimal level that maximizes skin friction. But what are the mechanisms that control and allow optimal moisture modulation? Several authors have previously shown that the palmar eccrine sweat glands are more sensitive to emotional stimuli (Kerassidis 1994) and that they potentially increase friction (Adams and Hunter 1969; Adelman et al. 1975). From our data, different hypotheses can be made. One possibility is passive regulation, with increased moisture due to occlusion at fingertip/object interface or decreased moisture due to reabsorption when the moisture level is high. Another possibility is active CNS control, which would regulate the sweat gland rate to optimize fingertip friction. It could also be hypothesized that an efference copy of the sweat motor command would be sent to the internal forward model and/or grip controller to account for changes in fingertip moisture content. This would explain the continuous modulation of grip force with the moisture level, given that friction is estimated using moisture variation predictions.

Finally, we began to analyze the differences in EEG responses between partial and complete slippage at the fingertip (see Appendix 1). These data revealed intensity variations in the evoked-potential responses between the partial and complete slippage scenarios. Moreover, we showed that we could quantify the size of the partial slippage using the stick ratio parameter, and that the CNS probably uses this partial slippage to code fingertip friction. We hypothesized that the intensity of the evoked-potential could be correlated to the quantity of partial slippage, which helps the brain to better estimate the likelihood that an object will slip.

Limitations and future investigations

The experiments and results detailed in this thesis had some limitations, which led us to design new experimental setups and consider new experiments to be performed. When we studied the skin surface (Chapter 2), we asked the subject to perform slippages with their index finger on a glass surface. Subjects had visual feedback and were asked to keep the normal force exerted by their finger as constant as possible. Nevertheless, we did not control the normal force, tangential force rate, angle between the fingertip and the surface, or slippage velocity. We did not continuously measure the fingertip moisture and did not test different surface structures (bump, hole, texture variations, etc.). Such enhancements would allow better control of the fingertip pressure distribution and help avoid fingertip roll. A better model of the skin surface could be found by determining the stiffness and viscosity, or an FE model could be developed. We could also study ridge deformation using a video camera with a stronger resolution. Accordingly, a new platform is being developed in collaboration with the Scuola Superiore Sant'Anna. This Skin Moisture Platform will allow complete control of the forces exerted and the fingertip positions; a complete range of translational and rotational movements of the surface in contact with fingertip; improved resolution and frequency acquisition to enhance video recording; continuous measurement of fingertip moisture; and different surface textures. We plan to study the life span of skin deformation under a linear tangential strain, to perform rotation of the contact surface, to better model the surface skin deformation, and to study CNS activity under different deformation conditions.

Further investigations to enhance the Moisture-Evaluator (Chapter 3) could also be performed. After long-term tool use, we observed notable instrument corrosion, mainly due to mechanical usury that removed the gold layer and due to the chemical reaction between the electrodes and the ions in sweat. To avoid contact between the skin and electrodes, we could develop an instrument based on the capacitance principle, with a thin isolator layer prohibiting this contact. The dielectric constant of the system would be influenced by the moisture content of the skin touching the probe. Nevertheless, this design would require a completely different electronic circuit, such as one based on an RLC circuit for which the resonance frequency could be measured. This design would require the use of a high-frequency circuit, since the capacitance variation would be on the order of picofarads. These kinds of circuits are complicated to design, because all parasitic capacitances must be considered and their effects minimized. Moreover, the circuits must be manufactured using clean-rooms. Presently, the Moisture-Evaluator measures the conductance of the contact region between the fingertip and the probe. Nevertheless, further investigations could evaluate the total impedance of this region. It could also be interesting to differentiate the impedance of the skin and the impedance of the interface skin/probe. Indeed, the skin impedance model used in chapter 3 is simplified comparing to the complete model that takes into account impedance of both skin and interface skin/probe. More tests could be performed to try to improve the Moisture-Evaluator: use smaller probe to decrease the influence of the contact surface, design another probe that aims at measuring both moisture and contact surface, replace gold with platinum, describe and evaluate the influence of experiments conditions

When studying the effect of moisture content on the grip strategy (Chapter 5), we used a 260-g manipulandum. Considering this weight and the grip force exerted by subjects, we observed that the effect of moisture on the frictional variation was attenuated due to the range of the normal force. Further experiments could be performed using a newly designed manipulandum with a smaller weight. The grip force exerted would be smaller and the moisture variations would strongly influence the frictional variation. The adaptation of the grip force with friction could be further studied. Moreover, none of our subjects covered the whole range of moisture levels. It would be interesting to analyze the grip modulation of various individual subjects covering a large range of moisture levels or subjects with diabetes (neuropathology of the non-myelinated fibers, the peripheral parasympathetic system is impaired). Eccrine sweat secretion at the fingertip is mainly induced by emotive stimuli (Kerassidis 1994). We could study grip modulation due to sweat rate variations when a stressful situation is provoked during performance of a dexterous manipulation task. For instance, during the manipulation task, the subject would have to answer questions in a short period of time to receive rewards. We could also show emotional images or movies to induce greater sweat gland activity. In order to locally change the fingertip moisture level, injections of hormones could be administrated in order to increase or decrease the sweating rate and to observe whether the precision grip control is modulated. If grip force changed with moisture, it could be an indication that the grip force modulation is a consequence of moisture change. Indeed, even if the causality between grip force modulation and the moisture variation is likely, our data does not allow to exclude the hypothesis that the variation of grip force and moisture are both the consequence of another variable. We could also increase the acquisition frequency of the fingertip moisture in order to detect the sweat secretion waves induced by the myoepithelium contractions and controlled by the CNS. The latter observation could be an indicator for a central control of the sweat secretion aiming at an increase of fingertip friction.

Another possibility would be to control and/or change the sympathetic nervous system activity. Several authors have shown that microgravity alters the sympathetic nerve activity, increasing the sympathetic response to Valsalva straining (Cox et al. 2002) and suppressing muscle sympathetic activity when subjects are quietly seated with their knee joints extended during the microgravity phase of parabolic flights (Iwase et al. 1999). Recently, Shibasaki et al. (2006) presented different studies showing that microgravity decreases the sweat rate for a given internal temperature and changes the thermoregulative control of eccrine sweat glands. These observations provide evidence that measuring fingertip moisture is of primary importance when studying dexterous manipulation on Earth or in space. Adaptations of the sympathetic nervous system to long-term microgravity exposure cannot be ignored, and changes in sweat activity should be measured.

Current investigations in the field of robotic and prostheses

Finally, some of the current advances in robotics and prostheses will be briefly presented in this section, with the goal of representing why improved knowledge of the human tactile system is of primary importance when designing an efficient tool that can mimic the hand. As Richard Crowder (2006) recently stated: “a key advance for new robots is the development of sensors or set of sensors that can replicate the human sense of touch”. Howe et al. (1989) first investigated a sensor to detect incipient slip, based on a thin rubber skin covering a soft inner layer of foam rubber (Figure 6-1.A). An accelerometer attached to the inner skin surface measured large local accelerations. They proved that sensing skin acceleration is an effective and reliable method to detect incipient slip. Tremblay and Cutkosky (1993) later developed a sensor to detect incipient slip using an artificial skin covered with “nibs”; when the finger was about to slip, some of the lightly loaded nibs near the periphery broke free and vibrated. Two accelerometers measured these skin vibrations (Figure 6-1.B).

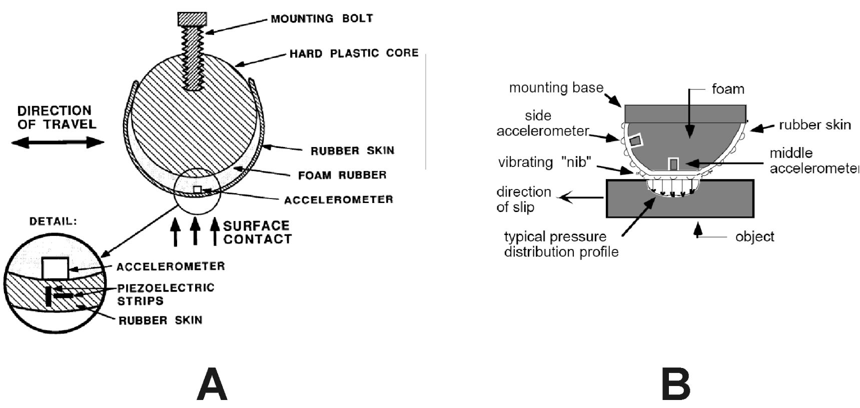

Figure 6-1 : The system developed by Howe et al. (A) and Tremblay and Cutkosky (B).

Others have sought to develop thin and flexible films that act as an artificial electronic skin that can be bonded to any instrument. Someya et al. (2004; 2005) presented an artificial skin consisting of a matrix of pressure sensors (Figure 6-2.A). The pressure sensors were based on organic field-effect transistors and pressure-sensitive rubber sheets, in which the resistance changes when a pressure is applied to the device. As a consequence, the electrical characteristics of the transistor changed with the pressure applied. The complete matrix of sensors, called the "E-skin", formed a thin film that had a large area and mechanical flexibility. Maheshwari and Saraf (2006) developed a large, thin-film device such that the change in current density through the film and the electroluminescent light intensity were linearly proportional to the local stress. More recently, Edin et al. (2008) developed a contact sensor that could be applied to the surface of a robotic finger and that was sensitive to indentation and had a spatial resolution comparable to that of human glabrous skin. The contact sensor comprised two Kapton layers with embedded copper electrodes spaced by two layers of foam with an upper thick silicone layer (Figure 6-2.B1).

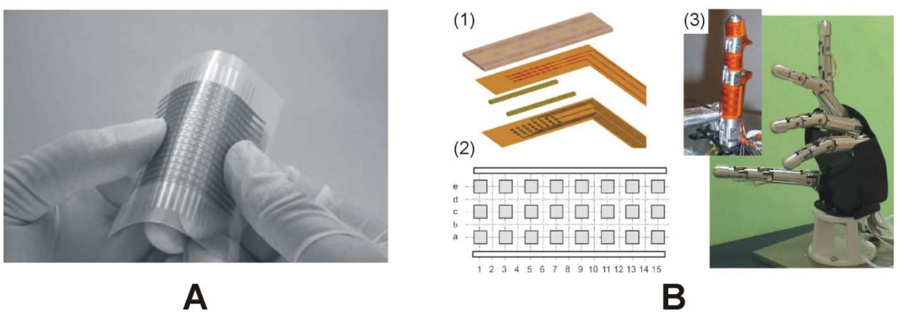

Figure 6-2 : The E-skin (A) and the contact sensor developed by Edin et al. (B)

Others have developed completely integrated fingers with embedded sensors. Hosada et al. (2006) designed an anthropomorphic robotic soft fingertip with randomly distributed receptors (Figure 6-3.A). It consisted of a metal bar (which represented the bone), a body, and a skin layer, inspired by the structure of the human finger. The randomly distributed receptors were strain gauges and PVDF films. The anthropomorphic fingertip was mounted on a robot and slipped against different materials. They differentiated between the materials using the output of the strain gauges and the signal variance from the PVDF films.

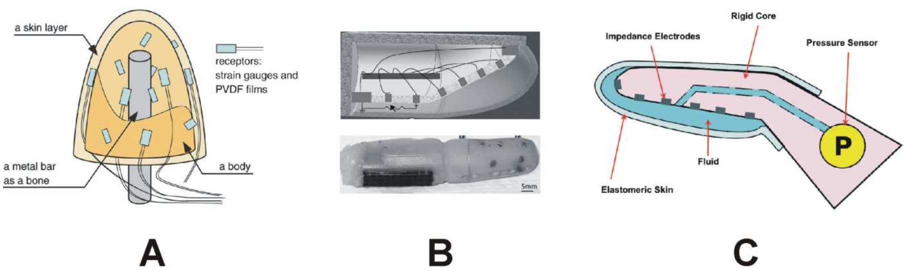

Figure 6-3 : The artificial fingertips developed by Hosada et al. (A), Wettels et al. (B) and Fischel et al. (C).

Wettels et al. (2008) developed a tactile sensor array that mimicked the mechanical properties and distributed touch receptors of the human fingertip. This array consisted of a rigid core surrounded by a weakly conductive fluid contained within an elastomeric skin (Figure 6-3.B). External forces deformed the fluid path around the electrodes, resulting in a distributed pattern of impedance changes containing information about those forces and the objects that applied them. Finally, Fischel et al. (2008) presented an artificial fingertip based on pressure variations due to vibration (Figure 6-3.C). Performing slippages with the artificial fingertip, they showed that the power spectral density of the pressure measurement provided information about the presence of slipping, the normal force exerted, and the sliding velocity. Some groups have also worked on developing artificial fingers without receptors, but that maximally mimic the skin properties (Shao et al. 2009).

Cybernetic hands already exist (Figure 6-2.B3) (Carrozza et al. 2006) and are now integrated with sensor systems to mimic the human hand as well as possible. However, substantial work remains. The anthropomorphic dexterous robot hand DLR-Hand II (Figure 6-4) is comprised of four fingers, each containing position, velocity, and torque sensors (Butterfab et al. 2001). The three independent joints of each finger are equipped with actuators, which essentially consist of brushless dc-motors, tooth belts, harmonic drive gears, and bevel gears. Each fingertip includes a first layer of rubber skin and a tiny six-dimensional force torque sensor that allows force measurement at the finger-object interface. Although lacking an advanced sensory system, the DLR-Hand II shows very robust and efficient results when performing precision grip tasks with small and fragile objects (Borst et al. 2003).

Figure 6-4 : The DLR-Hand II

Chapter 7 - APPENDIX I:

ARE EEG RESPONSES TO LOAD FORCE VARIATIONS INFLUENCED BY THE SLIPPING OF OBJECTS DURING MANIPULATION?

Presented as a poster at the 38th Annual Meeting of the Society for Neuroscience, Washington, USA (2008) and adapted from the proceeding **"Does slippage influence the EEG response to load force variations during object manipulation?"**, André T., Delbeke J., Lefèvre P. and Thonnard J-L. IFMBE Proceedings; Vol. 22. 4th European Conference of the International Federation for Medical and Biomedical Engineering (2008): 2097-2100.

Abstract

During object manipulation, sensory information from fingertip skin mechanoreceptors is of primary importance to correctly modulate grip forces according to load force (LF) variations. Here, we investigated the EEG responses to LF transients with and without slippage of a pinched object. Subjects used the precision grip to maintain a manipulandum mounted to a

mechanical device, which generated LF variations at the fingertips. The EEG was recorded synchronously. There were two types of LF variations: short-range variations without slippage (NS-task) and large variations generating finger slippage along the pinched object (S-task). We observed several differences between the somatosensory evoked potentials (SEP) related to LF transients with or without slippage. In addition to marked shape differences, a significant increase in the amplitude of the SEPs was observed during the S-task. Despite the small numbers involved and the noisy signals, very similar findings in all subjects indicated that the cortical information related to LF variations is clearly different depending on whether the manipulated object is slipping or not.

Introduction

When moving a hand-held object, the grip force is automatically modulated in parallel with fluctuations in the load force (LF) generated by the weight and acceleration of the object (Flanagan and Wing 1995). The grip force must be adapted to avoid object slippage, and sensory information is critical in this process. The performance of a subject dramatically decreases when the cutaneous feedback is suppressed by locally anesthetizing the thumb and index finger (Augurelle et al. 2003b). Human digital skin receptors generate bursts of activity on contact with an object during grasp. Microneurography provides information on such feedback signals provided by hand skin receptors during precision grip (Johansson and Westling 1987). Srinivasan et al. (1990) explored the tactile detection of slip in humans and monkeys using psychophysical and neurophysiological experiments, respectively, and found that specific neural codes indicated slip or the direction of skin stretch. Kourtis et al.

(2008) studied the anticipatory and reactive EEG responses of participants who were instructed to hold an object without letting it slip during load perturbations. They found an N58-P58 evoked response potential complex that was modulated by the preparation state.

Here, we investigated the EEG response to load variations with or without slippage of a pinched object.

Methods

Subjects

Eleven subjects (5 males and 6 females; aged 20-23 years) participated in this study. They washed their hands 15 minutes before the beginning of the experiment. None of them had a prior history of any neurological disorder. All gave their informed consent before the experiment and the experimental protocol was approved by the local ethics committee.

Recordings and materials

For somatosensory evoked potentials (SEPs), electroencephalographic (EEG) signals were recorded from 15 electrodes using an average reference (silver/silver chloride electrodes placed according to the international 10/20 system), bandpass-filtered between a 5-s time constant and a 1-kHz anti-aliasing filter and sampled at 2 kHz. The Biosemi software was used. A square trigger pulse recorded in the status channel provided synchronization between the EEG signals and the stimulus.

The mechanical stimulations applied to the fingertip skin were generated by a linear motor (Figure 7-1.A). An instrumented object equipped with force-torque transducers (Mini40 F/T transducer; ATI Industrial Automation, NC, USA) was linked to the mobile stage of the linear motor (NLS4 Series Precision Linear Stage, 6'' Travel, Newmark System Inc, CA, USA). Signals from the force-torque transducers were digitized on-line at 1000 Hz by a 12-bit 6071E analog-to-digital converter in a PXI chassis (National Instruments, Austin, TX, USA). A specific software program (written with CVI-LabWindows) acquired these digitized signals, controlled the displacement and velocity of the linear motor, and produced the trigger signal recorded with the EEG.

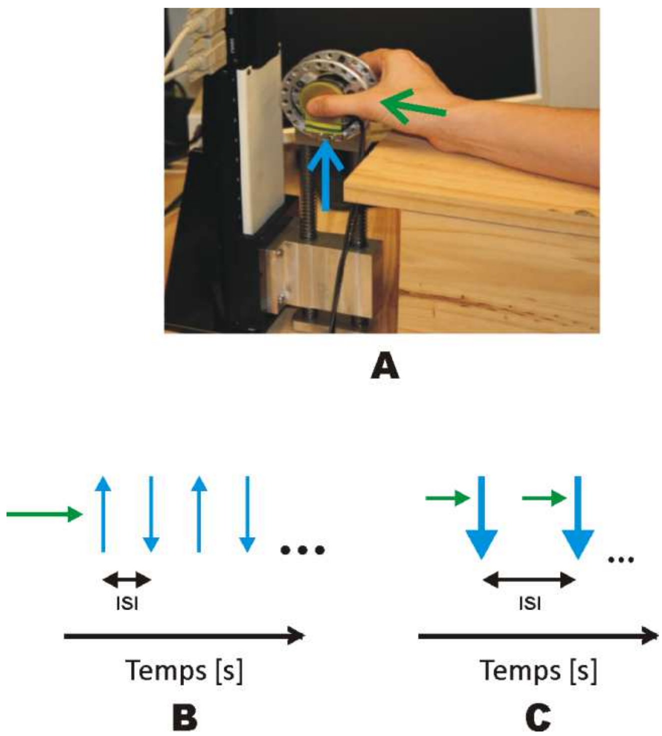

Figure 7-1 : A- Illustration of the general set up. B- The NS-task. C- The S-task.

Experimental design and mechanical stimulations

General set-up. Subjects were seated comfortably with their arm and wrist resting on a wooden support. They gripped the instrumented object between their thumb and index finger (Figure 7-1.A). Subjects were instructed to stare at a neutral visual target during the whole experiment and could not see the manipulandum or their hand. They had an audio helmet producing a white noise that masked sound in both ears to eliminate any acoustic stimulation.

NS-task. Fast upward and downward, vertical, 1-mm displacements of the hand-held object were produced by the linear motor, resulting in tangential mechanical stress of the skin without slippage. Two blocks of 100 upward/downward displacements were performed. The time delay between stimuli (ISI: inter-stimulus interval) varied randomly from 2.5 to 4 s (see Figure 7-1.B).

S-task. Subjects were instructed to exert a constant grip force, but were not provided a feedback of the grip force exerted. After an unknown delay of 8.5 to 10 s, the linear motor generated a fast downward displacement that caused the object to slip over the fingertip skin (see Figure 7-1.C). This experiment was repeated 100 times with each subject (2 blocks of 50 slippages).

Data analysis

Original EEG data, from which trials with eye-blinks, other excessive eye movements, or muscle artifacts had been excluded, were filtered with a digital zero-phase filter (Finite Impulse Response filter, pass band 0.2 to 30

Hz). The responses were averaged. Each sample started 500 ms before and ended 1500 ms after the stimulus.

Results

Figure 7-2 shows the average responses at electrode Cz (average reference) to a lateral stretch of the skin without (NS-task) or with (S-task) slippage for all subjects. ERP components P80, N90, P120, N200, and P300 were easily identified. The amplitude of the component varied between tasks. For P120 and N200, the peaks were greater for S-task than for NS-task, but the positive peak P300 was greater for NS-task. Moreover, an important long-latency activity was observed for S-task.

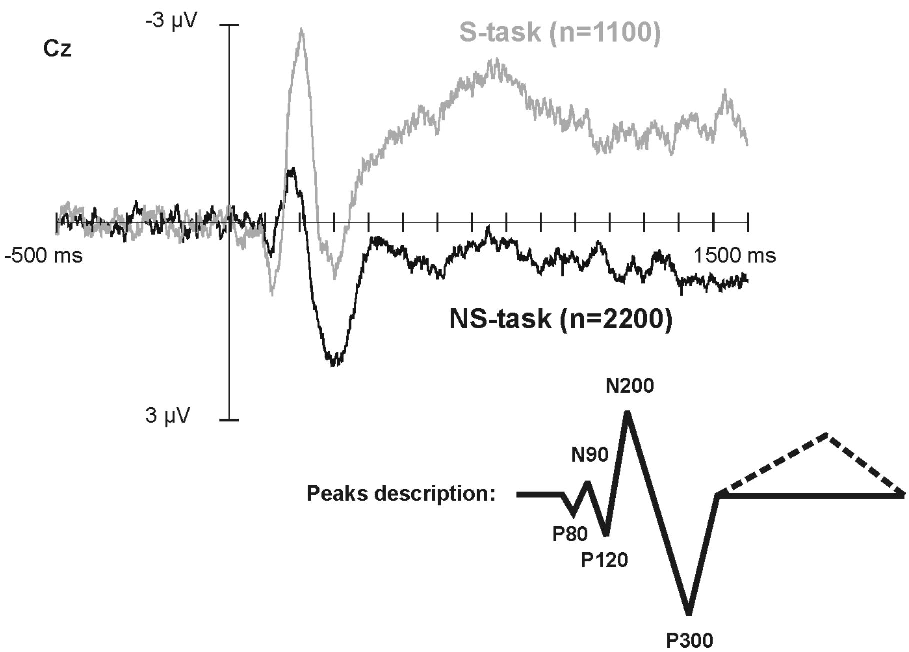

Figure 7-2 : Average of all subjects for NS-task and S-task

Figure 7-3 shows the topography associated with the average trace presented on Figure 7-2. There were small differences in the topography for components N90, P120, and N200, but the EEG profiles for NS-task and S-task presented significant differences for the P80 and P300 components.

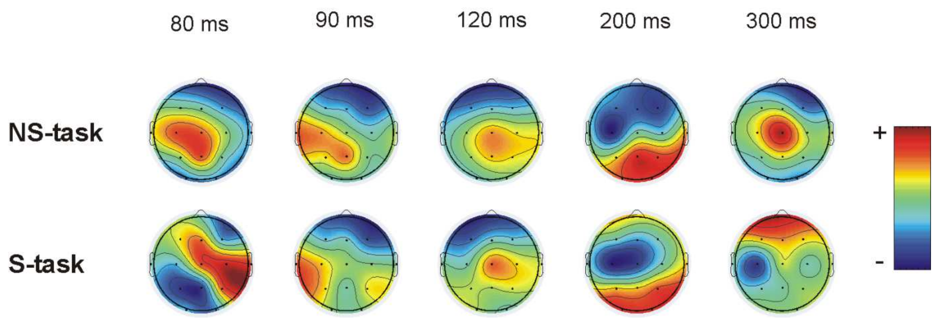

Figure 7-3 : Topography corresponding to the grand-average

Finally, the effects of the normal force and moisture were analyzed for some individual subjects presenting interesting differences in the normal force exerted or important fingertip moisture variations (Figure 7-4). The normal force exerted on the object and fingertip moisture (or frictional coefficient) did not influence the EEG responses, whatever the task.

Discussion

The aim of this study was to assess whether the presence of slippage influences the SEPs related to fingertip lateral skin deformation.

Important differences in the EEG profiles and amplitude ranges were shown. These preliminary results indicate that the neural information is different depending on the presence of slip.

The effects of slip on SEP have not been studied in great depth. Srinivasan et al. (1990) described the neural codes caused by slippage and dealt with slippage detection, but no previous work has analyzed the cortical activity caused by slippage. We showed that the SEP profiles related to 'lateral skin deformation with slippage' tactile stimuli were different from those profiles related to classical tactile stimulation previously described.

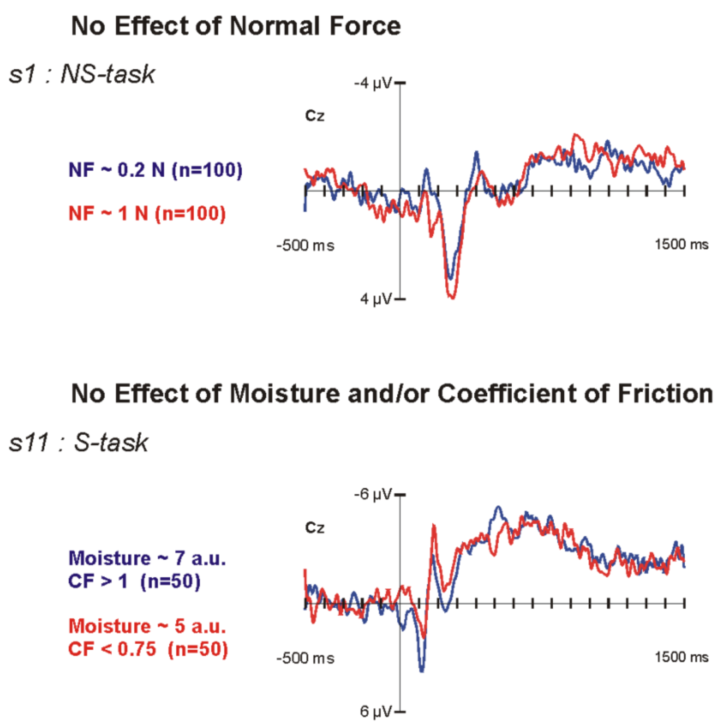

Figure 7-4 : Effects of normal force and moisture on the EEG profiles

This preliminary study should be improved before firm conclusions can be made. Such improvements include an increased number of subjects, allowing for improved statistical evaluation, and a reduction in noise by increasing the sample number. However, we must first ensure that habituation would not fade out the responses. The evoked potentials observed have relatively long latencies, indicating that they are most likely generated by cognitive processes. Therefore, the exact task is of major importance and variations in the paradigm could help to pinpoint the real significance of the results. A source localization effort would also be helpful.

REFERENCES

Adams MJ, Briscoe BJ, and Johnson SA. Friction and lubrication of human skin. *Tribology Letters* 26: 239-253, 2007.

Adams T, and Hunter WS. Modification of skin mechanical properties by eccrine sweat gland activity. *J Appl Physiol* 26: 417-419, 1969.

Adelman S, Taylor CR, and Heglund NC. Sweating on paws and palms: what is its function? *Am J Physiol* 229: 1400-1402, 1975.

Alanen E, Nuutinen J, Nicklén K, Lahtinen T, and Mönkkönen J. Measurement of hydration in the stratum corneum with the MoistureMeter and comparison with the Corneometer. *Skin Res Technol* 10: 32-37, 2004.

André T, Lefèvre P, and Thonnard JL. A continuous measure of fingertip friction during precision grip. *J Neurosci Methods* 179: 224-229, 2009.

André T, Lefèvre P, and Thonnard JL. Fingertip moisture is optimally modulated during object manipulation. *J Neurophysiol* 103: 402-408, 2010.

André T, Dewan M, Lefèvre P, and Thonnard J-L. Moisture Evaluator: a direct measure of fingertip skin hydration during object manipulation. *Skin Res Technol* 14: 385-389, 2008.

Atkeson CG. Learning arm kinematics and dynamics. *Annu Rev Neurosci* 12: 157-183, 1989.

Augurelle AS, Penta M, White O, and Thonnard JL. The effects of a change in gravity on the dynamics of prehension. *Exp Brain Res* 148: 533-540, 2003a.

Augurelle AS, Smith AM, Lejeune T, and Thonnard JL. Importance of cutaneous feedback in maintaining a secure grip during manipulation of hand-held objects. *J Neurophysiol* 89: 665-671, 2003b.

Barel AO, and Clarys P. In vitro calibration of the capacitance method (Corneometer CM 825) and conductance method (Skicon-200) for the evaluation of the hydration state of the skin. *Skin Res Technol* 3: 107-113, 1997.

Birznieks I, Jenmalm P, Goodwin AW, and Johansson RS. Encoding of direction of fingertip forces by human tactile afferents. *J Neurosci* 21: 8222-8237, 2001.

Birznieks I, Macefield VG, Westling G, and Johansson RS. Slowly adapting mechanoreceptors in the borders of the human fingernail encode fingertip forces. *J Neurosci* 29: 9370-9379, 2009.

Birznieks I, Wheat HE, Redmond SJ, Salo LM, Lovell NH, and Goodwin AW. Encoding of tangential torque in responses of tactile afferent fibres innervating the monkey's fingerpad. *J Physiol* 2010.

Blau PJ. The significance and use of friction coefficient. *Tribology International* 34: 585-591, 2001.

Bligh J. A thesis concerning the processes of secretion and discharge of sweat. *Environ Res* 1: 28-45, 1967.

Bolton CF, Winkelmann RK, and Dyck PJ. A quantitative study of Meissner's corpuscles in man. *Neurology* 16: 1-9, 1966.

Bonola A, Caroli A, and Celli L. *La main*. Padova, Italia: Piccin Nuova Libraria, 1988.

Borst C, Fischer M, Haidacher S, Liu H, and Hirzinger G. DLR Hand II: Experiment and Experiences with an Anthropomorphic Hand. *IEEE International Conference on Robotics and Automation* 702-707, 2003.

Bowden FP, and Tabor D. *Friction and lubrication*. London: Methuen, 1967.

Bowden FP, and Tabor D. *Friction. An introduction to tribology.* Krieger, Florida: 1982.

Buchholz B, Frederick LJ, and Armstrong TJ. An investigation of human palmar skin friction and the effects of materials, pinch force and moisture. *Ergonomics* 31: 317-325, 1988.

Buettner KJK. The moisture of human skin as affected by water transfer. *J Soc Cosmetic Chemists* 16: 133-143, 1965.

Butterfab J, Grebenstein M, Liu H, and Hirzinger G. DLR-Hand II: Next Generation of Dextrous Robot Hand. *IEEE International Conference on Robotics and Automation* 109-114, 2001.

Cadoret G, and Smith AM. Friction, not texture, dictates grip forces used during object manipulation. *J Neurophysiol* 75: 1963-1969, 1996.

Carrozza MC, Cappiello G, Micera S, Edin BB, Beccai L, and Cipriani C. Design of a cybernetic hand for perception and action. *Biological Cybernetics* 95: 629-644, 2006.

Castiello U. The neuroscience of grasping. *Nat Rev Neurosci* 6: 726-736, 2005.

Cohen JC, Makous JC, and Bolanowski SJ. Under which conditions do the skin and probe decouple during sinusoidal vibrations? *Exp Brain Res* 129: 211-217, 1999.

Cole KJ. Grasp force control in older adults. *J Mot Behav* 23: 251-258, 1991.

Cole KJ, and Johansson RS. Friction at the digit-object interface scales the sensorimotor transformation for grip responses to pulling loads. *Exp Brain Res* 95: 523-532, 1993.

Collins K. In: *A textbook of Clinical Disorders of the Autonomic Nervous System*. Oxford, New York, Toronto: Oxford University Press, pp. 1988.

Comaish S, and Bottoms E. The skin and friction: deviations from Amontons' laws, and the effects of hydration and lubrication. *Br J Dermatol* 84: 37-43, 1971.

Cox JF, Tahvanainen KU, Kuusela TA, Levine BD, Cooke WH, Mano T, Iwase S, Saito M, Sugiyama Y, Ertl AC, Biaggioni I, Diedrich A, Robertson RM, Zuckerman JH, Lane LD, Ray CA, White RJ, Pawelczyk JA, Buckey JC, Jr., Baisch FJ, Blomqvist CG, Robertson D, and Eckberg DL. Influence of microgravity on astronauts' sympathetic and vagal responses to Valsalva's manoeuvre. *J Physiol* 538: 309-320, 2002.

Crevecoeur F, Thonnard JL, and Lefevre P. Forward models of inertial loads in weightlessness. *Neuroscience* 161: 589-598, 2009a.

Crevecoeur F, Thonnard JL, and Lefevre P. Optimal integration of gravity in trajectory planning of vertical pointing movements. *J Neurophysiol* 102: 786-796, 2009b.

Critchley HD, Elliott R, Mathias CJ, and Dolan RJ. Neural activity relating to generation and representation of galvanic skin conductance responses: a functional magnetic resonance imaging study. *J Neurosci* 20: 3033-3040, 2000.

Crowder R. Applied physics - Toward robots that can sense texture by touch. *Science* 312: 1478-1479, 2006.

Daly CH. Biomechanical properties of dermis. *J Invest Dermatol* 79 Suppl 1: 17s-20s, 1982.

Danion F, Descoins M, and Bootsma RJ. When the fingers need to act faster than the arm: coordination between grip force and load force during oscillation of a hand-held object. *Exp Brain Res* 193: 85-94, 2009.

Danion F, and Sarlegna FR. Can the human brain predict the consequences of arm movement corrections when transporting an object? Hints from grip force adjustments. *J Neurosci* 27: 12839-12843, 2007.

Darrow CW. The galvanic skin reflex (sweating) and blood pressure as preparatory and facilitative function. *Psychol Bull* 33: 73-94, 1936.

Davidson PR, and Wolpert DM. Internal models underlying grasp can be additively combined. *Exp Brain Res* 155: 334-340, 2004.

Derler S, Kausch F, and Huber R. Analysis of factors influencing the friction coefficients of shoe sole materials. *Safety Science* 46: 822-832, 2008.

Derler S, Schrade U, and Gerhardt L-C. Tribology of human skin and mechanical skin equivalents in contact with textiles. *Wear* 263: 1112-1116, 2007.

Desmurget M, Pelisson D, Rossetti Y, and Prablanc C. From eye to hand: planning goal-directed movements. *Neurosci Biobehav Rev* 22: 761-788, 1998.

Dinç OS, Ettles CM, Calabrese SJ, and Scarton HA. Some parameters affecting tactile friction. *ASME Journal of Tribology* 113: 512-517, 1991.

Dizio P, and Lackner JR. Motor adaptation to Coriolis force perturbations of reaching movements: endpoint but not trajectory adaptation transfers to the nonexposed arm. *J Neurophysiol* 74: 1787-1792, 1995.

Edin BB, Ascari L, Beccai L, Roccella S, Cabibihan JJ, and Carrozza MC. Bio-inspired sensorization of a biomechatronic robot hand for the grasp-and-lift task. *Brain Res Bull* 75: 785-795, 2008.

Edin BB, Westling G, and Johansson RS. Independent control of human finger-tip forces at individual digits during precision lifting. *J Physiol* 450: 547-564, 1992.

Edwards C, and Marks R. Evaluation of biomechanical properties of human skin. *Clin Dermatol* 13: 375-380, 1995.

Fawcett D. *Text Book of Histology*. Philadelphia: W.B. Sauders Co., 1986.

Fishel JA, Santos VJ, and Loeb GE. A robust micro-vibration sensor for biomimetic fingertips. *International Conference on Biomedical Robotics and Biomechatronics* 659-663, 2008.

Flanagan JR, Bowman MC, and Johansson RS. Control strategies in object manipulation tasks. *Curr Opin Neurobiol* 16: 650-659, 2006.

Flanagan JR, and Lolley S. The inertial anisotropy of the arm is accurately predicted during movement planning. *J Neurosci* 21: 1361-1369, 2001.

Flanagan JR, and Tresilian JR. Grip-load force coupling: a general control strategy for transporting objects. *J Exp Psychol Hum Percept Perform* 20: 944-957, 1994.

Flanagan JR, and Wing AM. Modulation of grip force with load force during point-to-point arm movements. *Exp Brain Res* 95: 131-143, 1993.

Flanagan JR, and Wing AM. The role of internal models in motion planning and control: evidence from grip force adjustments during movements of hand-held loads. *J Neurosci* 17: 1519-1528, 1997.

Flanagan JR, and Wing AM. The stability of precision grip forces during cyclic arm movements with a hand-held load. *Exp Brain Res* 105: 455-464, 1995.

Flanagan JR, Wing AM, Allison S, and Spenceley A. Effects of surface texture on weight perception when lifting objects with a precision grip. *Percept Psychophys* 57: 282-290, 1995.

Flash T, and Hogan N. The coordination of arm movements: an experimentally confirmed mathematical model. *J Neurosci* 5: 1688-1703, 1985.

Fluhr J, Elsner P, Berardesca E, and Maibach HI. *Bioengineering of the skin: Water and the Stratum Corneum*. CRC PRESS, 2000.

Fluhr J, Gloor M, Lazzerini S, Kleesz P, Grieshaber R, and Berardesca E. Comparative study of five instruments measuring stratum corneum hydration (Corneometer CM 820 and CM 825, Skicon 200 Nova DPM 9003, DermaLab). Part I. In vitro. *Skin Res Technol* 5: 161-170, 1999.

Folk GE, Jr., and Semken HA, Jr. The evolution of sweat glands. *Int J Biometeorol* 35: 180-186, 1991.

Forrest WJ, and Basmajian JV. Functions of human thenar and hypothenar muscles; an electromyographic study of twenty-five hands. *J Bone Joint Surg Am* 47: 1585-1594, 1965.

Fung Y. *Biomechanics: Mechanical Properties of Living Tissue, 2nd ed.* New-York: Springer-Verlag, 1993.

Gee MG, Tomlins P, Calver A, Darling RH, and Rides M. A new friction measurement system for the frictional component of touch. *Wear* 259: 1437-1442, 2005.

Gordon AM, Forssberg H, Johansson RS, and Westling G. Visual size cues in the programming of manipulative forces during precision grip. *Exp Brain Res* 83: 477-482, 1991.

Gulati R, and Srinivasan MA. Human fingerpad under indentation I: Static and Dynamic force response. *Bioengineering Conference ASME* BED-Vol. 29: 1995.

Harris CM, and Wolpert DM. Signal-dependent noise determines motor planning. *Nature* 394: 780-784, 1998.

Heinrich U, Koop U, Leneveu-Duchemin M-C, Osterrieder K, Bielfeldt S, Chkarnat C, Degwert J, Häntschel D, Jaspers S, Nissen H-P, Rohr M, Schneider G, and Tronnier H. Multicentre comparison of skin hydration in terms of physical-, physiological- and product-dependent parameters by the capacitive method (Corneometer CM 825). *Int J Cosmet Sci* 25: 45-53, 2003.

Hermsdorfer J, Marquardt C, Philipp J, Zierdt A, Nowak D, Glasauer S, and Mai N. Moving weightless objects. Grip force control during microgravity. *Exp Brain Res* 132: 52-64, 2000.

Hogan N. An organizing principle for a class of voluntary movements. *J Neurosci* 4: 2745-2754, 1984.

Hosoda K, Tada Y, and Asada M. Anthropomorphic robotic soft fingertip with randomly distributed receptors. *Robotics and Autonomous Systems* 54: 104-109, 2006.

Howe RD, and Cutkosky MR. Sensing Skin Acceleration for Slip and Texture Perception. *International conference on Robotics and Automation* 1: 145-150, 1989.

Iggo A. Cutaneous receptors and their sensory functions. *J Hand Surg Br* 9: 7-10, 1984.

Iggo A, and Andres KH. Morphology of cutaneous receptors. *Annu Rev Neurosci* 5: 1-31, 1982.

Iwase S, Mano T, Cui J, Kitazawa H, Kamiya A, Miyazaki S, Sugiyama Y, Mukai C, and Nagaoka S. Sympathetic outflow to muscle in humans during short periods of microgravity produced by parabolic flight. *Am J Physiol* 277: R419-426, 1999.

Jeannerod M. *Attention and Performance IX*. Erlbaum, Hillsdale: 1981.

Jeannerod M. The timing of natural prehension movements. *J Mot Behav* 16: 235-254, 1984.

Jenmalm P, Dahlstedt S, and Johansson RS. Visual and tactile information about object-curvature control fingertip forces and grasp kinematics in human dexterous manipulation. *J Neurophysiol* 84: 2984-2997, 2000.

Jenmalm P, Goodwin AW, and Johansson RS. Control of grasp stability when humans lift objects with different surface curvatures. *J Neurophysiol* 79: 1643-1652, 1998.

Johansson RS. In: *Motor control: Concepts and Issues*. John Wiley and sons Ltd, pp. 331-355, 1991.

Johansson RS, and Cole KJ. Sensory-motor coordination during grasping and manipulative actions. *Curr Opin Neurobiol* 2: 815-823, 1992.

Johansson RS, and Flanagan JR. Coding and use of tactile signals from the fingertips in object manipulation tasks. *Nat Rev Neurosci* 10: 345-359, 2009.

Johansson RS, and Vallbo AB. Tactile Sensory Coding in the Glabrous Skin of the Human Hand. *Trends in Neurosciences* 6: 27-32, 1983.

Johansson RS, and Westling G. Coordinated isometric muscle commands adequately and erroneously programmed for the weight during lifting task with precision grip. *Exp Brain Res* 71: 59-71, 1988.

Johansson RS, and Westling G. *Influences of cutaneous sensory input on the motor coordination during precision manipulation*. London: MacMillan Press, 1984a.

Johansson RS, and Westling G. Roles of glabrous skin receptors and sensorimotor memory in automatic control of precision grip when lifting rougher or more slippery objects. *Exp Brain Res* 56: 550-564, 1984b.

Johansson RS, and Westling G. Signals in tactile afferents from the fingers eliciting adaptive motor responses during precision grip. *Exp Brain Res* 66: 141-154, 1987.

Johnson KO. The roles and functions of cutaneous mechanoreceptors. *Current Opinion in Neurobiology* 11: 455-461, 2001.

Jordan MI, and Wolpert DM. In: *The cognitive Neuroscience*. Cambridge: MIT Press, pp. 1999.

Kawato M. Internal models for motor control and trajectory planning. *Curr Opin Neurobiol* 9: 718-727, 1999.

Kawato M. In: *Attention and Performance, XIV: Synergies in Experimental Psychology, Artificial Intelligence, and Cognitive Neuroscience - A Silver Jubilee*. Cambridge, Massachusetts: MIT press, pp. 821-849, 1992.

Kerassidis S. Is palmar and plantar sweating thermoregulatory? *Acta Physiol Scand* 152: 259-263, 1994.

Kim I, Ohtsuka H, and Inooka H. Impedance model for human fingertips. *SICE* 30: 112-114, 1994.

Kinoshita G, and Mori M. An elastic model of the skin and some proerties on the variable threshold processing of an artificial tactile sense. *Trans Soc Instrument and Control Eng* 8: 398-405, 1972.

Koudine AA, Barquins M, Anthoine P, Aubert L, and Lévèque J-L. Frictional properties of the skin: proposal of a new approach. *Int J Cosmet Sci* 22: 11-20, 2000.

Kourtis D, Kwok HF, Roach N, Wing AM, and Praamstra P. Maintaining grip: anticipatory and reactive EEG responses to load perturbations. *J Neurophysiol* 99: 545-553, 2008.

Kurtzer I, DiZio PA, and Lackner JR. Adaptation to a novel multi-force environment. *Exp Brain Res* 164: 120-132, 2005.

Lackner JR, and DiZio P. Motor control and learning in altered dynamic environments. *Curr Opin Neurobiol* 15: 653-659, 2005.

Lackner JR, and Dizio P. Rapid adaptation to Coriolis force perturbations of arm trajectory. *J Neurophysiol* 72: 299-313, 1994.

Landsmeer JM. Power grip and precision handling. *Ann Rheum Dis* 21: 164-170, 1962.

Lévêque JL, and de Rigal J. Impedance methods for studying skin moisturization. *J Soc Cosmet Chem* 34: 419-428, 1983.

Leveque JL, and Querleux B. SkinChip, a new tool for investigating the skin surface in vivo. *Skin Res Technol* 9: 343-347, 2003.

Levesque V, and Hayward V. Experimental Evidence of Lateral Skin Strain During Tactile Exploration. *Eurohaptics* 2003.

Li FX, Margetts S, and Fowler I. Use of 'chalk' in rock climbing: sine qua non or myth? *Journal of Sports Sciences* 19: 427-432, 2001.

Long C, 2nd, Conrad PW, Hall EA, and Furler SL. Intrinsic-extrinsic muscle control of the hand in power grip and precision handling. An electromyographic study. *J Bone Joint Surg Am* 52: 853-867, 1970.

Lucas BD, and Kanade T. An Iterative Image Registration Technique with an Application to Stereo Vision. *Intl Joint Conf on Artificial Intelligence* 674-679, 1981.

Macefield VG, Hager-Ross C, and Johansson RS. Control of grip force during restraint of an object held between finger and thumb: responses of cutaneous afferents from the digits. *Exp Brain Res* 108: 155-171, 1996.

Maeno T, Hiromitsu S, and Kawai T. Control of Grasping Force by Detecting Stick/Slip Distribution at the Curved Surface of an Elastic Finger. *IEEE International conference on Robotics and Automation* 2000.

Maeno T, Kobayashi K, and Yamazaki N. Relationship between the structure of human finger tissue and the location of tactile receptors. *Jsme International Journal Series C-Mechanical Systems Machine Elements and Manufacturing* 41: 94-100, 1998.

Maheshwari V, and Saraf RF. High-resolution thin-film device to sense texture by touch. *Science* 312: 1501-1504, 2006.

Maier MA, and Hepp-Reymond MC. EMG activation patterns during force production in precision grip. I. Contribution of 15 finger muscles to isometric force. *Exp Brain Res* 103: 108-122, 1995.

McDonnell MN, Ridding MC, Flavel SC, and Miles TS. Effect of human grip strategy on force control in precision tasks. *Exp Brain Res* 161: 368-373, 2005.

Melzack R, and Wall PD. On the nature of cutaneous sensory mechanisms. *Brain* 85: 331-356, 1962.

Miall RC, Weir DJ, Wolpert DM, and Stein JF. Is the cerebellum a smith predictor? *J Mot Behav* 25: 203-216, 1993.

Mon-Williams M, and Murray AH. The size of the visual size cue used for programming manipulative forces during precision grip. *Exp Brain Res* 135: 405-410, 2000.

Monzee J, Lamarre Y, and Smith AM. The effects of digital anesthesia on force control using a precision grip. *J Neurophysiol* 89: 672-683, 2003.

Mountcastle VB. *The Hensory Hand: neural mechanisms of somatic sensation*. Cambridge, Massachussetts, and London, England: Harvard University Press, 2005.

Müller J. *Elements of Physiology*. London: Taylor and Walton, 1842.

Nacht S, Close JA, Yeung D, and Gans EH. Skin Friction Coefficient - Changes Induced by Skin Hydration and Emollient Application and Correlation with Perceived Skin Feel. *Journal of the Society of Cosmetic Chemists* 32: 55-65, 1981.

Nakazawa N, Ikeura R, and Inooka H. Characteristics of human fingertips in the shearing direction. *Biological Cybernetics* 82: 207-214, 2000.

Napier JR. The prehensile movements of the human hand. *J Bone Joint Surg Br* 38-B: 902-913, 1956.

Naylor PF. The skin surface and friction. *Br J Dermatol* 67: 239-246, 1955.

Nowak DA, Hermsdorfer J, Glasauer S, Philipp J, Meyer L, and Mai N. The effects of digital anaesthesia on predictive grip force adjustments during vertical movements of a grasped object. *Eur J Neurosci* 14: 756-762, 2001a.

Nowak DA, Hermsdorfer J, Philipp J, Marquardt C, Glasauer S, and Mai N. Effects of changing gravity on anticipatory grip force control during point-to-point movements of a hand-held object. *Motor Control* 5: 231-253, 2001b.

O'goshi K, and Serup J. Inter-instrumental variation of the skin capacitance measured with the Corneometer. *Skin Res Technol* 11: 107-109, 2005.

Papaxanthis C, Pozzo T, and McIntyre J. Kinematic and dynamic processes for the control of pointing movements in humans revealed by short-term exposure to microgravity. *Neuroscience* 135: 371-383, 2005.

Papaxanthis C, Pozzo T, Popov KE, and McIntyre J. Hand trajectories of vertical arm movements in one-G and zero-G environments. Evidence for a central representation of gravitational force. *Exp Brain Res* 120: 496-502, 1998.

Pare M, Behets C, and Cornu O. Paucity of presumptive ruffini corpuscles in the index finger pad of humans. *J Comp Neurol* 456: 260-266, 2003.

Pare M, Elde R, Mazurkiewicz JE, Smith AM, and Rice FL. The Meissner corpuscle revised: a multiafferented mechanoreceptor with nociceptor immunochemical properties. *J Neurosci* 21: 7236-7246, 2001.

Pare M, Smith AM, and Rice FL. Distribution and terminal arborizations of cutaneous mechanoreceptors in the glabrous finger pads of the monkey. *J Comp Neurol* 445: 347-359, 2002.

Pataky TC, Latash ML, and Zatsiorsky VM. Viscoelastic response of the finger pad to incremental tangential displacements. *Journal of Biomechanics* 38: 1441-1449, 2005.

Pawluk DT, and Howe RD. Dynamic contact of the human fingerpad against a flat surface. *J Biomech Eng* 121: 605-611, 1999a.

Pawluk DTV, and Howe RD. Dynamic lumped element response of the human fingerpad. *Journal of Biomechanical Engineering-Transactions of the Asme* 121: 178-183, 1999b.

Persson BNJ, Sivebaeck IM, Samoilov VN, Zhao K, Volokitin AI, and Zhang Z. On the origin of Amonton's friction law. *Journal of Physics: Condensed Matter* 20: 395006(395011pp), 2008.

Phillips JR, and Johnson KO. Tactile spatial resolution. III. A continuum mechanics model of skin predicting mechanoreceptor responses to bars, edges, and gratings. *J Neurophysiol* 46: 1204-1225, 1981.

Pigeon P, Bortolami SB, DiZio P, and Lackner JR. Coordinated turn-and-reach movements. I. Anticipatory compensation for self-generated coriolis and interaction torques. *J Neurophysiol* 89: 276-289, 2003.

Robertshaw D. Neuroendocrine control of sweat glands. *J Invest Dermatol* 69: 121-129, 1977.

Saels P, Thonnard JL, Detrembleur C, and Smith AM. Impact of the surface slipperiness of grasped objects on their subsequent acceleration. *Neuropsychologia* 37: 751-756, 1999.

Sato K, Kang WH, Saga K, and Sato KT. Biology of sweat glands and their disorders. I. Normal sweat gland function. *J Am Acad Dermatol* 20: 537-563, 1989.

Savescu AV, Latash ML, and Zatsiorsky VM. A technique to determine friction at the fingertips. *J Appl Biomech* 24: 43-50, 2008.

Sekiguchi N, Komeda T, Funakubo H, Chabicovsky R, Nicolics J, and Stangl G. Microsensor for the measurement of water content in the human skin. *Sensors and Actuators B: Chemical* 78: 326-330, 2001.

Serina ER, Mockensturm E, Mote CD, and Rempel D. A structural model of the forced compression of the fingertip pulp. *Journal of Biomechanics* 31: 639-646, 1998.

Serina ER, Mote CD, and Rempel D. Force response of the fingertip pulp to repeated compression - effects of loading rate, loading angle and anthropometry. *Journal of Biomechanics* 30: 1035-1040, 1997.

Shadmehr R, and Mussa-Ivaldi FA. Adaptive representation of dynamics during learning of a motor task. *J Neurosci* 14: 3208-3224, 1994.

Shao F, Childs THC, and Henson B. Developing an artificial fingertip with human friction properties. *Tribology International* 42: 1575-1581, 2009.

Shibasaki M, Wilson TE, and Crandall CG. Neural control and mechanisms of eccrine sweating during heat stress and exercise. *J Appl Physiol* 100: 1692-1701, 2006.

Sinclair D. *Mechanisms of cutaneous sensation*. New York, Toronto: Oxford University Press, 1981.

Sinclair DC. Cutaneous sensation and the doctrine of specific energy. *Brain* 78: 584-614, 1955.

Sivamani RK, Goodman J, Gitis NV, and Maibach HI. Friction coefficient of skin in real-time. *Skin Res Technol* 9: 235-239, 2003.

Smeets JB, and Brenner E. A new view on grasping. *Motor Control* 3: 237-271, 1999.

Smith AM. The coactivation of antagonist muscles. *Can J Physiol Pharmacol* 59: 733-747, 1981.

Smith AM, and Bourbonnais D. Neuronal activity in cerebellar cortex related to control of prehensile force. *J Neurophysiol* 45: 286-303, 1981.

Smith AM, Cadoret G, and St-Amour D. Scopolamine increases prehensile force during object manipulation by reducing palmar sweating and decreasing skin friction. *Exp Brain Res* 114: 578-583, 1997.

Someya T, Kato Y, Sekitani T, Iba S, Noguchi Y, Murase Y, Kawaguchi H, and Sakurai T. Conformable, flexible, large-area networks of pressure and thermal sensors with organic transistor active matrixes. *Proceedings of the National Academy of Sciences of the United States of America* 102: 12321-12325, 2005.

Someya T, Sekitani T, Iba S, Kato Y, Kawaguchi H, and Sakurai T. A large-area, flexible pressure sensor matrix with organic field-effect transistors for artificial skin applications. *Proceedings of the National Academy of Sciences of the United States of America* 101: 9966-9970, 2004.

Srinivasan MA, and Dandekar K. An investigation of the mechanics of tactile sense using two-dimensional models of the primate fingertip. *Journal of Biomechanical Engineering-Transactions of the Asme* 118: 48-55, 1996.

Srinivasan MA, Gulati R, and Dandekar K. In Vivo Compressibility of the Human Fingertip. *ASME* BED-Vol. 22: 1992.

Srinivasan MA, Whitehouse JM, and LaMotte RH. Tactile detection of slip: surface microgeometry and peripheral neural codes. *J Neurophysiol* 63: 1323-1332, 1990.

Tada M, Imai M, and Ogasawara T. Development of Simultaneous Measurement System of Incipient Slip and Grip/load Force. *IEEE Workshop on Human and Robot Interaction Communication* 57-62, 2000.

Tada M, Mochimaru M, and Kanade T. How does a fingertip slip? - Visualizing partial slippage for modeling of contact mechanics. *Eurohaptics* 2006a.

Tada M, Mochimaru M, and Kanade T. How does a fingertip slip? - Visualizing partial slippage for modeling of contact mechanics. *Eurohaptics* 2006b.

Tada M, Nagai N, Yoshida H, and Maeno T. Iterative FE analysis for non-invasive material modeling of a fingertip with layered structure. *Eurohaptics 2006* 2006c.

Tada M, Shibata T, and Ogasawara T. Investigation of the touch processing model in human grasping based on the stick ratio within a fingertip contact interface. *IEEE International Conference on Systems, Man and Cybernetics* 2002.

Todorov E. Optimality principles in sensorimotor control. *Nat Neurosci* 7: 907-915, 2004.

Tomlinson SE, Lewis R, and Carré MJ. Review of the frictional properties of finger-object contact when gripping. *J Engineering Tribology* 221: 841-851, 2007.

Tremblay MR, and Cutkosky MR. Estimating friction using incipient slip sensing during a manipulation task. *International Conference on Robotics and Automation* 429-434, 1993.

Turrell YN, Li FX, and Wing AM. Estimating the minimum grip force required when grasping objects under impulsive loading conditions. *Behav Res Methods Instrum Comput* 33: 38-45, 2001.

Uno Y, Kawato M, and Suzuki R. Formation and control of optimal trajectory in human multijoint arm movement. Minimum torque-change model. *Biol Cybern* 61: 89-101, 1989.

Vallbo AB, and Johansson RS. Properties of cutaneous mechanoreceptors in the human hand related to touch sensation. *Hum Neurobiol* 3: 3-14, 1984.

van Beers RJ, Wolpert DM, and Haggard P. When feeling is more important than seeing in sensorimotor adaptation. *Curr Biol* 12: 834-837, 2002.

Venables PH, and Christie MJ. In: *Electrodermal Activity in Psychological Research*. New York and London: Academic Press, pp. 2-124, 1973.

Wang Q, and Hayward V. In vivo biomechanics of the fingerpad skin under local tangential traction. *Journal of Biomechanics* 40: 851-860, 2007.

Warman PH, and Ennos AR. Fingerprints are unlikely to increase the friction of primate fingerpads. *Journal of Experimental Biology* 212: 2015-2021, 2009.

Weiner JS, and Hellman K. The sweat glands. *Biol Rev Cambridge Phil Soc* 35: 141-186, 1960.

Westling G, and Johansson RS. Factors influencing the force control during precision grip. *Exp Brain Res* 53: 277-284, 1984.

Wettels N, Santos VJ, Johansson RS, and Loeb GE. Biomimetic Tactile Sensor Array. *Advanced Robotics* 22: 829-849, 2008.

White O, Bleyenheuft Y, Ronsse R, Smith AM, Thonnard JL, and Lefevre P. Altered gravity highlights central pattern generator mechanisms. *J Neurophysiol* 100: 2819-2824, 2008.

White O, McIntyre J, Augurelle AS, and Thonnard JL. Do novel gravitational environments alter the grip-force/load-force coupling at the fingertips? *Exp Brain Res* 163: 324-334, 2005.

Wilke K, Martin A, Terstegen L, and Biel SS. A short history of sweat gland biology. *Int J Cosmet Sci* 29: 169-179, 2007.

Witney AG, Wing A, Thonnard JL, and Smith AM. The cutaneous contribution to adaptive precision grip. *Trends Neurosci* 27: 637-643, 2004.

Wolfram LJ. Friction of skin. *J Soc Cosmet Chem* 34: 465-476, 1983.

Wolpert DM, and Flanagan JR. Motor prediction. *Curr Biol* 11: R729-732, 2001.

Wolpert DM, Ghahramani Z, and Jordan MI. An internal model for sensorimotor integration. *Science* 269: 1880-1882, 1995.

Yantis S, and Pashler H. *Stevens' handbook of experimental psychology*. New York: John Wiley & Sons, Inc., 2002.

Zackrisson T, Eriksson B, Hosseini N, Johnels B, and Krogstad AL. Patients with hyperhidrosis have changed grip force, coefficient of friction and safety margin. *Acta Neurol Scand* 117: 279-284, 2008.

Zitova B, and Flusser J. Image registration methods: a survey. *Image and Vision Computing* 21: 977-1000, 2003.